

ROADMAP • OPEN ACCESS

## Roadmap on industrial imaging techniques

To cite this article: Jung-Ryul Lee *et al* 2025 *Meas. Sci. Technol.* **36** 013001

View the [article online](#) for updates and enhancements.

### You may also like

- [Special section on imaging](#)  
M Bertero and O Scherzer
- [Imaging systems and techniques](#)  
Wuqiang Yang, George Giakos,  
Konstantina Nikita et al.
- [Advances in physics-informed deep learning for imaging data: a review of methods and applications](#)  
Yogita Yogita and Thomas Bocklitz

## Roadmap

# Roadmap on industrial imaging techniques

Jung-Ryul Lee<sup>1,\*</sup>, Hongki Yoo<sup>2</sup>, Chia Chen Ciang<sup>1</sup>, Young-Jin Kim<sup>2</sup>, Daehee Kim<sup>2</sup>, Teow Wee Teo<sup>3</sup>, Zeinab Mahdavi pour<sup>3</sup>, Azizi Abdullah<sup>4</sup>, Bee Ee Khoo<sup>5</sup>, Mohd Zaid Abdullah<sup>5</sup>, Dimitris K lakovidis<sup>6</sup>, Panagiotis Vartholomeos<sup>6</sup>, Andrew Yacoot<sup>7</sup>, Tao Cai<sup>8</sup>, Mirae Kim<sup>8</sup>, Kyung Chun Kim<sup>8</sup>, Jiamin Ye<sup>9</sup>, Xiao Liang<sup>9</sup>, Lidan Cao<sup>10</sup>, Xingwei Wang<sup>10</sup>, Jianqing Huang<sup>11,12</sup>, Weiwei Cai<sup>11</sup>, Yingchun Wu<sup>13</sup>, Marco J da Silva<sup>14</sup>, Chao Tan<sup>9</sup>, Sayantan Bhattacharya<sup>15</sup>, Pavlos Vlachos<sup>16</sup>, Christian Cierpka<sup>17</sup> and Massimiliano Rossi<sup>18</sup>

<sup>1</sup> Department of Aerospace Engineering, Korea Advanced Institute of Science and Technology (KAIST), 291 Daehak-ro, Yuseong-gu, Daejeon 34141, Republic of Korea

<sup>2</sup> Department of Mechanical Engineering, Korea Advanced Institute of Science and Technology (KAIST), 291 Daehak-ro, Yuseong-gu, Daejeon 34141, Republic of Korea

<sup>3</sup> TT Vision Technologies Sdn. Bhd., Plot 106, Hilir Sungai Keluang 5, Bayan Lepas Industrial Zone, Phase 4, Penang 11900, Malaysia

<sup>4</sup> Faculty of Information Sciences and Technology, Universiti Kebangsaan Malaysia, 43600 Bangi, Selangor, Malaysia

<sup>5</sup> School of Electrical and Electronics Engineering, Engineering Campus, Univerisiti Sains Malaysia, 14300 Nibong Tebal, Penang, Malaysia

<sup>6</sup> Department of Computer Science and Biomedical Informatics, University of Thessaly, Papasiopoulou 2-4, Lamia, Greece

<sup>7</sup> National Physical Laboratory, Hampton Road, Teddington, Middlesex TW11 0LW, United Kingdom

<sup>8</sup> School of Mechanical Engineering, Pusan National University, Busan 46241, Republic of Korea

<sup>9</sup> School of Electrical and Information Engineering, Tianjin University, Tianjin 300072, People's Republic of China

<sup>10</sup> Electrical and Computer Engineering Department, University of Massachusetts Lowell, One University Ave, Lowell, MA 01854, United States of America

<sup>11</sup> KeyLaboratory of Education Ministry for Power Machinery and Engineering, School of Mechanical Engineering, Shanghai Jiao Tong University, People's Republic of China

<sup>12</sup> Department of Electrical and Electronic Engineering, The University of Hong Kong, People's Republic of China

<sup>13</sup> State Key Laboratory of Clean Energy Utilization, Zhejiang University, Hangzhou 310027, People's Republic of China

<sup>14</sup> Institute of Measurement Technology, Johannes Kepler University Linz, Austria

<sup>15</sup> Department of Mechanical Engineering, University of Maryland, Baltimore County, MD 21250, United States of America

<sup>16</sup> School of Mechanical Engineering, Purdue University, West Lafayette, IN 47907, United States of America

<sup>17</sup> Institute of Thermodynamics and Fluid Mechanics, Technische Universität Ilmenau, Helmholtzring 1, 98693 Ilmenau, Germany

<sup>18</sup> Department of Industrial Engineering, Alma Mater Studiorum Università di Bologna, Via Fontanelle 40, 47121 Forlì, Italy

\* Author to whom any correspondence should be addressed.



Original content from this work may be used under the terms of the [Creative Commons Attribution 4.0 licence](https://creativecommons.org/licenses/by/4.0/). Any further distribution of this work must maintain attribution to the author(s) and the title of the work, journal citation and DOI.

E-mail: [leejrr@kaist.ac.kr](mailto:leejrr@kaist.ac.kr)

Received 20 March 2024

Accepted for publication 4 September 2024

Published 3 December 2024



## Abstract

Imaging plays a vital role in enabling the visualization and analysis of objects and phenomena across various scientific disciplines and industrial sectors, spanning a wide range of length and time scales. This roadmap presents a critical overview of 13 industrial imaging techniques, which are organized into three thematic categories according to their applicability to either solid, fluid, or both solid and fluid targets. The objectives of this roadmap are to highlight challenges and provide perspectives for next-generation imaging systems, which can serve as a guide to researchers and funding agencies in identifying new prospects. It has been found that the common challenges of imaging techniques have remained fundamentally unchanged over the years, including improving coverage, speed, resolution, accuracy, and robustness; however, there is an increasing reliance on data-driven or artificial intelligence (AI) approaches. Addressing these challenges necessitates easy access to high-performance computing resources. Notably, the trustworthiness and traceability of AI approaches should be enhanced through the sharing of benchmarking data, balancing with physics-based techniques, and the adoption of more explainable AI.

Keywords: signal processing, image processing, computer vision, machine learning, nondestructive testing and evaluation, imaging informatics, multimodal imaging

---

## Contents

1. Introduction	3
2. LIDAR imaging	5
3. Ultrasound propagation imaging (UPI)	8
4. Luminescence imaging	11
5. Endoscopy	15
6. Confocal microscopy	18
7. Atomic force microscopy	21
8. Phosphor thermometry	23
9. Electrical tomography (ET)	26
10. Photoacoustic imaging (PAI)	29
11. Holography	31
12. Multiphase flow process imaging	33
13. Particle image velocimetry (PIV)	35
14. Microscopic particle image velocimetry ( $\mu$ PIV)	38
Data availability statement	40
References	40

## 1. Introduction

A picture is worth a thousand words. Imaging technology has come a long way since the first camera obscura was invented in ancient Greece. Since then, imaging technology has been continually evolving, driven by human curiosity to better comprehend and record the world around us, and the need to find solutions to the challenges we face. Imaging technology offers a plethora of techniques, each with its unique characteristics and capabilities. They range from generating visualizations directly through mechanical waves to reconstructing images indirectly via electromagnetic interference. While some techniques excel in producing detailed 2D still images, others bring scenes to life through animated videos. Additionally, the versatility of these methods is evident as some are optimized for examining vast macroscopic landscapes, whereas others excel in the intricate world of nanoscale phenomena. Their development has supported vivid, detailed visualization of the targets and provided insights that would have been impossible to obtain just a few decades ago.

Among all imaging techniques, some have been identified as having significant potential to revolutionize our ways of life through improved healthcare, easier daily navigation, and access to high-quality products, yet, some of them have received comparatively less attention than their substantial potential for industrial enhancement in relevant sectors warrants. Against this backdrop, this roadmap presents a critical overview of 13 industrial-relevant techniques, aiming to highlight challenges and provide perspectives for upgrades that may profoundly alter the future landscape. Nevertheless, it is important to clarify that the selection is certainly not exhaustive, and there is no intention to suggest that those not included are of lesser potential or significance.

The remainder sections of this roadmap present the selected imaging techniques according to the physical forms of targets to which they can be applied. Specifically, with reference to figure 1, Category A is dedicated to techniques that can perform imaging on targets in solid form; Category B to techniques capable of imaging both solids and fluidic targets; while Category C is reserved for those techniques suitable for targets in fluid form only. Note that the term ‘fluids’ encompasses both liquids and gases. It is important to clarify that the classification is based on the general applicability of the techniques, without being confined to the examples provided or the specific application fields focused on in the respective sections. For instance, while photoacoustic imaging (PAI) (section 10) is presented primarily based on biomedical imaging of biological tissues, which are effectively solids, this technique is classified under Category B due to its suitability for flow-field imaging [1] as well. Similarly, electrical tomography (ET) (section 9), which is being presented leaning more towards fluid-flow applications, is classified under Category B because of its ability to image property inhomogeneity or damage in solids [2]. In order to give a rough idea where a technique stands relative to the other, the presentation order of the techniques within their respective categories is generally arranged by the descending physical size of the targets. It is therefore easy to find that the techniques can be broadly

divided into two groups in each category: one for macroscopic targets and the other for microscopic targets, as depicted in figure 1. Exceptions are the PAI (section 10) and holography (section 11) techniques, which are applicable to both macroscopic and microscopic targets.

Discussions on the 13 imaging techniques, presented in the subsequent sections of this roadmap, reveal that the common challenges encountered by these techniques today are not significantly different from those faced decades ago; namely, the need to improve spatial and/or temporal resolution, enhance accuracy, increase imaging speed, and ensure robustness in highly variable environments. While delving into the technical specifics of each technique is beyond the scope of this introduction—with detailed information available in the respective sections or cited references—it is noteworthy that these challenges and inherent possibilities converge at several key junctures. For instance, many techniques are still limited to two-dimensional visualizations at specific moments, despite the fact that the targets exist in three-dimensional physical spaces and evolve over time. This limitation in coverage is particularly apparent for techniques like multiphase flow process imaging (section 12), which restricts the visualization to phase fraction distribution at specific locations within a larger system. Addressing this constraint could significantly enhance our understanding of the targets, thereby unlocking new possibilities. For example, in the context of multiphase flow process imaging, achieving comprehensive coverage in both spatial and temporal dimensions could enable precise automatic control of complex systems.

Secondly, the imaging speed restricts the overall throughput and temporal resolution across many imaging techniques. For instance, phosphorescence activities at high temperatures can occur within microseconds or nanoseconds, necessitating frame rates for phosphor thermometry (section 8) in the MHz or GHz range. Yet, the highest frame rate currently stands at approximately 100 kHz. Additionally, spatial point-scanning methods, such as PAI (section 10) and ultrasound propagation imaging (UPI) (section 3), are typically limited in terms of throughput. This limitation is especially pronounced in UPI (section 3) where the targets, such as thin-walled engineering structures like airplanes, require larger imaging regions of interest (ROIs) compared to the smaller biomedical targets used in PAI (section 10). Overcoming the speed limitation by developing faster hardware or implementing compressive sensing for reduced measurement points would, obviously, enable imaging of more targets or larger ROIs in a shorter time and enhance our ability to understand and address more dynamic problems.

Thirdly, as highlighted in some sections, imaging accuracy, robustness, and contextual understanding can be significantly improved by fusing complementary information from more than one set of data, each acquired using different measurement modalities or parametric settings. This approach is applicable even for techniques beyond the 13 selected ones. For example, distortion in the imaging plane of UPI (section 3) can be reduced or corrected by incorporating depth information from LIght Detection and Ranging (LIDAR) imaging (section 2); a comprehensive temperature-velocity history of

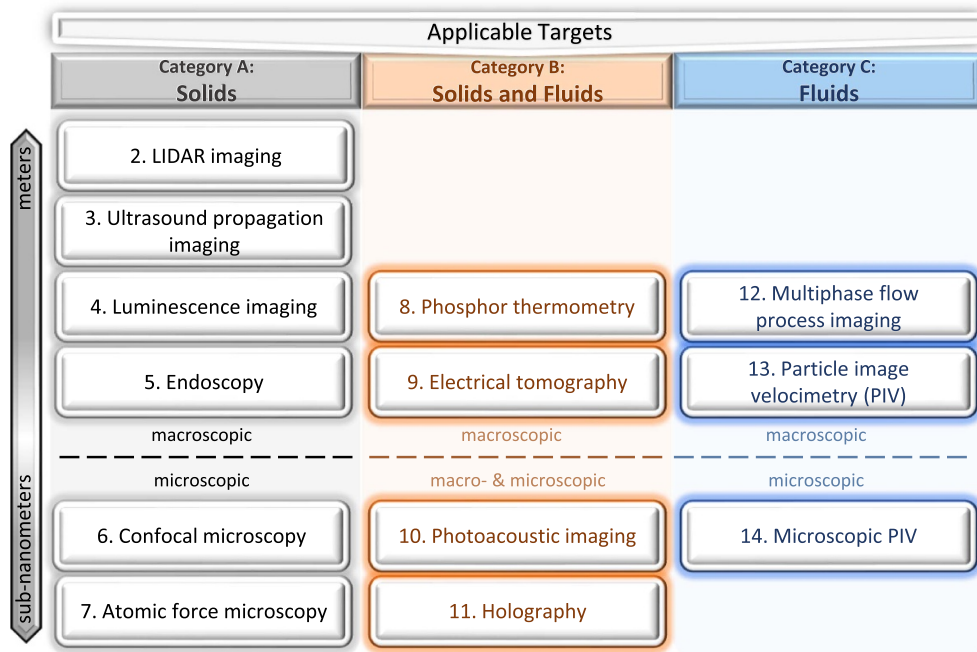


**Figure 1.** Classification of selected imaging techniques based on their applicability to solid, fluid, or both solid and fluid targets.

a flow field can be obtained by merging temperature data from phosphor thermometry (section 8) with velocity data from particle image velocimetry (PIV) (section 13); imaging accuracy can be enhanced by integrating ET (section 9) data with data from other techniques such as radiometric and ultrasonic imaging; contextual understanding of scanning electron microscopy can be improved by amalgamating topological information from atomic force microscopy (section 7). Potential fusions applicable for both the selected techniques as well as for other techniques not covered in this roadmap, remain to be discovered. This includes possibilities within the existing scope of example applications and to applications beyond those outlined in the sections. For instance, although endoscopy is described under the context of the biomedical industry in section 5, it is also commonly employed for the inspection of airplane turbine engines and industrial pipelines. In this broader applications, combining endoscopy (section 5), which provides visual information, with techniques like luminescence imaging (section 4), which can provide information regarding material degradation, might enhance understanding of the target through an information-rich, fused image.

Fourthly, artificial intelligence (AI) technologies, particularly deep learning (DL) and machine learning (ML), are revolutionizing imaging techniques through improved image reconstruction, interpretation, and measurement accuracy. However, their trustworthiness is often compromised by the notorious scarcity of benchmarking data, which is crucial for training and validating AI models, as well as for fair comparisons and quantification of advancements. Therefore, the sharing of diverse and well-annotated benchmarking datasets is essential, as exemplified commendably by the authors of [3]. Moreover, while AI algorithms vary in transparency, DL networks are particularly noted as ‘black-box’ algorithms,

with their input–output relationships being largely opaque. Thus, it is imperative for all stakeholders, particularly imaging technologists, researchers, and the broader AI community, to enhance transparency and traceability by directing more efforts toward explainable AI [4]. Last but not least, the significant increase in data-driven approaches due to AI should be complemented by physics-based approaches, ensuring that they support one another for a holistic understanding.

To fundamentally address the previously delineated challenges and fully leverage the potential of imaging techniques, access to high-performance computing resources, such as parallel graphics processing units (GPUs) and tensor processing units, has become more of a requirement than an option. Consequently, the development of scalable computing architectures and next-generation processing technologies should progress concurrently with advancements in imaging techniques. Furthermore, revisiting and learning from more mature techniques by defining performance metrics, ensuring traceability, and establishing standardization is beneficial. The discussions on traceability in section 7 ‘atomic force microscopy’ and on uncertainty in section 13 ‘particle image velocimetry’ serve as good examples. Only when these aspects are defined and established can a technique be considered a measurement tool rather than merely a visualization tool, thereby paving the way for it to be widely embraced by industries.

In conclusion, it is hoped that this roadmap, constituted by the overall discussion presented in this Introduction and the status and challenges of all techniques detailed in the respective sections, will catalyze cross-disciplinary collaborations and dismantle existing barriers. The aim is to foster a unified approach that synergizes diverse expertise and state-of-the-art technological resources for the comprehensive advancement of imaging techniques, thereby aiding the continuous and sustainable progress of global society.

## 2. LIDAR imaging

Young-Jin Kim and Daehee Kim

Department of Mechanical Engineering, Korea Advanced Institute of Science and Technology (KAIST), 291 Daehak-ro, Yuseong-gu, Daejeon 34141, Republic of Korea

E-mail: yj.kim@kaist.ac.kr and d.h.kim2754@kaist.ac.kr

### Status

LIDAR is one of the most discussed 3D machine vision technologies due to their growing demands in autonomous vehicles [5–7], object detection in smart manufacturing [8–10], human–machine interaction for collaborative robots [10–13], automated guided vehicles in smart factories, which commonly requires machine intelligence [14, 15]. LIDAR has been also the prerequisite in other broad applications of geodetic survey, formation flying of smart satellites, environmental monitoring of chemical leakages, and understanding of global warming effects. General machine vision technologies are split into 2D and 3D imaging; LIDAR technologies currently span over a large part of 3D machine vision over passive-type stereovision, active-type optical triangulation, and active-type interferometry, as shown in figure 2. The principle of LIDAR is strongly dependent on the required measurement range and precision. In most LIDAR applications requiring mm-level precision, fast and simple geometrical optics and time-of-flight detection principles are readily applied. However, when the target precision approaches sub-millimeter or even down to a few micrometer-level, the time-of-flight detection resolution or the wave nature of light, optical diffraction starts to limit the attainable precision. Therefore, the other wave nature of light, the optical interference, should be introduced for realizing sub-micrometer-level precision.

The basic principle of LIDAR was first demonstrated in 1961 [18], shortly after the invention of the laser; 3D imaging LIDARs determine the absolute distances from the LIDAR to the target objects by measuring the time-of-flight of the reflected or back-scattered photons from the objects and multiplying the times-of-flight ( $\Delta t$ ) by the speed-of-light ( $c = 299\,792\,458\text{ m s}^{-1}$ ), one of the fundamental physical constants, as shown in figure 3(a) [19, 20]. The time-of-flight can be detected by detecting ultrashort light pulses having a pulse duration of nanosecond ( $10^{-9}\text{ s}$ ), picosecond ( $10^{-12}\text{ s}$ ) or even down to femtoseconds ( $10^{-15}\text{ s}$ ). The state-of-the-art photodetectors and event timers [21] support picosecond-level time resolution, which is converted into 0.15 mm level precision considering the double-path configuration.

For higher sub-millimeter-level precision, the optical interference can be introduced as demonstrated in FMCW (frequency-modulated continuous wave) LIDAR [22, 23], as shown in figure 3(b). A fast wavelength-swept laser is used as the light source in the FMCW LIDAR system. The laser beam is split into two parts; one works as the measurement beam that is transmitted to the target (Tx) and the returns from the target (Rx), while the other beam works as the reference

(local oscillator (LO)) without any travel. These two beams are recombined so as to form the optical beat frequency,  $f_{\text{beat}}$ , at the high-speed photodetector. Because the time-of-flight to the target makes the  $f_{\text{RX}}$  and  $f_{\text{LO}}$  different, FMCW can detect the  $f_{\text{beat}}$  as the difference between  $f_{\text{RX}}$  and  $f_{\text{LO}}$ ; therefore, the  $f_{\text{beat}}$  can be converted to the time-of-flight  $\Delta t$  for the distance measurement. Because FMCW utilizes the coherent nature of the laser beam, the measurement range and attainable precision are strongly dependent on the spectral linewidth and signal-to-noise ratio (SNR) of the  $f_{\text{beat}}$ , as shown in figure 3(b). The spectral linewidth and SNR are governed by the coherence degree of the swept laser in use and other system background noise.

For the time-of-flight detection with lower timing jitters, high-frequency amplitude modulation can be utilized with internal injection current modulation or external electro-optic modulators, instead of using short laser pulses with a fast photodetector, as shown in figure 3(c) [24]. Periodic sinusoidal waves (with the modulation frequency of  $f_{\text{AM}}$ ) can be generated with a simple amplitude modulator in front of the laser; then, the phase difference ( $\Delta\varphi$ ) between the reflected or back-scattered beam (Rx) and the local reference beam (Tx) can be measured at the phase meter. The resulting phase difference can be converted to the time-of-flight information  $\Delta t$  for the distance measurement. In AMCW (amplitude-modulated continuous wave) LIDAR, however, the phase ambiguity hinders the absolute determination of the target distances; therefore, some objects having complicated large-stepped surface structures or having fast motions cannot be measured.

### Current and future challenges

The measurement range, precision, and speed are the three key performances of 3D LIDAR imaging technologies. Therefore, we will discuss four critical challenges in these three key performances for state-of-the-art LIDAR systems based on direct TOF, FMCW TOF and AMCW TOF detections. The first challenge is in the beam scanning mechanism. All LIDAR systems are based on the TOF detection of a single point at a time; therefore, a beam scanning mechanism should be involved for reconstructing the 3D information of the object. Wide-angular mechanical scanning with rotating mirrors, small-angular mechanical scanning with MEMS (micro-electro-mechanical system) mirrors [25] and OPA (optical phased array) scanners [26] are the available scanning mechanisms. An ideal scanning system should have a wide scanning range, high angular resolution, high scanning speed, high reliability, and low production cost at the same time, which cannot be realized with a single system. The second challenge is in multi-path interference (MPI). Because the laser beam has a physical beam size and the beam is later expanded during the propagation, the returned beam can come from different sections of the target objects or even from intermediate obstacles. This MPI effect should be suppressed by post-processing, whose algorithms are different for different LIDAR principles. The third challenge is in 3D object detection. The LIDAR provides

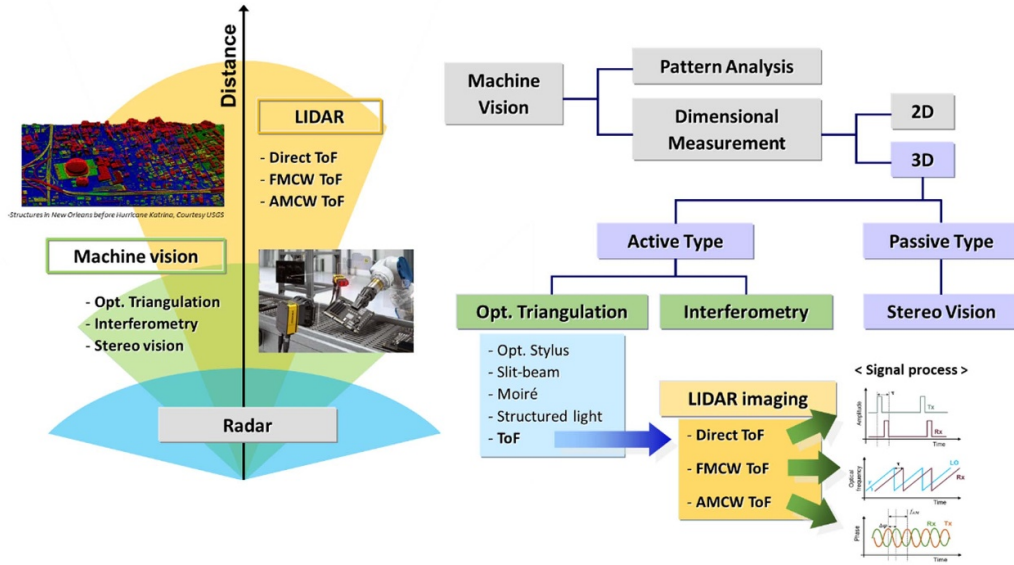


**Figure 2.** LIDAR as a 3D machine vision technology. LIDARs currently span over a large part of 3D machine vision over passive stereovision, active-type optical triangulation, and active-type interferometry. LIDAR image courtesy USGS. Machine vision image courtesy Cognex Corp. Reproduced from [16]. CC BY 4.0. Reproduced with permission from [17].

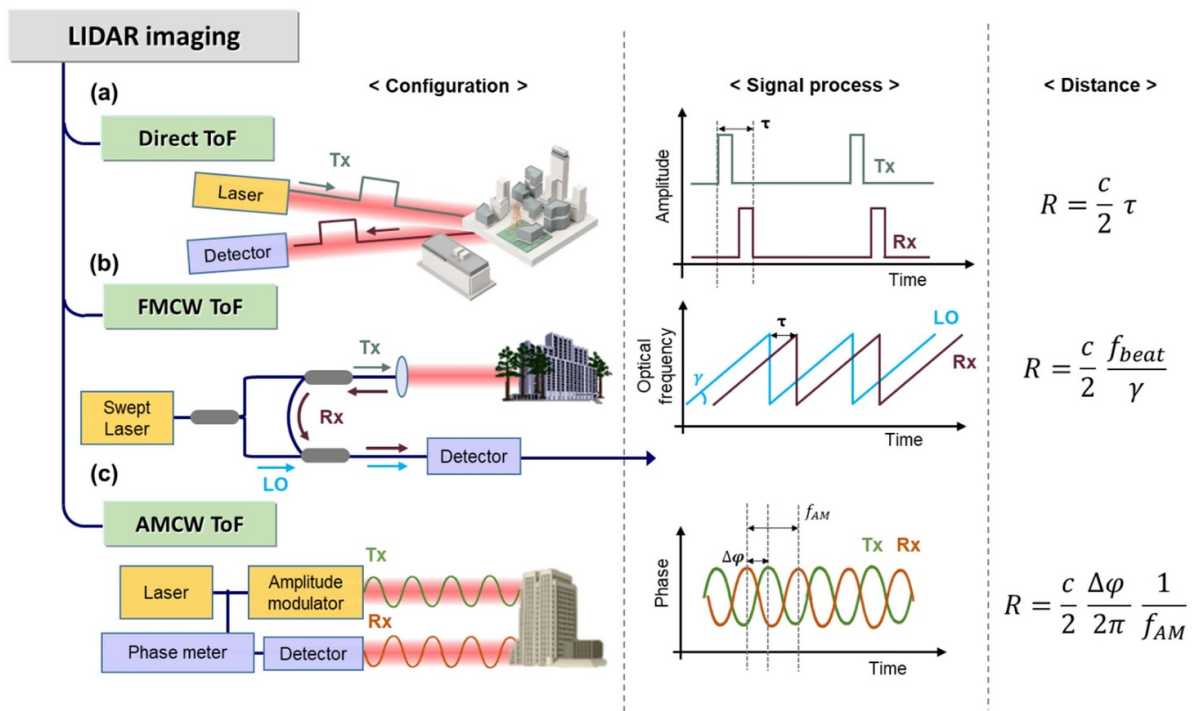


**Figure 3.** Schematics of ToF-based LIDAR 3D imaging techniques. This figure represents LIDARs’ system configuration, signal processing procedure and distance calculation method of (a) direct ToF, (b) FMCW (frequency-modulated continuous wave) ToF, (c) AMCW (amplitude-modulated continuous wave) ToF LIDAR, respectively.

the object information in the form of 3D point clouds only. Therefore, the 3D point data should be processed for easier object detection with background noise removal. However, the distance information may not be enough for object detection because one cannot tell whether the target object is a human being or a static obstacle. The fourth challenge lies in

weather and environmental sensitivity. The water vapors can absorb, scatter, or reflect the laser beam in different directions. Therefore, the LIDARs can be strongly influenced by wet targets, heavy rain or heavy fog. For the more ubiquitous application of LIDARs, the above-mentioned four challenges should be overcome.

## Advances in science and technology to meet challenges

Regarding the four technological challenges of LIDAR, there have been a series of important advances in the last two decades. Regarding the first beam scanning challenge, the advanced OPA concepts have been realized with the aid of semiconductor lithography processes; one concept realized the active 2D phase-shifter array by combining the MEMS actuator layer with sub-wavelength grating layer, and the other concept by realizing the on-chip optical-waveguide OPA. Regarding the second challenge on MPI and the third challenge of 3D object detection, the introduction of reinforcement learning or other AI technologies could resolve the key issues in distinguishing the unwanted multi-path information from the target information or in recognizing the 3D objects out of the numerous point clouds. About the fourth challenge of weather/environmental sensitivity, other types of sensors that are immune to environmental conditions can be used in parallel for making appropriate decisions. GPS, RADARs, ultrasonic sensors, and infrared sensors can work for this purpose. The partial data loss in LIDAR due to environmental issues can be reconstructed with the aid of ML technology.

## Concluding remarks

LIDARs have received extreme attention in the last decade owing to the solid technological trends in machine intelligence for autonomous vehicles, Industry 4.0, smart factories, collaborative robots, and AI. Therefore, many non-precedented research efforts and investments have been addressed in terms of system hardware, software, computing powers and searching for business chances. These have resulted in consistent performance improvement of 3D LIDAR imaging with real market opportunities. Nowadays, many LIDAR market leaders are waiting for the tipping points where real business chances are open. Three key requirements, the measurement range, precision and speed, that the business model requires will determine who is the first market leader. Then, the other groups will try to catch up with them with advanced concepts. By this series of market competition, we will be able to enjoy an opulent lifestyle with the bright future of LIDAR technologies in the next decade.

## Acknowledgements

This work was supported by the National Research Foundation of Korea (2020R1A2C210233813, 2021R1A4A1031660), KAIST UP program.



### 3. Ultrasound propagation imaging (UPI)

Chen Ciang Chia and Jung-Ryul Lee

Department of Aerospace Engineering, Korea Advanced Institute of Science and Technology (KAIST), 291 Daehak-ro, Yuseong-gu, Daejeon 34141, Republic of Korea

E-mail: chiacc@kaist.ac.kr and leejrr@kaist.ac.kr

#### Status

Since the magnetostriction excitation of elastic waves by James Prescott Joule in 1847 [27], ultrasound rapidly became a major modality for nondestructive testing and evaluation of aero-mechanical structures. Continuous use and adoption of thin-walled design for these safety-critical structures lead to active research of UPI of thin-walled structures using guided waves and bulk waves (see figure 4 and [28, 29] for differences). In the recent decade, we have witnessed the imaging of large (about 1 m<sup>2</sup> [30]) ROI at high speed (4 m<sup>2</sup> min<sup>-1</sup> [31] or higher with compressive sensing) due to the availability of galvanometric laser scanners. The great applicability of UPI is demonstrated by the successful visualization of all common flaw types associated with conventional materials and the hybrid use of new functional materials, including delamination and crushed honeycomb core. Research focus has also shifted from geometrically simple specimens, such as isotropic metallic plates, to *in-situ* inspection of full-scale structures, such as in-service airplanes and wind turbines. Aside from flaw visualization, UPI also has great potential for material evaluation and wave physics study. It is used in topological acoustics [32] to visualize wave propagation in metamaterials with a specific acoustic property, such as directionality [33]. Similar studies for ‘natural’ materials, i.e. materials without repetitive features like metamaterials, have also been validated using UPI, for example, for acoustic superlensing, trapping, and cloaking [34].

Despite significant advances, material degradation that does not have an abrupt material discontinuity, such as the weakening of interfacial adhesion [35], the onset of material fatigue [36], and incipient thermal degradation, remained an open problem for UPI. With the widespread use of UPI in research laboratories worldwide, improving the UPI for more industrial acceptance would logically be the next step. Potential targets include silicon wafers at one end of the physical scale, with aircraft, petrol-chemical tanks, and bridges at the other end. More focus could be directed toward large-scale structures because the micro/nanomanufacturing environment is laboratory-like. Along this line, for minimization of system footprint and flexibility of operation without any scanning scaffolding, an ideal UPI system should be an angular-scanning pump-probe system. With a bolder imagination, ultimately, it could be a mobile cobot-borne or airborne system equipped with a high-speed camera for ultrasound measurement. Diverse challenges originated from

different aspects of the UPI can be identified, and those related to hardware are addressed in the next section.

#### Current and future challenges

Currently, there are many variants of UPI, distinguishable according to the use of guided or bulk waves; angular, translation, or robotic scanning; and functionality for flaw detection, material evaluation, or wave study. Their common challenge is the limited SNR when measuring surface displacement (or velocity) from attenuative materials, such as thick composites and additively manufactured parts. Even with measurement averaging, getting a clear image for such materials above 10 mm thickness is often difficult. For Lamb waves-based UPI, frequency optimization is another challenge affecting both data acquisition and result processing. Theoretical or numerical analysis could be done if the material properties of the specimen are known; else, it becomes an educated-guessing process. Furthermore, when inspecting geometrically complex structures, it is difficult to effectively extract useful information from the complicated interferences of multimodal and dispersive Lamb waves. For angular-scanning UPI, large and complex three-dimensional (3D) imaging planes may suffer from pincushion distortion. In addition, if the measurement is performed by angular-scanning a laser Doppler vibrometer (LDV), the signal strength could be inconsistent or lost with increasing laser incident angles. Increasing the stand-off distance (SoD) could reduce the incident angle, but the advantage gained would be offset by the reduction of its numerical aperture (NA).

We envision that the UPI will advance according to the timeline given in figure 5 in the near future and will let us visualize flaws *and* distribution of material properties in large and complex structures by synchronously scanning both the pump and probe lasers using an angular scanner in an autonomous fashion. The above-stated challenges of SNR, image-plane distortion, and inconsistent LDV signal strength remain for this future UPI. Some of the challenges are even greater. To image material properties, the distortion of the scanner must be reduced, and a confocal state or a micron-scale displacement between the pump and probe laser focus must be maintained, at least within a few meters of SoD regardless of the angular displacement. To inspect 3D curved or multifaceted structures, keeping a normal incident angle for the lasers is critical. Even if the ultrasound were successfully measured, a subsequent challenge is to geometrically morph the imaging plane according to the specimen surfaces so that an intuitive interpretation of the result is possible. Ultimately, the UPI will be mobile cobot-borne or airborne by unmanned aerial vehicles. Foreseeable challenges include the miniaturization of system packaging suitable for deployment in the industrial environment, considering the confined space, extreme temperatures, vibration, dust, precipitation, etc. Measurement must also be completed at a photographic speed, perhaps without any time-consuming grid point scanning.

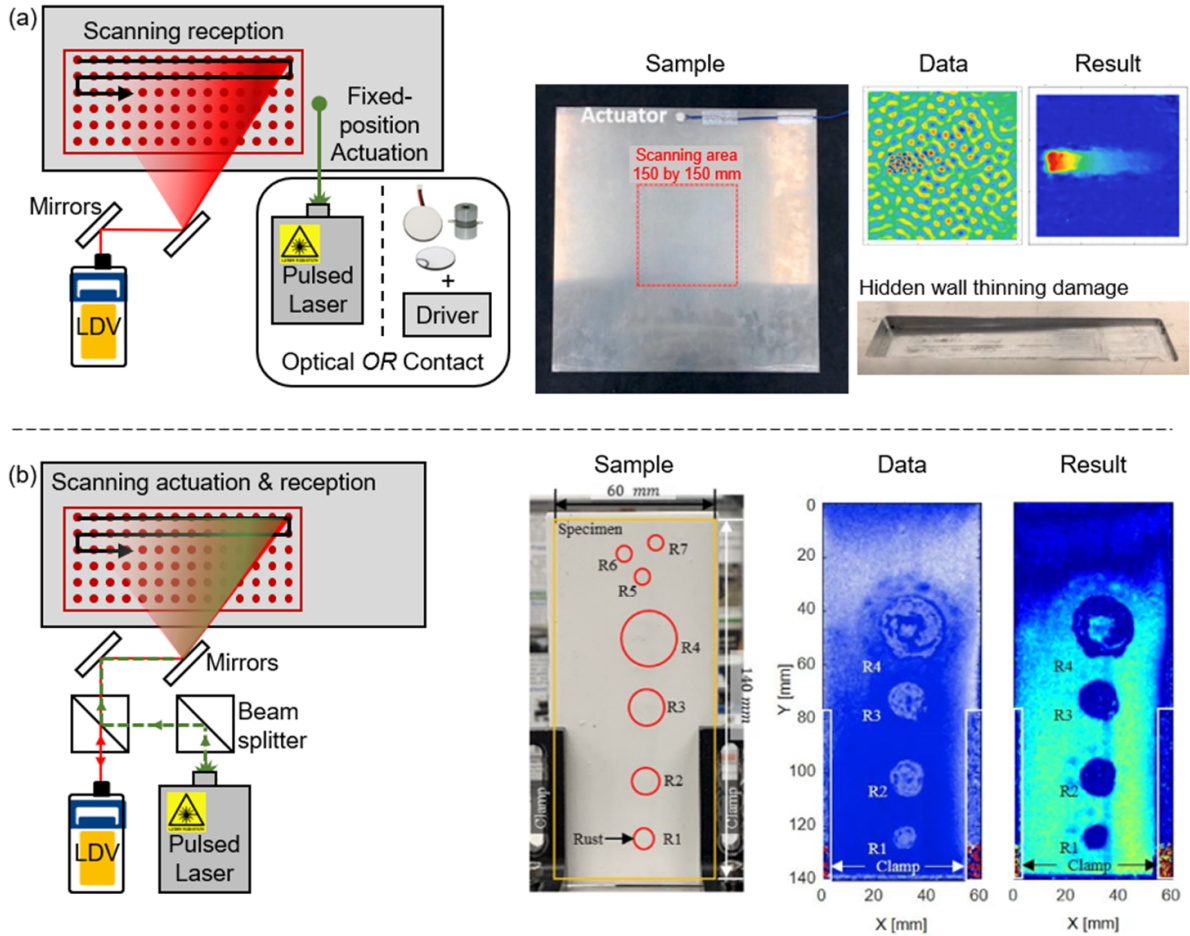


**Figure 4.** Measurement principle of ultrasound propagation imaging (UPI) using (a) guided waves and (b) bulk waves. Application (a) shows hidden wall thinning damages in an aluminum plate. Reproduced with permission from [37]. Application (b) shows hidden corrosions in a steel plate. Reproduced with permission from [38].

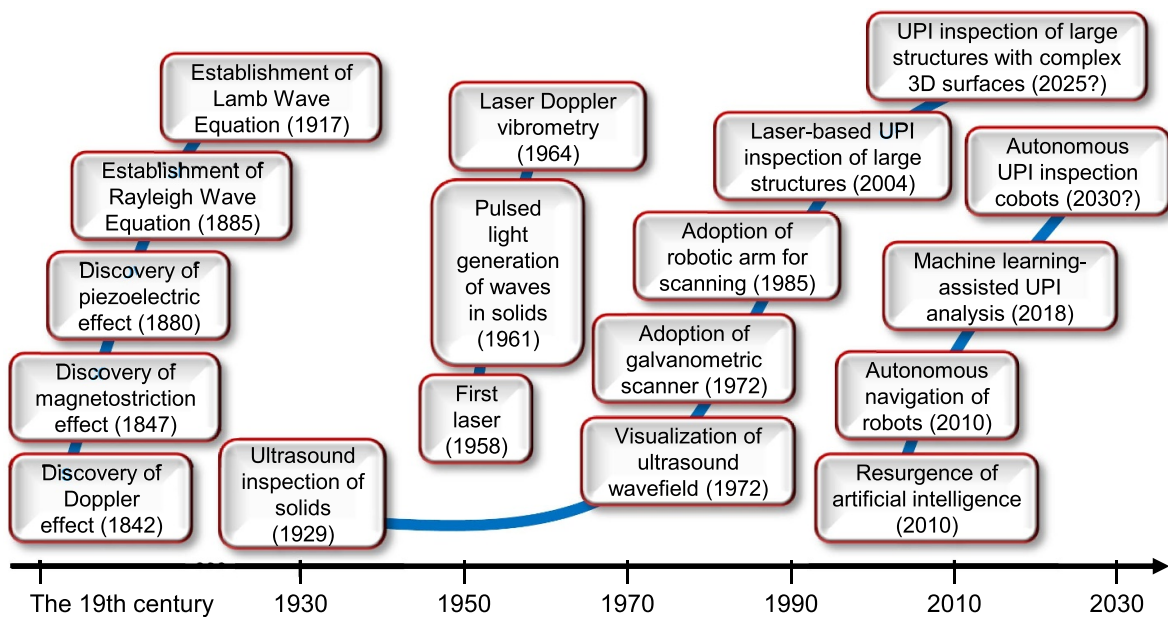


**Figure 5.** Roadmap of the key developments related to UPI in the past and in the near future.

## Advances in science and technology to meet challenges

Increment of SNR is currently performed using a continuous steady-state excitation [31] and optimizing the pump laser's spatial and/or temporal profiles [39]. These technologies come along with some limitations; thus, there is still a craving for better transducers. More research to improve SNR, for example, by fully exploiting existing or new functional materials [40] or by developing a laser with an arbitrarily tunable wavelength for optimum depth penetration in specimens [41], is very much welcomed. For frequency optimization without material information, spectroscopy imaging could be done during result processing, provided that the ultrasound is measured using a broadband transducer. Otherwise, with appropriate material information, it is good to optimize the imaging frequency at a narrow band. Perhaps better still, at one selected ultrasound mode [42–44], for easier image processing. Note that the frequency linearity of the transducer and related equipment is important because the sensitivity of UPI could be increased for material evaluation through non-linear ultrasound [45], similar to that used in [36] for fatigue evaluation.

Distortion of the imaging plane due to large angular displacement in the scanner can be corrected through better control [46]. Distortion caused by 3D specimen surfaces must be corrected using depth-of-field information, which could be measured using a depth sensor such as LIDAR or surface profiler. It appears that inconsistent or loss of signal at large laser incident angles will remain the biggest challenge. Before a solution emerges, it is necessary to demarcate the 3D surfaces into multiple smaller ROIs according to the limitation of laser incident angle and then perform imaging for each ROI after matching the normal angle of the imaging plane with that of the ROI. An algorithm is needed to collect the results from all ROIs and 'stitch' them into the final result. Considering a large number of ROI for large 3D structures, delegating the laborious imaging works to a mobile cobot-borne or airborne

UPI must be considered. To realize this, we need to at least miniaturize the system components, such as the LDV [47] and pump laser. High-precision position and attitude reference system must be established so that the UPI platform has sufficient environmental awareness to perform ROI demarcation and subsequent imaging. For the reduction of imaging time, a multi-sensing-points LDV [48] or a high-speed camera [33, 49] could be used to measure the ultrasound wavefield, but the sampling/frame rate, spatial resolution, sensitivity, and vibration immunity [50] must be significantly improved.

## Concluding remarks

The UPI is perhaps the most powerful ultrasonic imaging tool available for flaws visualization and material evaluation of plate-like specimens in the laboratory. The main challenges to getting the UPI into the field for imaging of large-scale thick-walled 3D structures are identified, i.e. the increment of measurement SNR, frequency linearity of the measurement system, and mode selectivity of transducers. But, perhaps, the game-changing technology is the realization of remote ultrasound measurement at large incident angles or wireless ultrasonic propagation sensing. These advancements, together with the growth in related fields, including robotics, signal processing, and DL, would prime the evolution of next-generation autonomous UPI.

## Acknowledgements

This research was supported by the Brain Pool program funded by the Ministry of Science and ICT through the National Research Foundation of Korea (2021H1D3A2A01100011) and by Defense Acquisition Program Administration and the Agency for Defense Development of the Republic of Korea under Grant No. 99-402-805-032 (The integration of wireless sensing into aerial vehicles for structural damage identification).

#### 4. Luminescence imaging

Teow Wee Teo<sup>1</sup>, Zeinab Mahdavi<sup>1</sup>, Azizi Abdullah<sup>3</sup>, Bee Ee Khoo<sup>2</sup> and Mohd Zaid Abdullah<sup>2</sup>

<sup>1</sup> TT Vision Technologies Sdn. Bhd., Plot 106, Hilir Sungai Keluang 5, Bayan Lepas Industrial Zone, Phase 4, Penang 11900, Malaysia

<sup>2</sup> School of Electrical and Electronics Engineering, Engineering Campus, Universiti Sains Malaysia, 14300 Nibong Tebal, Penang, Malaysia

<sup>3</sup> Faculty of Information Sciences and Technology, Universiti Kebangsaan Malaysia, 43600 Bangi Selangor, Malaysia

E-mail: twteo@ttvision-tech.com, zeinab@ttvision-tech.com, azizia@ukm.edu.my, beekhoo@usm.my and mza@usm.my

#### Status

One key challenge encountered in the PV (photovoltaic) industry is the removal of defective crystalline Silicon solar cells before they are assembled to become PV modules. Among different types of defects, micro-crack is one of the most common defects which occurs during the various stages of manufacturing. The trend of manufacturing thinner Silicon wafers makes PV cells vulnerable to micro-cracks. This type of defect is typically invisible to naked eyes and therefore require specialized tools to enable detection. The optical transmission (OT) method [51] is one of the popular instruments used in visual inspection of PV modules, particularly during the bare Silicon wafer manufacturing stage. However, the new diamond-wire slicing technology [52, 53] leaves saw marks that can camouflage micro-cracks, thus reducing the effectiveness of OT. Emerging technique such as the transflection (TF) system [54] are a very promising since this method is less vulnerable to interference caused by these saw marks. Another two popular methods, especially for downstream segments of PV manufacturing, are the photoluminescence (PL) [55] and the electroluminescence (EL) [56] imaging techniques. In addition to micro-cracks, these technologies can also be used to detect other types of defects such as dark regions, finger interruptions, stains, scratches, etc. Important components of OT, EL, PL and TF are shown schematically in figures 6(a)–(d) (i) respectively. A good perspective overview of these imaging technologies is published elsewhere [57]. Meanwhile figures (a)–(d) (ii) show examples of images captured by OT, EL, PL and TF techniques respectively. Close examination of these figures revealed that images produced by TL and EL are visually very complex and relatively noisy. This is most prevalent for polycrystalline cells where different crystals produce luminescence of different intensity [58, 59]. This is the main drawback of TL and EL techniques. Hence, these technologies require a very sophisticated algorithm for image analysis and data automation [57]. For this reason, TF offers a good alternative solution as this modality is not influenced by the different crystalline structure. Unlike EL

and PL, unfortunately, TF is sensitive to micro-cracks only. Hence, EL and PL remain popular with PV manufacturers as these technologies can map micro-crack and other types of manufacturing defects. Nevertheless, the difficulty in interpreting EL and PL images remains an issue, and this field, constitutes an active area of research. One recent development is the application of AI and DL such as the convolution neural network (NN) [60]. The use of AI-driven software can help enhance decision making and refine predictive analytics which are essential for efficient and accurate image interpretation.

#### Current and future challenges

To-date there is no single ideal modality which is suitable for inspecting PV modules in manufacturing-based environment. Though OT, EL, PL and TF provide valuable information about solar cells or silicon wafers, however, these imaging technologies are largely complementary. This means that they have their own characteristics, strengths and weaknesses. Trends in the future may lead to the development of a hybrid inspection system, with a combination of different types of luminescence modalities. In the case of micro-crack, TF is very promising since this modality produces clean and less noisy images. In contrary PL offers a good solution for other types of defects since this technology has speed advantage compared to OT or EL. Therefore the fusion between TF and PL has many advantages compared to the fusion of other modalities. The development of line-scan PL imaging system is prerequisite as most currently deployed PL systems are based on area scan. While line-scan PL imaging for solar cells currently exists [61, 62], it would be significantly more challenging for Silicon wafers as PL emission is significantly less intense. This poses a speed limitation especially for on-the-fly inspection as much longer exposure time is required to compensate for the weak PL signal. For a hybrid TF and PL to work harmoniously, speed is very crucial factor to be considered and these modalities have to share the same inspection station or space in the manufacturing line. While it may be possible to use a single camera for both TF and PL, both techniques require very different illumination set-up. In this case TF requires light source with wavelength longer than 1200 nm. In contrast PL operates at much shorter wavelength, preferably less than 950 nm in order to avoid interference caused by Silicon emission which peaks at around 1040 nm. Currently, the design of such a system is active under development.

#### Advances in science and technology to meet challenges

The availability of highly sensitive sensors in the near infrared (NIR) range such the indium gallium arsenide (InGaAs) cameras could potentially enable high-speed acquisition of PL and TF emissions. However, the limitations on resolution and cost

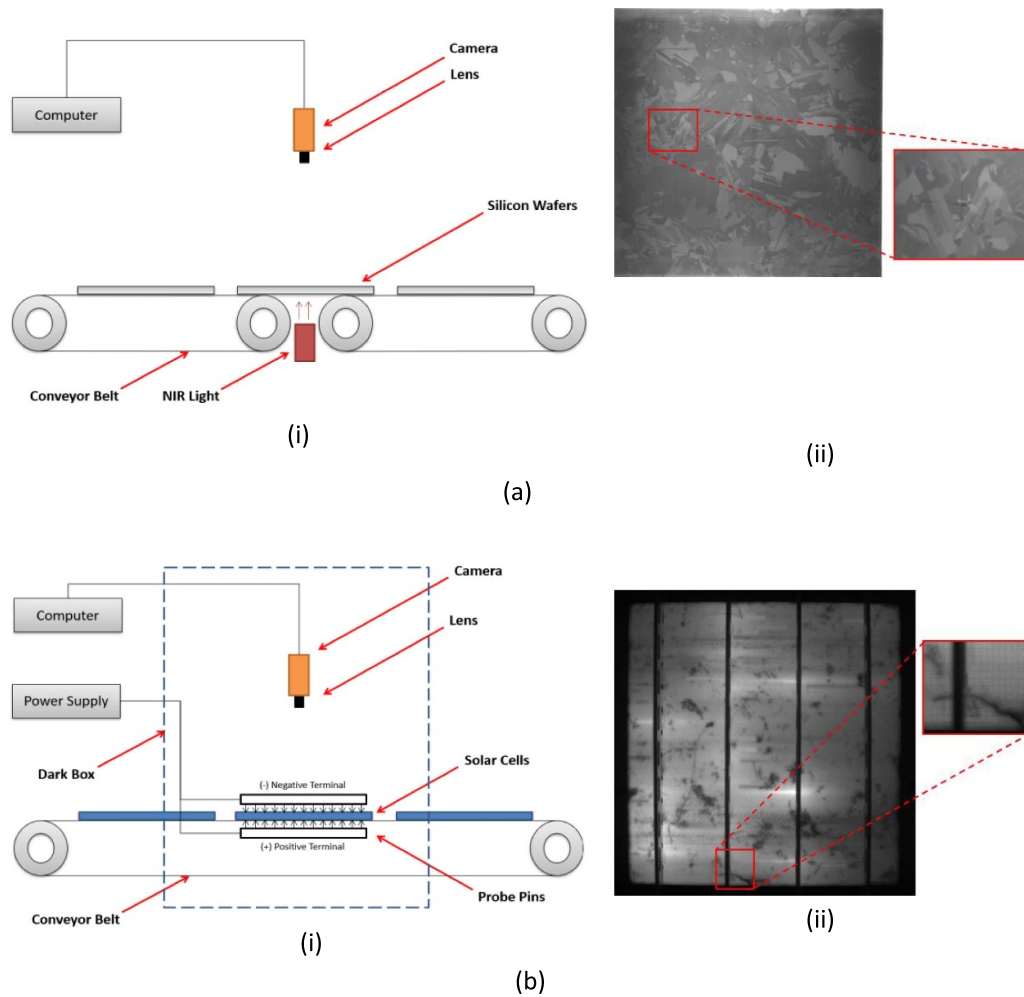


**Figure 6.** The schematics of (a) the optical transmission, (b) the electroluminescence, (c) the photoluminescence and (d) the transflection methods. Important components are shown in (i) while (ii) shows one example of luminescence image produced by each imaging set-up. The square box in each image depicts the area containing defect, in this case a micro-crack defect. Reproduced from [59]. © IOP Publishing Ltd. All rights reserved.

factor of such cameras are hindrance to large scale installation. In future it is envisioned that the high resolution but cheaper NIR sensor would be available commercially as many major camera producers are actively investing and working to mass produce such a device. This would speed-up the deployment of PV inspection system integrating TF and PL modalities. Despite the positive outlook, the challenge of processing PL images remains, especially with polycrystalline solar cells. While micro-cracks can be dealt effectively with TF, other artifacts may not appear distinctively since they are camouflaged by complex polycrystalline structures. Polycrystalline solar cell image is inherently more complex to process since it contains many interfering artifacts such as the crystalline patterns, the dislocation clusters, etc. Recent development in AI, in particular the DL framework, has a potential in solving this complicated image processing problem as results from current research in this area suggest. For instance, Rahman and Chen [63] designed a multi-attention U-Net for classification of polycrystalline solar cells. Using a five-fold

cross-validation technique, these authors reported an accuracy of 99.1% when distinguishing good from defective cells. In another study, Wang *et al* [64] developed a hybrid NN-based defect detection model that combines the advantages of ResNet152 and Xception networks. An accuracy of 96.2% was reported by these authors when solving a binary classification problem. Nevertheless, the performance of the algorithm dropped slightly to 92.1% when multiclass classification problem was attempted. More recently Binomairah *et al* [65] compared the performance of various convolution neural network (CNN) algorithms based on the you only look once framework (YOLO). The algorithm was designed to inspect several types of defects in monocrystalline cells. Results from this study suggest that the heavy-weighted YOLO is the best performing algorithm, resulting in accuracy of 98.8%. Nevertheless, this algorithm is relatively slow since it recorded a runtime of approximately 62.9 ms. In contrast the tiny-weighted YOLO with spatial pyramid pooling for improved ML resulted in accuracy of 91.0% and runtime of 28.2 ms. Hence a trade-off

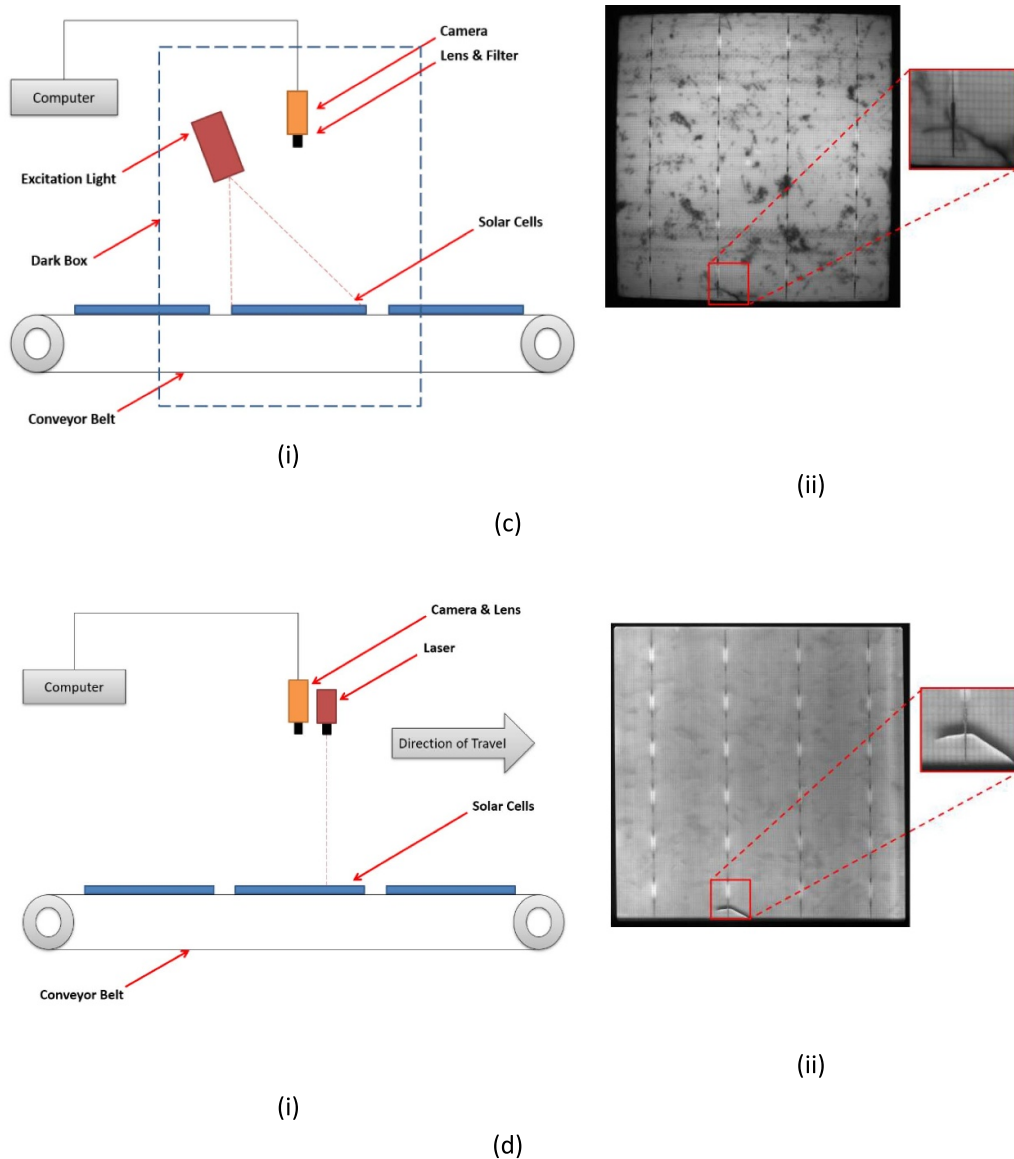


Figure 6. (Continued.)

between speed and accuracy is essential to in-order to arrive with acceptable solutions. Results from this research and other studies suggest the potential in applying AI with DL capabilities in solving complex EL or PL images. The combined improvements in the image acquisition systems and software would inherently yield much improved inspection accuracies. Even though polycrystalline is less efficient than monocrystalline, however, the former is relatively cheaper to produce compared to the latter. In future, it is predicted that the monocrystalline, particularly the passivated emitter rear cell solar cells, would be a dominant Silicon used in assembling PV modules, possibly reaching more than 95% of the total PV production worldwide [61]. As this trend continues, the challenges associated with processing polycrystalline solar cells diminish as more manufacturers shift to producing monocrystalline cells. Hence, the CNN driven solutions in the future would be targeting monocrystalline instead of polycrystalline Silicon wafers and solar cells.

### Concluding remarks

In summary the primary modalities used for luminescence imaging of Silicon wafers and PV cells include EL, PL and very recently TF. Each of these modalities has technical advantages and disadvantages. PL has slightly better merit compared to EL since the latter enables a fully contactless-based inspection and rapid in-line instrumentation. However, both modalities produce complex images which constitutes their main drawback. In contrast TF produces much cleaner image with less noise. However, this technology is suitable for inspecting mechanically induced fractures especially micro-cracks. This is the principal weakness with this imaging modality. In future such an inspection is best conducted by the combination of different luminescence modalities or a hybrid system. In this regard the integration between PL and TF offers distinct advantages over other available luminescence modalities. Advances in AI

and DL together with hardware breakthrough further fuelled this interest, enabling high-throughput and high-resolution image capturing at unprecedented performance and speed. For this reason, many leading PV processors continue to escalate their investment and support for AI for different applications.

### **Acknowledgements**

The authors acknowledge TT Vision Technologies Sdn. Bhd. for funding this research (304.PELECT.6050420.T148) and matching grant from Universiti Sains Malaysia (1001.PELECT.8070009).

## 5. Endoscopy

*Dimitris K Iakovidis and Panagiotis Vartholomeos*

Department of Computer Science and Biomedical Informatics,  
University of Thessaly, Papasiopoulou 2-4, Lamia, Greece

E-mail: diakovidis@uth.gr and pvartholomeos@uth.gr

### Status

Endoscopy is a primarily optical imaging technique for screening internal structures of the human body. It appeared in the early 1800s, and since then, it is preferred because it enables direct visual examination of tissues, and minimally invasive interventions. Today, the application of endoscopy spans various systems of the human body, including the digestive, the respiratory, the cardiopulmonary, the urinary, the reproductive, and the musculoskeletal system. Also, it can be complemented by emerging imaging technologies offering enhanced information about the examined tissues, in terms of detail and/or tissue composition. These include optical coherence tomography, near-infrared fluorescence imaging, confocal laser endomicroscopy, endocytoscopy, and multispectral/hyperspectral imaging technologies [66, 67].

The endoscopic devices are evolving towards an improved trade-off between the size of the endoscope and image fidelity, enhanced safety, less invasiveness, and convenience for both the patients and their operators. Rigid endoscopes (REs) and flexible endoscopes (FEs) have a sufficiently large tip to accommodate high-resolution image sensors, e.g. the diameter of a standard colonoscope is  $\sim 13$  mm [68]. Ultrathin FEs enable transnasal esophagogastroduodenoscopy and bronchoscopy, with a very small diameter ( $\sim 3$ – $5$  mm). Such FEs are typically based on bundles of optical fibers for image and light transmission. High-resolution images can be obtained by miniature FEs with diameters that can reach up to sub-millimeter level, by using a single fiber and a scanning laser light [69]. Wireless capsule endoscopes (WCEs) appeared in the early 2000s. They are swallowable alternatives for the examination of the gastrointestinal (GI) tract, with a size of a large vitamin pill. Most of them have a length of 24–27.9 mm, a diameter of 10.8–13 mm, and a wide field of view ranging between  $140^\circ$  and  $170^\circ$ . The image resolution of such endoscopes is limited, not only by the size of the sensor, but also by their energy requirements, e.g. for wireless image transmission. Various miniature robotic endoscopic systems coping with the lack of navigation, biopsy, and targeted drug delivery of the conventional WCE devices, have been proposed [68, 70]. Robotic mechanisms have already been integrated into commercially available RE/FE solutions, mainly offering enhanced precision and convenience with respect to motion control and navigation [68, 71]. Virtual endoscopy (VE), performed by 3D reconstruction of the internal body structures from computed tomography (CT) images, offers non-invasive screening; however, although there are studies indicating that VE can provide a comparable sensitivity with optical endoscopy for lesion detection, it involves radiation exposure, and unlike

optical endoscopy alternatives, it does not allow neither biopsy nor surgical interventions [72]. AI provides tools for clinical decision support (CDS) by detection/recognition of findings, and *in vivo* visual measurements [73]. Virtual/augmented reality (VR/AR) offers immersive visualizations that can contribute to easier endoscope navigation, lesion recognition, and clinical training [74].

### Current and future challenges

The miniaturization of the endoscopes to have millimeter or even sub-millimeter diameters, while maintaining an imaging fidelity sufficient for diagnostic purposes, is still one of the major challenges. Miniaturization does not refer only to the imaging sensors, but also to the tools required for endoscopic interventions, as well as the design of the robotic systems to support safe endoscopic procedures. Despite increasing interest in minimally invasive surgical techniques and related developments in FEs and catheters, follow-the-leader motion remains elusive [76]. Following the path of least resistance through a tortuous environment requires the control of many degrees of freedom. This typically results in large-diameter instruments. Furthermore, the capability of miniaturized FEs to apply sufficient lateral forces is currently limited by the low stiffness of the mechanical structure. This is a critical challenge, which when solved will enable effective physical interaction between the endoscope tool and the tissue, and it paves the way for conducting a broad range of interventional procedures. Advancements in this direction open perspectives for less invasive screening procedures and interventions, as well as navigating in narrow anatomical regions, such as those encountered in nasal, urological, and endovascular interventions for repairing vascular-related abnormalities.

WCE offers a model paradigm of applied innovation in GI endoscopy. However, there are still a lot of challenges with respect to enhancing WCE with capabilities such as controlled navigation, biopsy sampling, and targeted drug delivery. These capabilities require actuation mechanisms, e.g. mechanisms to manipulate forceps and needles, which are demanding in terms of energy. Research towards the development of energy-efficient WCEs (figure 7), could pave the way for next-generation robotic capsules with autonomy to perform diagnostic and therapeutic interventions. Although a lot of WCE designs have been proposed, timely traversing the pathway from a theoretical design to the market is by itself another challenge.

Image enhancement and visualization techniques can address limitations of the imaging hardware. Image super-resolution (ISR) reconstruction techniques can be used to address the ill-posed inverse problem of converting a given low-resolution image with coarse details to a corresponding high-resolution image with better visual quality and refined details [77]. Also, the 2D images of a monocular endoscope can be used to create enhanced 3D visualizations, which may contribute to improved diagnostic yield, e.g. by reducing abnormality miss rates through 3D reconstruction and panoramic visualization, in combination with VR/AR devices. The



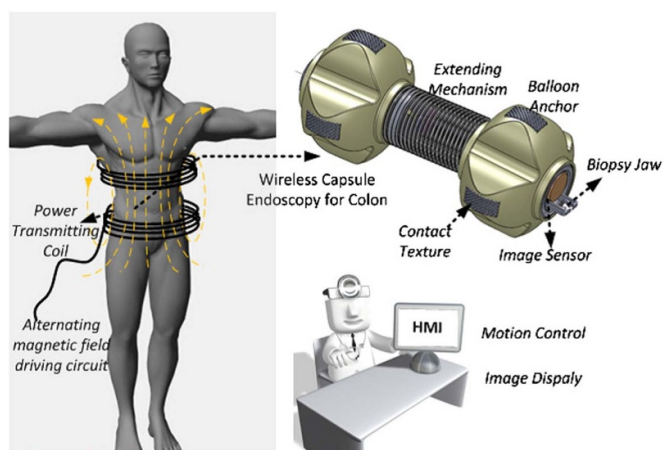


**Figure 7.** Design concept of a wirelessly powered WCE for colonoscopy. Reproduced from [75]. © IOP Publishing Ltd. All rights reserved.

visualizations can be improved by fusing information from different endoscopic modalities, e.g. optical endoscopy and CT colonography [78]. Enhanced visualizations can also be considered in conjunction with VE and AI methods inferring missing information, e.g. the prediction of tissues appearance from the CT images. Coping with the drawbacks of CT imaging for VE, the improvement of magnetic resonance (MR)-based is a promising alternative; however, cost-efficiency issues should be considered.

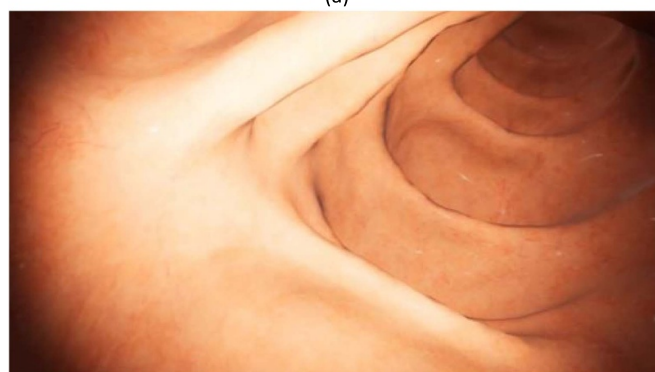
AI-based CDS in endoscopy faces two main challenges: data availability and system interpretability/explainability. DL methods have significantly progressed during the last decade; however, their performance is limited by the limited availability of sufficiently large and diverse annotated datasets. Such datasets have slowly started becoming available mainly in the context of GI endoscopy and laparoscopy [79–81]; however, the availability of appropriate datasets for other endoscopic modalities remains a gap. Interpretability indicates the degree to which a human can understand the cause of a system's decision [82], and it can effectively contribute in earning clinicians' trust.

### Advances in science and technology to meet challenges

The miniaturization and the energy efficiency requirements can be addressed by considering novel bio-inspired designs. Nature has a lot of successful paradigms to offer, that can act as a source of inspiration for the development of novel imaging sensors and actuators [83]. The advantages of soft robotics in biomedicine are increasingly becoming evident, offering enhanced safety, adaptability, and flexibility [84]. First steps towards this direction indicate the feasibility and the potentials of their application, both in FE and WCE [68, 70]. Further advances should be considered with respect to (a) the materials used, aiming to achieve improved interaction of the soft robotic components with mucosal surfaces; (b) the robot locomotion, which should ensure stability for both imaging and



(a)



(b)

**Figure 8.** Digital twin of the GI tract for medical device testing, being developed by our research group. (a) Multiphysics model for *in silico* testing of a WCE device. (b) Appearance model showing a respective camera-view of the digital twin GI tract from the virtual WCE device.

surgical interventions, while maintaining energy efficiency; (c) the variable stiffness of the FE structure, and the actuation mechanisms employed for distal force transmission. A promising technology for achieving atraumatic follow-the-leader endoscope motion and solving the force transmission limitations is magnetic guidance and control of the FE structure and tip [76, 85]. To speed up the traditionally long translation times from research to market, multiphysics, digital-twin platforms of human organs, such as the GI tract, are under investigation for endoscopic device testing and *in-silico* clinical trials within a realistic simulation environment [86] (figure 8). Regulatory bodies responsible for the approval of medical devices, such as the US Food and Drug Administration, are becoming increasingly supportive of such platforms.

Today, AI is an integral part of most state-of-the-art image processing methods for ISR, and CDS systems. Considering the limited availability of endoscopic training data for supervised DL algorithms, research should focus on algorithms with fewer training requirements, such as weakly supervised, self-supervised and zero-shot learning techniques [70, 77], as well as physics-informed approaches, considering the image acquisition physics, and the characteristics of the endoscopic images under investigation. Fuzzy set theory is a promising direction towards interpretable CDS systems that needs further investigation, since it offers a sound mathematical framework for linguistic representation of numerical data under

uncertainty [87]. Uncertainty is inherent in real-world data, e.g. due to measurement errors, the diversity of the structures being measured, and the subjectivity of expert opinions being considered for the development of a CDS system. Establishing uncertainty estimates in measurement outputs enable a confidence level approximation that can be decisive for clinical decision making and user trust.

DL is also promising for the development of methods inferring image contents across modalities. Visual measurement methods need to be further investigated, since they can contribute to *in vivo* assessment of useful parameters, such as the size of abnormal findings during endoscopy, image depth, and the distance travelled by the endoscope [73]. Depth assessment is also useful for the implementation of the 2D to 3D image transformation required for immersive VR/AR visualizations. Pre-operative 3D models of anatomical structures under investigation can be enhanced using intra-operatively collected imaging data, and application of rendering techniques; thus, offering complementary information with respect to realistic appearance of the examined tissues.

### Concluding remarks

The technologies related to endoscopy span various disciplines, including optics, instrumentation and measurement, mechanical engineering, image processing and computer vision, AI, and robotics. This paper highlighted research

challenges and future directions considering the multidisciplinary nature of the domain, which has a high socioeconomic impact, considering that early detection of diseases, such as cancer, can improve lifespan and reduce healthcare expenditure. AI-based image processing and CDS applications can enhance the diagnostic yield of endoscopy and increase clinicians' productivity by being able to examine more patients in less time. Therefore, meeting the related challenges identified in this paper, within the next decade, should be prioritized. The evolution in imaging sensors and robotics, which include hardware aspects, is also important; however, considering the current advancements and the steps to follow, a milestone for the next 20 years is to increase the level of autonomy of the endoscopes, which also necessitates the standardization of medical, legal, and ethical concerns. Advancements in miniaturization, force transmission, precision and motion dexterity could offer miniature flexible robotic endoscopes for performing interventions in the central nervous system.

This paper focused on endoscopy, addressing the biomedical domain. However, endoscopy can have impactful industrial applications as well, and most of the identified challenges are also applicable to borescopes for non-destructive testing, e.g. inspection of airplane engines [88] and industrial pipes [89]. Also, the advances in endoscopy can have impact in the evolution of imaging systems used in other domains, e.g. energy-efficient miniature camera-enabled robots with increased autonomy for inspection and exploration [88, 90].

## 6. Confocal microscopy

Hongki Yoo

Department of Mechanical Engineering, Korea Advanced Institute of Science and Technology (KAIST), 291 Daehak-ro, Yuseong-gu, Daejeon 34141, Republic of Korea

E-mail: h.yoo@kaist.ac.kr

### Status

Confocal reflectance microscopy (CRM) is an optical imaging technique that provides high-speed three-dimensional (3D) surface profiling of objects [91]. It provides highly accurate 3D images with a lateral resolution of less than 200 nm and a depth resolution of less than 10 nm [92]. In particular, its ability to measure both large areas quickly and small features accurately in a non-destructive manner makes CRM a valuable tool in many industries. This makes it ideal for applications such as surface topography analysis and high-throughput metrology in industrial manufacturing applications including semiconductors and displays.

The working principle behind CRM involves the use of a laser beam that is focused onto a focal point on the sample surface [93]. The reflected light is then detected by a photodetector through a confocal pinhole aperture. Since the confocal pinhole removes out-of-focus light, it only detects light coming from the focal point. Therefore, it is easy to find the surface of a sample, which exhibits strong intensity. By accumulating these data points into a 3D volume, highly detailed 3D images can be generated. The intensity profile along the depth is called the axial response curve, and the peak position of the axial response curve is the surface position of the sample.

CRM has several advantages over conventional optical microscopy or other types of 3D metrology [94]. Most importantly, CRM produces 3D images, whereas optical microscopy only provides magnified two-dimensional (2D) images without precise depth information [95]. Another major advantage is the non-destructive acquisition of the 3D surface profile of a sample without or with minimal sample preparation, whereas other types of 3D measurement techniques, such as electron microscopy, atomic force microscopy and stylus, require extensive sample preparation or unavoidable sample damage [96]. In addition, CRM works on different types of surfaces as long as the light is either reflected or back-scattered from the surface.

The lateral resolution of CRM is determined by the NA of the objective lens and the wavelength of light because the spot size is limited by diffraction [97]. Lateral resolution of less than 200 nm can be achieved by using short-wavelength light, i.e. blue or violet, and high-NA objectives. The axial resolution essential for depth profiling, which is determined by the objective lens and wavelength, is highly dependent on the depth profiling algorithm and surface reflectance. Typically, the axial resolution can be on the order of nanometers when measuring flat surfaces with an objective lens with an NA

of 0.95 and a light source with a wavelength of 405 nm. In addition, a hybrid confocal technique combined with interferometry can be employed to achieve a robust and improved vertical resolution [98].

The surface profiling speed of CRM is quite fast, offering the capability to generate over 1 volume per second, each accompanied by a height map of  $1024 \times 1024$ , depending on the measurement parameters [92]. However, the field of view is very small because of the use of high-magnification lenses and the need for 3D volume data acquisition. Additionally, obtaining high-precision surface profiling requires a large number of image stacks, which inevitably increases measurement time.

While the measurement speed is considered relatively fast compared to other 3D surface profiling techniques, much higher speeds are always needed, especially in manufacturing processes where in-line total inspection is required. Therefore, technology development to achieve faster 3D measurements continues as optical and electronical technologies advance and new ideas are developed.

### Current and future challenges

As the axial and lateral resolutions of CRMs are considered to be physically limited by diffraction, not much effort has been made to improve resolutions, unlike their fluorescent counter-parts, where several super-resolution techniques have been successfully implemented [100]. Instead, many advances have been made to improve imaging speed, especially by applying various scanning methods. Typically, laser beam scanning using fast- and slow-axis scanners combined with depth scanning has been used to cover 3D volumes. Galvano-scanning mirrors, resonant-scanning mirrors, polygon mirrors, and acousto-optic deflectors can also be used as fast-axis scanners, and provide scan rates up to tens of kHz. Because of the fast scanning unit, real-time 2D confocal images can currently be acquired. Figure 9 shows the different scanning methods used in CRM.

However, precise 3D surface profiling requires 2D confocal image stacks consisting of tens to hundreds of frames, which make 3D imaging time consuming. Acquiring multiple confocal points instead of a single point is one way to speed up imaging. For example, using a rotating Nipkow disk can potentially increase the pixel acquisition rate, which is limited only by the acquisition rate of 2D image sensors such as CMOS and CCD [101]. Another solution would be to use line beams instead of points [102]. In this case, the acquisition rate of the linear detector can be the limiting factor. Although these methods can improve the 2D imaging speed, mechanical focus scanning to acquire 2D image stacks with different depths will also affect the 3D surface acquisition speed. Depth scanning is usually performed by mechanical scanning of the objective lens, using a precise stage such as high resolution piezo stages. There are faster alternatives such as deformable mirrors, micro-mirror array lens, and electrically tunable lens, but stacking multiple 2D images is still a limiting factor for speed [103]. Therefore, the speed limit can be overcome by using

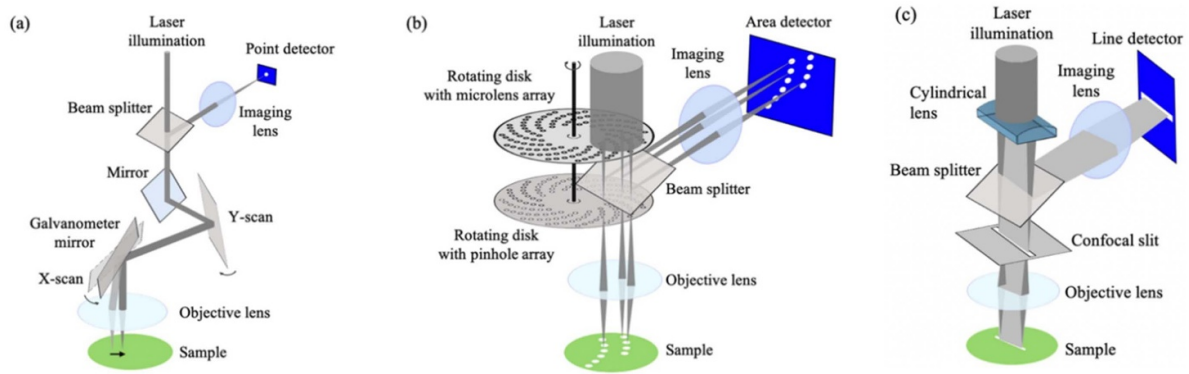


**Figure 9.** Confocal reflectance microscopy scanning methods. (a) Beam scanning with two scanning mirrors. (b) Multi-beam scanning using rotating Nipkow disk. (c) Line scanning using a slit and linear detector. Reproduced from [99]. © IOP Publishing Ltd. All rights reserved.

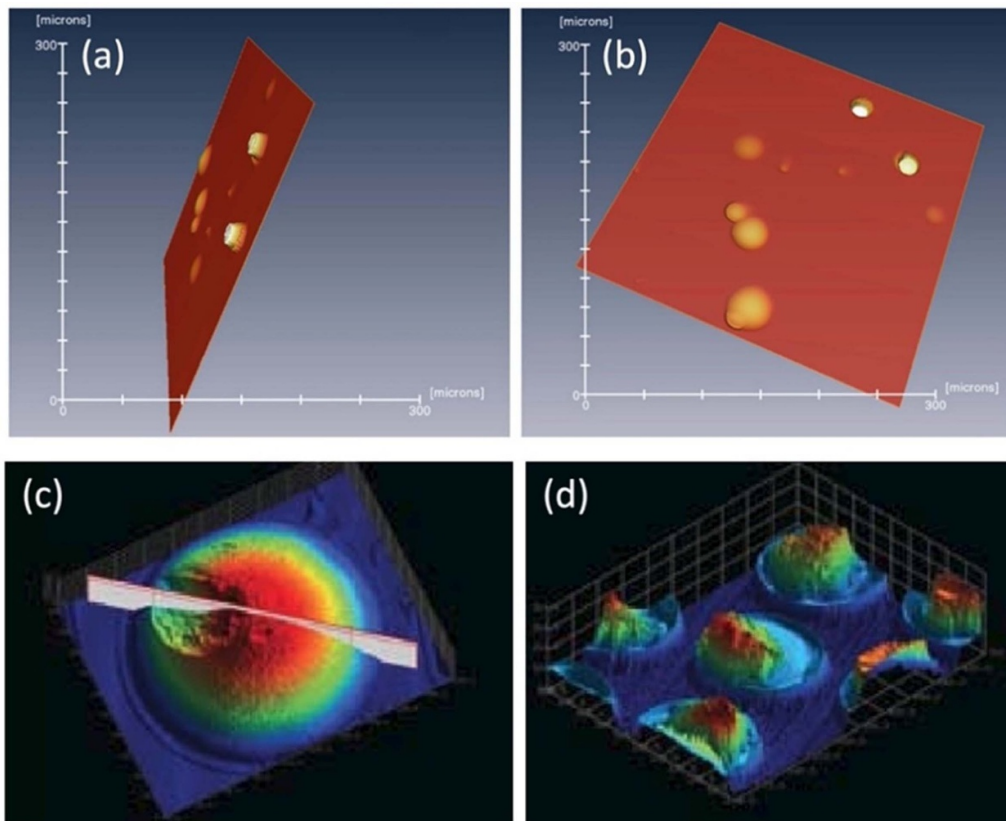


**Figure 10.** Examples of 3D surface images taken by confocal reflectance microscopy. (a) Side view and (b) top view of the detector surface. Reproduced with permission from [111]. (c) Bump. (d) Diamond. Reproduced with permission from [112].

depth scanning techniques without mechanically changing the focal depth.

**Advances in science and technology to meet challenges**

While confocal microscopy acquires information one point at a time, if we create multiple foci along the depth direction, depth information can be acquired without mechanical depth scanning. One clever way to accomplish this is to utilize the

chromatic focal shift of a broadband light source [104]. Instead of using a monochromatic light source, a broadband light source and axial chromatic aberration can create a rainbow-like pencil beam at the focal point. As it covers a specific depth range, the axial response curve is simultaneously acquired by the spectrometer [105]. Therefore, the surface height is determined immediately without any mechanical depth scanning. In this case, the speed of depth profiling is limited by the speed of the spectrometer used to detect color information from the chromatic focal beam. Spectrometers are basically array detectors made up of thousands of pixels, so their readout

rate is much slower than point detectors such as PMTs and PDs. As a result, chromatic confocal microscopy is not significantly faster than general confocal microscopy, even if the mechanical depth scanning is eliminated.

In fact, colors containing depth information can be determined without using a spectrometer. For example, our eyes only have three different types of cones to perceive all natural colors. Likewise, only two photo-multiplier tubes can be used to determine the color of the light returned through a confocal pinhole, which corresponds to the surface height [106]. This allows height acquisition rates that are over 1000 times faster.

Other methods have been recently reported which acquire depth information using only a few detectors, such as differential confocal microscopy (DCM) and dual detection confocal microscopy (DDCM). DCM uses axially shifted axial response curves from two pinhole detectors with different focal positions to acquire the height information without depth scanning [107]. DDCM uses two confocal detectors of different sizes [108]. Surface height can be directly measured by calculating the intensity ratio between the two confocal detectors. Using multiple pinhole detectors at different focal positions can be another way to increase imaging range without mechanical axial scanning [109]. In addition, the recently introduced 3D volumetric imaging technique in the field of biomedical optics can also be employed for high-speed surface profiling [110].

## Concluding remarks

CRM, often regarded as the gold standard for non-invasive precision surface profiling, is widely used in research and industry. As the demand for faster acquisition rates increases, great efforts have been made to improve imaging speeds. This has made CRM increasingly efficient and reliable in industrial inspection applications and it will continue to be an important tool for quality control in production processes (figures 10).

With the introduction of faster and more sensitive high-speed detectors, images can now be captured in a fraction of the time that was previously required. Recent advances in DL technology allow the three-dimensional surface topography of a sample to be estimated with a reduced amount of data, which will also speed up imaging. In addition, the enhanced computational power allows the use of sophisticated image processing algorithms in real-time. Furthermore, novel light sources and detectors offer distinct opportunities for accelerating the measurement speed. Due to the unique advantages of confocal surface profilers, including precise microscopic three-dimensional surface measurements, they will continue to evolve to meet industrial measurement needs.

## Acknowledgements

This work was supported by the National Research Foundation of Korea (NRF-2020R1A2C3006745 & RS-2023-00208888).

## 7. Atomic force microscopy

Andrew Yacoot

National Physical Laboratory, Hampton Road, Teddington, Middlesex TW11 0LW, United Kingdom

E-mail: andrew.yacoot@npl.co.uk

### Status

The invention of the atomic force microscope (AFM) in 1986 [113] closely followed the invention of the scanning tunneling microscope (STM). Both opened the nanoscale world enabling imaging of surfaces at the nanoscale and opening the area of nanoscale science and technology. These microscopes have transformed from the initial homemade instruments into sophisticated commercial instruments found in virtually every laboratory concerned with nanoscale science and technology. An AFM, unlike an STM, can image either conductive or nonconductive samples as well as very soft (biological) structures. The basic principle of operation of an AFM is shown in figures 11 and 12 shows an AFM image of a silicon amphitheater structure that can be used for calibration of the AFM's vertical axis. The imaging part of the microscope is a small cantilever, typically a few tens of micrometers wide and about 150  $\mu\text{m}$  long with a sharp tip underneath it; the radius of the tip ranges from a few tens of nanometers to  $<5$  nm. For a comprehensive review of AFM cantilevers and tips, together with illustrative examples see [114]. There are several modes of operation, the simplest being contact mode where the tip is scanned along the sample surface, rather like a profilometer. The cantilever bends as it follows the surface topography. A light beam is reflected from the cantilever surface onto a quadrant photodiode. The position of the light spot on the photodiode varies with cantilever bending and gives an indication of the cantilever deflection. The photodiode signal is used as the process variable for a servo control system that is used to provide a signal to a voltage amplifier that is connected to a piezoelectric tube. The length of the piezoelectric tube varies as a function of the applied voltage such that the force applied by the cantilever on the sample remains constant. The other most commonly used modes are non-contact and intermittent contact, where the cantilever is oscillated at or near to its resonant frequency just above the sample. Depending on the mode of operation the tip either taps the surface gently or remains just above the sample. As the tip approaches the sample, the interaction of forces between the atoms at the end of the tip and on the sample surface causes a reduction in the amplitude of oscillation of the tip. This change in oscillation is used as the process variable with the servo system being used to keep the amplitude of oscillation constant and hence the distance between the tip and the sample constant. In whichever mode of operation is used, the output voltage from the servo system can be related to the sample topography. Following on from the development of

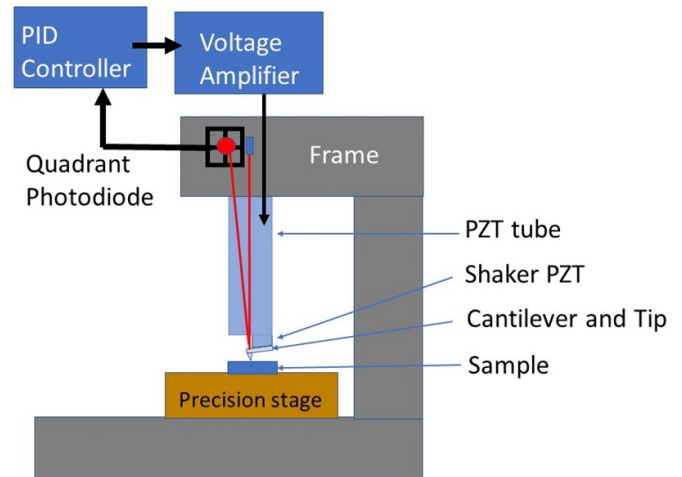


**Figure 11.** Schematic diagram showing the major components of an atomic force microscope. Note that in practice the cantilever is much smaller than shown in the diagram.

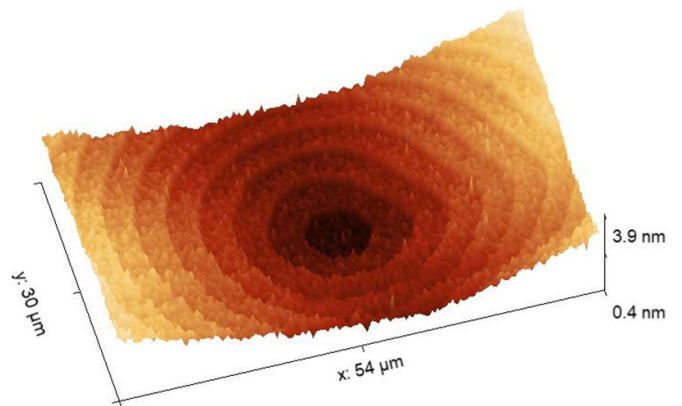


**Figure 12.** Monoatomic steps in an amphitheater construction, each step 0.314 nm.

the AFM and STM other variants have been developed all of which are fall into the generic family of scanning probe microscopes. These include, for example, conductive force AFM [115], contact resonance force microscopy [116], kelvin probe force microscopy [117], magnetic force microscopy [118], scanning near-field optical microscopy [119], photon scanning tunneling microscopy [120], scanning capacitance microscopy [121], scanning thermal microscopy [122] and scanning resistive probe microscopy [123].

### Current and future challenges

Many imaging techniques, including those based on AFMs are making the transition from qualitative imaging to quantitative imaging where users are wanting to extract absolute measurements rather than a relative indication of differences within an image. To achieve this, traceable calibration is required. For dimensional measurements this has been

realized through the development of metrological AFMs that use optical interferometry to measure traceability the relative movement between the tip and sample resulting in a traceable three-dimensional set of coordinates of the surface of the calibration sample [124]. These can then be processed to provide a traceable measurement of either a lateral (grating) or step height standard that can then be used to calibrate an AFM. Nevertheless, a recent comparison of AFM measurements shows that accurate calibration of an AFM is still a challenge for many users [125]. It is possible that some degree of automation of the calibration process could be beneficial to users.

A major weakness of an AFM has been its slow scanning speed, of the order of micrometres per second. In the last few years there have been many advances in the area of high-speed AFMs [126, 127] with scan rates of several millimeters per second and images recorded with video rate now available commercially. However, in these cases the scan range of the AFM is still limited, often to a few square micrometers and data density may be compromised, as may be the linearity of the scanning stage.

Particularly within the life sciences, there is increasing interest in correlative microscopy to combine results from difference techniques [128]. This requires both traceable calibration and a thorough understanding of AFM instrumentation and imaging artifacts [129]. The ever-increasing drive towards miniaturization and measurement of smaller structures, meaning that instrumentation artifacts, i.e. features that appear in an image but are not a genuine measurement of the sample properties, will need to be understood to reduce their contribution to the measurement uncertainty.

Tip shape has been a major source of uncertainty for AFMs; when the tip scans the surface the image obtained is dilated by the shape of the tip. There are several samples available for determining the tip shape and the blind tip reconstruction routines initially developed by Villarubia [130] have been refined over the years together with the development of sharper tips. Nevertheless, as structure sizes are reduced, particularly for semiconductors [131] and critical dimension metrology, quantum structures and devices are fabricated with more complex structures and the shape of the tip will make an increasingly large contribution to the measurement uncertainty.

### Advances in science and technology to meet challenges

Over the last few years there have been significant developments in atomic force microscopy. In addition to the numerous modes developed (see status section), many commercial systems are moving away from scanning using piezoelectric tubes for lateral scanning and moving towards precision stages, sometimes combined with non-raster scan paths for more efficient data collection [132]. There are now continually

developing software packages for AFM data processing [133] that can also accommodate non-raster scanning and data from different modes of operation. Routines are also available for correction of multi-axis drift [134] in AFM data when operating AFMs in less benign environments.

In the last few years photothermal actuation of the cantilever is becoming more widespread [135]. This uses an additional light beam for exciting the cantilever and has the advantages of direct oscillation of the cantilever without excitation of other components in the AFM leading to lower noise levels and better operation in liquid environments thereby supporting biological studies. There have been improvements in the efficiency of the excitation leading to reduced damage to delicate biological samples [136].

The development of piezo active cantilevers and MEMS based AFM on a chip has led to miniaturization of AFMs making them potentially suitable for integration into larger measurements systems. For example, placing an AFM in a scanning electron microscope [137]. Other approaches to detecting the cantilever motion including using a miniaturized interferometric readout [138] have also been developed. Piezo active cantilevers have also opened the possibility of combined dimensional and electrical investigations of samples. The developments in AFM as a microscopy technique also support its development for use for probe lithography [139], offering the potential for imaging and fabrication from the same tool.

### Concluding remarks

Atomic force microscopy has developed rapidly over the last three and a half decades and made a major contribution to science opening many new areas and posing challenges for the instrumentation engineer. The technique is used in research laboratories and in industrial sectors, life sciences, material science and the semiconductor industry. The transition from qualitative high-resolution imaging to high accuracy metrology at high speed is well under way, with the need for ever smaller measurement uncertainties being particularly important for semiconductor applications as well as the ability to measure more complex structures that may require adaptive scanning routines. As a result, numerous challenges still exist for the instrument developer and scientist in achieving these goals. With the support of improved data processing, developments in instrumentation such as scanning technology, and fabrication of lower cost MEMS type AFM systems, the potential for AFM to support the nanoscale world will undoubtedly grow.

### Acknowledgements

AY acknowledges funding from the National Measurement System Programme from the Department of Business Energy and Industrial Strategy, UK.

## 8. Phosphor thermometry

Tao Cai, Mirae Kim and Kyung Chun Kim

School of Mechanical Engineering, Pusan National University, Busan 46241, Republic of Korea

E-mail: caitao@pusan.ac.kr, futurekim@pusan.ac.kr and kckim@pusan.ac.kr

### Status

High-accuracy non-invasive or minimally invasive temperature measurements are continual challenges for thermal science. In this context, phosphor thermometry has attracted considerable attention in recent years owing to its advantages of low intrusiveness, high accuracy, and high spatial resolution. Phosphor thermometry realizes real-time non-contact measurement through the quantitative relationship between phosphorescence and temperature. Phosphors used for temperature measurements are mainly ceramic oxides doped with lanthanides or transition metals [140], which was first attempted as a tool for temperature measurement in the late 1930s [141]. Due to the continuous improvement of laser and camera devices, it has developed rapidly in the past 20 years.

Figure 13(a) summarizes a phosphor thermometry system: excitation light, detector (camera), and phosphor are the primary measurement units. Auxiliary measurement units include filters, controllers for excitation signals, etc. From the earliest relatively low-accuracy temperature measurement based on phosphorescence intensity, a variety of higher-precision phosphor thermometry methods based on the phosphorescence characteristics in intensity (intensity ratio) and in the time domain (rise and decay) have been developed (shown in figures 13(b) and (c)). Especially with the rapid development of high-speed cameras, it is possible to record the rise and decay behavior of phosphorescence in milliseconds or even microsecond time scales, which greatly assisted the improvement of the accuracy of phosphor thermometry. Currently, mature temperature imaging systems based on phosphorescence have been developed. Generally, it tends to use the intensity ratio method to achieve temperature imaging in the fluid [142] (figure 13(d)), and use phosphorescence decay or rise to achieve wall temperature imaging [143] (figure 13(e)). The temperature measuring range has also been expanded from near room temperature to  $-190\text{ }^{\circ}\text{C}$  [144]  $\sim 1700\text{ }^{\circ}\text{C}$  [145].

Phosphor thermometry has already demonstrated its application potential in a variety of aspects. First of all, it is superior to conventional optical temperature measurement technologies readings in harsh environments with complicated geometries and optical noise interference. As temperature probes, phosphor particles can be easily sprayed on the target surface with any shape to achieve *in-situ* temperature monitoring. And due to the selectivity of the measurement spectrum provided by a variety of phosphors [146], phosphor thermometry can be used to measure temperature in harsh environments such as flames and strong radiations by selecting

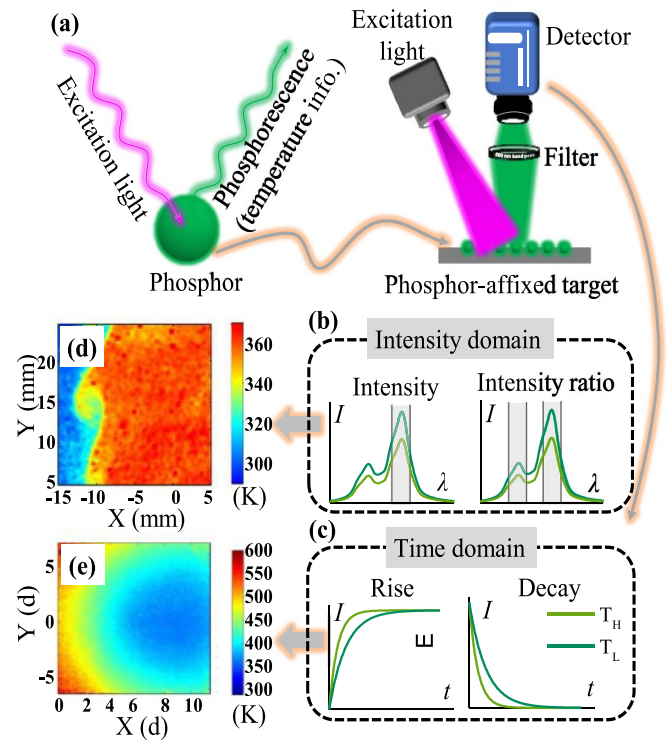


**Figure 13.** Phosphor thermometry system (a); phosphor thermometry based on the characteristics of phosphorescence in intensity domain (b) and time domain (c); temperature imaging using intensity ratio methods. Reproduced from [142]. CC BY 4.0. (d) Using rise time method (e). Reproduced from [143]. © IOP Publishing Ltd. All rights reserved.

the proper spectrum. Another advantage of phosphor thermometry is that it can be used in conjunction with thermal barrier coatings (TBCs). The TBC can be modified with rare earth ion doping to have the temperature measurement function while preserving the thermal insulation function [147]. This makes phosphor thermometry promising in the field of thermal research on high-temperature components of gas turbines and aero engines. Furthermore, utilizing phosphor particles as tracer particles in conjunction with PIV or PTV technology allows for temperature-velocity synchronic measurement in fluids [148], which makes phosphor thermometry gain interest in the field of experimental fluid dynamics and thermodynamics. Given the aforementioned advantages, it is evident that phosphor thermometry, which only started to gain popularity nearly 20 years, is considered a promising tool for temperature measurement.

### Current and future challenges

Despite the broad applicability and superior measurement capabilities of phosphor thermometry, there are still several limitations that impede its usage in more technological and scientific fields. The current and future challenges are summed up in the following points:

Firstly, the camera's performance such as sensitivity, recording rate, and memory storage capacity will be a major



obstacle to the advancement of phosphorescence-based temperature imaging.

- (1) The camera's sensitivity limits the maximum temperature of phosphor thermometry. Due to thermal quenching, the intensity of phosphorylation decreases in high temperature environments significantly. And the thermal radiation is intensifying dramatically and shifting into the measured spectrum. This makes it harder for the camera to obtain the phosphorescent signals.
- (2) The camera's sensitivity also limits the frequency of phosphor thermometry. High frequency measurement requires extremely short exposure time, which results in weak captured phosphorescence signals and leads to a sharp decrease in SNR.
- (3) The frame frequency of the camera restricts the frequency of phosphorescence-based temperature imaging. A time domain measurement method requires a high camera frame frequency even for low-frequency temperature imaging (for example, a 10 Hz temperature imaging requires a 1 kHz camera frame frequency, that is, 100 images of phosphorescence for each decay period is needed). Therefore, a very high recording frequency of camera is required if the frequency of temperature imaging is further increased.
- (4) The frame frequency of the camera will also restricts the upper limit of phosphor thermometry. Due to thermal quenching, the phosphorescence behavior in the time domain (rise and decay) in high-temperature will become very fast ( $\mu\text{s}$  level or even ns level), which poses a challenge to the recording frequency of the camera.
- (5) The memory of the camera limits the measurement duration of phosphor thermometry. As mentioned in the point (3), temperature imaging requires a large number of images in the time domain, therefore, it is necessary for the camera to have sufficient memory to ensure long-term temperature measurement.

Secondly, issues in the imaging, which mainly occur in fluid measurement.

- (1) Measurement errors brought on by multiple scattering. Phosphor particles dispersed in fluids can serve as temperature probes. However, there is strong scattering between particles and between walls and particles, resulting in the image containing a large amount of scattered light. Therefore, research on the removal (or correction) of scattering effects is a concern for in flow phosphorescence thermometry.
- (2) Particle movement. The movement of phosphor particles in the fluid makes it impossible to obtain the rise or decay curve of phosphorescence, which is the reason why the in-fluids phosphor thermometry can only be made using the intensity ratio method. In addition, the movement of phosphor particles along the camera's normal direction affects their signal intensity during the imaging process, which also brings errors to the measurement.

Thirdly, the challenges encountered in practical applications involve specific implementation strategies for phosphor thermometry.

- (1) The influencing conditions that lead to temperature measurement errors: the initial phosphor thermometry simply established the relationship between temperature and phosphorescence, but more recent studies have shown that the excitation energy, excitation duration, and oxygen concentration in the environment will all affect the phosphorescence-temperature relationship.
- (2) The problem of phosphor coating peeling off on the surface of high-speed moving, air-impacted, or deforming objects.
- (3) The extensive post-processing required when using high-precision time-domain based phosphor thermometry, as well as the demanding requirements for high-speed detectors.

Fourthly, the simultaneous measurement of multiple parameters is also on the agenda due to the connection of diverse thermophysical parameters in thermal situations. In addition to the developed phosphorescence-based temperature-velocity measurement, there is also an urgent need for temperature/strain, temperature/pressure, etc measurements, which also pose further challenges for the development of measurement technology.

### Advances in science and technology to meet challenges

Overcoming the above challenges will mainly depend on the development of advanced camera and optimized imaging strategy, the design of high-performance advanced phosphor materials, and the perfection of phosphor thermometry theory. Several needed advances are outlined below.

Relying on the development of advanced camera and optimized imaging strategy, phosphor thermometry continues to expand towards high-frequency, high-resolution, and high-precision.

- (1) With the continuous improvement of camera measurement frequency and sensitivity,  $\mu\text{s}$  and even ns level phosphorescence can be effectively recorded, which makes 2D phosphorescence temperature measurement at kHz or even 10 kHz levels possible [149]. In addition, the phosphorescence analysis in the time domain will be more detailed, which allows for the high measurement precision with sub- $^{\circ}\text{C}$ , even in high-frequency measurements [150].
- (2) New imaging strategies are constantly being developed, and optimization methods based on time domain imaging are constantly being proposed. This can achieve high spatial resolution while maintaining measurement accuracy [151]. And using high-frequency excitation methods and novelty temperature referencing methods [152], kHz-based time-domain phosphorescence thermometry can also be achieved in an optimized time-domain analysis manner.

- (3) The use of structured light technology [153] has made it possible to lessen measurement errors in fluid measurements caused by scattering.

According to recent studies, phosphorescence temperature imaging has achieved measurements at different scales from nm level [154] to meter level, while the maximum frequency has reached 100 kHz [149]. In terms of resolution, the full frame resolution can reach up to  $4000 * 2672$  pixels [151], and research on imaging methods is currently being conducted towards sub pixel algorithms [155]. Related research has also been conducted on phosphorescence temperature measurement imaging of moving objects (mainly in fluids), temperature analysis using the image of decaying phosphorescence will be affected by the displacement of particles [156]. According to Massing *et al's* study [157], there is a 20% change in the phosphorescence intensity values of the discrete particle images due to the shift in the sub-pixel position even without any additional noise. Thus, the influence of displacement and deformation of phosphorescence signals on temperature measurement should be focused on the future research.

On the development of phosphor materials, new design methods for thermographic phosphor materials need to be continuously proposed:

- (1) By selecting luminescent ions with a large energy gap between the radiatively emitting energy level and the next lowest energy level, phosphor for high-temperature sensing could be developed. Furthermore, the co-doping of sensitizers can further enhance the luminescence intensity. At this point, Dy ion-doped phosphors and multi-ion co-doped sensitized phosphors will be important materials for ultra-high temperature measurements. YAG: Dy phosphor thermometry capable of measuring up to 2033 K has been reported [158].
- (2) Via co-doping multiple rare earth ions, the sensitivity of phosphor thermometry for both the intensity ratio method [159] and the decay time method [160] can be improved.

The theory of phosphor thermometry also needs to be continuously improved. Franck–Condon's model [161] based on the configurational coordinate model explains the phosphorescence emission mechanism from the temperature in most cases. Its improvement will provide a theoretical basis for the

further development of the phosphorescence thermometry theory. Studies on excitation energy [162], excitation duration [163], oxygen concentration effects [164], etc have also been a significant development direction in the field of phosphor thermometry research. These studies will aid in the improvement of phosphor thermometry to measure temperatures accurately over a wider range and with fewer measurement errors.

In addition, based on phosphor thermometry, multi-parameters measurement methods could be developed. The development of 3D PIV/PTV technology makes it possible to measure 3D temperature velocity in fluids [165]. Method of phosphorescence-based temperature-thermal strain measurement [166] based on phosphor thermometry and digital image correlation has been proposed in high-temperature environments. The concept of temperature-oxygen concentration measurement [167] has also been proposed.

### Concluding remarks

In a conclusion, low-invasive temperature imaging technique utilizing phosphorescence has shown its strong development potential in the fields of scientific research and engineering applications. The multi-environmental applicability of phosphor particles also brings infinite possibilities for its application in various temperature measurement fields in the future. Higher temperature ranges, higher sensitivity, more convenient engineering application methods, and multi-functional measurement methods will all be the goals of future development. Phosphor thermometry will unquestionably continue to grow in popularity as a method for measuring surface and in-fluid temperatures as a result of the advancement of novel material preparation techniques and continuing improvement in the performance of imaging equipment.

### Acknowledgements

This research was supported by the Brian Pool Program from the National Research Foundation of Korea (NRF) Grant (KRF-2019H1D3A1A01071033). This research was also supported by the National Research Foundation of Korea (NRF) Grant, which is funded by the Korean government (MSIT) (Nos. 2020R1A5A8018822, 2021R1A2C2012469, 2021R1C1C2009287).

## 9. Electrical tomography (ET)

Jiamin Ye and Xiao Liang

School of Electrical and Information Engineering, Tianjin University, Tianjin 300072, People's Republic of China

E-mail: yejiamin\_19@tju.edu.cn and liangxiao@tju.edu.cn

### Status

ET is a non-invasive electrical detection method, and has been applied in the biomedical field and in the field of industrial process detection, e.g. the multiphase flow detection as described in section 12. To adapt to the detection needs, ET still needs to be greatly improved in terms of accuracy and resolution. This section is focused on discussing the challenges and advances in ET technology itself.

ET uses electromagnetic fields to detect the electrical properties of the object under test, including electrical capacitance tomography (ECT), electrical resistance tomography (ERT), and electromagnetic tomography (EMT). ECT and ERT detect the distribution of permittivity and conductivity respectively, while EMT detects the distribution of conductivity or permeability. In the biomedical field, EMT is also known as magnetic induction tomography. Figure 14 shows the components of the ET system [168], which can be divided into the sensor array, the signal control/acquisition unit, and the image reconstruction unit.

For the technical maturity or technology readiness level (TRL), ERT and ECT have achieved TRL 7 to TRL 9 [169]. They have been successfully applied to production-scale fluidized bed processes, hydrogeology, and other fields [170, 171]. Compared with the above two tomography technologies, the development of EMT is relatively backward. The technology maturity of EMT only reaches TRL 6 or lower [169], and the current research progress is still in the testing of the model/prototype. The optimization of sensor arrays, the enhancement of electronic circuits, and the application of new sensors are the main focus of EMT. As a soft-field measurement technology, the imaging accuracy of ET is limited. The improvement of image reconstruction algorithms is a research hotspot. Each reconstruction algorithm has its advantages. In addition to the improvement of the existing iterative algorithm, non-iterative algorithm, and direct algorithm, the combination of different algorithms can also improve the spatial resolution and quality of reconstructed images.

Due to the advantages of non-invasive, low cost, fast measurement speed, convenience, and safe operation, ET is suitable for the harsh industrial environment. Currently, ML techniques have opened up a new way to deal with nonlinear and ill-posed problems. Therefore, the reconstruction of electrical properties distribution and the extraction of useful information for industrial applications can be realized quickly and accurately. In addition, ET is radiation-free. With the development of sensor miniaturization and electronic circuit integration, the portable ET system will be suitable for long-term continuous monitoring in the biomedical field.

### Current and future challenges

Quantitative measurement is an inevitable requirement for the development of the technology. Since ET is a soft-field measurement technology, its natural nonlinearity, ill-condition, and ill-posedness make the true electrical parameter distributions difficult to obtain. Currently, the common solution is to linearize the nonlinear problem to ensure solvability and computational speed. The quantitative results are later obtained by linearly mapping the reconstruction results to the known interval of the electrical parameters. However, the medium distribution is complex in the actual process. Linearized solutions can only image the approximate electrical parameter distributions, making it difficult to achieve accurate quantitative measurements, which limits the further development of ET. Algorithms such as D-bar and Calderon algorithms have been proposed to solve the nonlinear problem directly and achieve quantitative measurement, but they still have limitations and cannot be generalized. The big challenge is to find a generalized solution for the nonlinearity, ill-condition, and ill-posedness from the mathematical and physical aspects.

Another challenge concerns the construction of the simulation model. To facilitate the study of the ET imaging mechanism, simple models such as the square/circular/cylindrical/sphere models have been adopted in the initial research phase. However, such models are too simple to represent the distribution of electrical properties of the real measured object. Future research will require the establishment of more realistic and complex simulation structures with reference to specific applications. Inevitably, the enormous amount of computation involved in building complex models needs to be taken into account.

Most of the current research has focused on imaging the distribution of electrical properties on 2D slices. In this case, it is usually assumed that the electrical properties remain constant in the axial direction. When the assumption is untenable, the reconstruction of the electrical properties of the cross-section is affected, leading to incorrect interpretation. Therefore, a correction to the 2D reconstruction or a direct implementation of the 3D reconstruction is required to fully demonstrate the spatial distribution of electrical properties and provide more accurate information.

### Advances in science and technology to meet challenges

To address the poor imaging accuracy of ET, ML methods provide an effective solution. ML methods are based on mathematical theories such as probability and statistics, and utilize computers with powerful calculation capacity to extract effective information from measurement data and to reconstruct the distribution of electrical properties. In some applications, ML methods have demonstrated higher imaging accuracy compared to traditional algorithms. In addition, multi-modality data fusion is also an approach for imaging accuracy improvement. Through the combination of different modalities of ET [172] or the combination of ET and other measurement

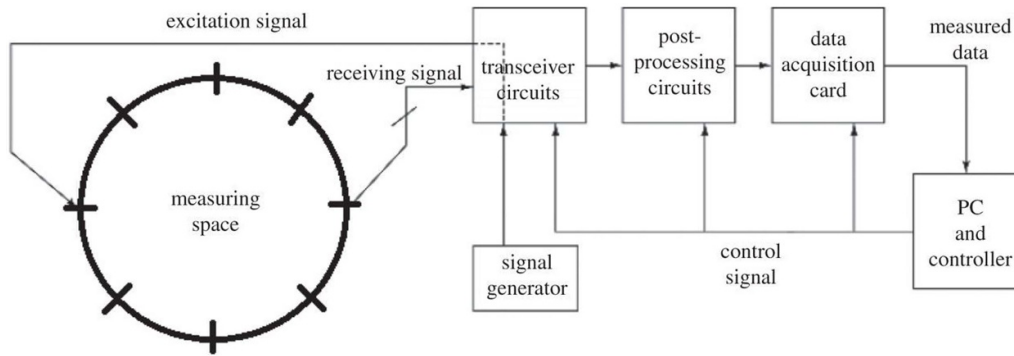


Figure 14. Block diagram of a typical ET system. Reproduced with permission from [168].

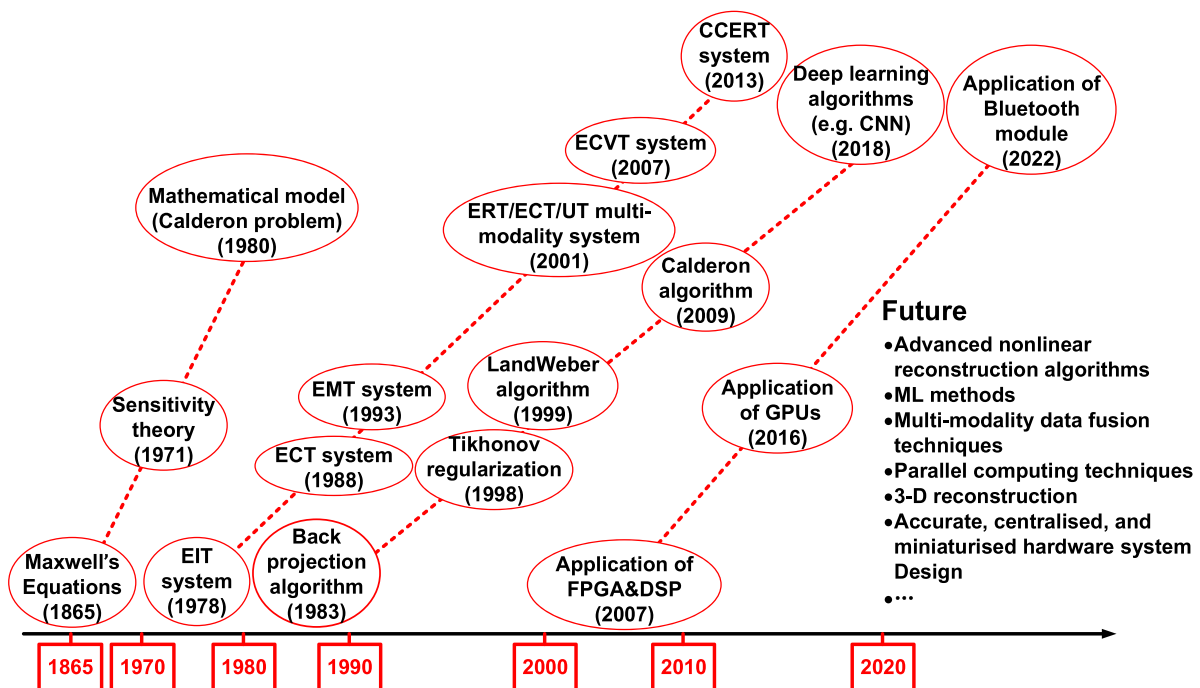


Figure 15. Roadmap of the key developments in ET in the past and future.

methods, such as the radiometric method [173], ultrasonic method [174], and differential pressure method [175], the information is complementary or redundant. Thereby, the measurement accuracy is improved, and the measurement uncertainty is reduced.

As computer hardware has evolved in terms of speed and data throughput, GPUs with high computational performance have been used to accelerate the tasks of complex model building and image reconstruction [176, 177]. Besides, parallel computing of multiple GPUs can also significantly reduce computation time. Parallel solutions and large-scale computer/GPU clustering technologies will be the focus of future investigation.

In order to improve the convenience of the system, centralized and miniaturized hardware system design is one of the future trends. Currently, the three parts of the ET system are in a separate state as shown in figure 14. By developing the small and economical sensor array as well as the

integrated data processing circuits, and connecting them to the remote image reconstruction unit using wireless transceiver technology, long-term continuous detection can be achieved, which will greatly expand the application field of ET [178, 179].

The 3D reconstruction of ET is a research hotspot. In order to obtain detailed information on the spatial distribution of electrical properties, more sensors are employed than in the 2D reconstruction. The spatial arrangement of the sensor array needs to be optimized [180]. In addition, more sensors open up more possibilities for data acquisition strategies. Good strategies can improve the ill-condition and ill-posedness of ET [181]. Besides, the design of the imaging algorithm is also an important part of the process. Compared with 2D reconstruction, the number of pixels to be calculated in 3D reconstruction increases exponentially, and the computational complexity increases significantly. The image reconstruction algorithms suitable for large-scale matrix calculations are

required. At this point, the compressed sensing techniques provide a solution [182, 183].

### Concluding remarks

With its low cost, adaptability to harsh environments, and absence of radiation, ET is suitable for continuous monitoring in industry and biomedicine. However, its soft-field characteristics limit spatial resolution and imaging accuracy. The huge computation time of solving forward and inverse problems for complex 3D models also constrains the further development of ET. ML methods, multi-modality data fusion techniques, parallel computing techniques, and large-scale computer/GPU

cluster techniques offer the possibility of breaking through these bottlenecks. In addition, with the development of hardware, a truly practical and portable ET system will appear. For clarity, the roadmap of the key developments in ET is summarized in figure 15.

### Acknowledgements

The author acknowledges the support by the National Natural Science Foundation of China (Nos. 61871366, 62271343 and 61627803) and Tianjin Research Innovation Project for Postgraduate Students (No. 2021YJ SB117).

## 10. Photoacoustic imaging (PAI)

Lidan Cao and Xingwei Wang

Electrical and Computer Engineering Department, University of Massachusetts Lowell, One University Ave, Lowell, MA 01854, United States of America

E-mail: lidan\_Cao@student.uml.edu  
and xingwei\_Wang@uml.edu

### Status

The concept of the photoacoustic effect, wherein sound waves are generated in a material following pulsed light irradiation, was initially proposed by Alexander Graham Bell in 1880 [184]. Over the subsequent century, this phenomenon garnered increasing attention within the biomedical domain, with the first documented investigation occurring in 1964 by Amar [185]. Transitioning into the late 20th century, the concept was introduced to the realm of biomedical imaging, with pioneering research by Oraevsky *et al* in 1994 [186]. The turn of the millennium marked a pivotal period for PAI, as technological advancements in laser sources, ultrasound detectors, and data acquisition and processing algorithms facilitated a significant surge in research activity. As a result, PAI emerged as one of the most rapidly expanding and focal areas within the field of biomedical imaging [187].

The fundamental principle underlying PAI is that a specific tissue was illuminated by a light source (a nano-second pulsed laser is commonly used) resulting in the generation of ultrasound waves that could be detected by detectors and form images (figure 16). Compared with traditional imaging methods like x-ray imaging, CT, MR imaging, and positron emission tomography, PAI has numerous advantages: high optical contrast into ultrasound waves that leads to a higher spatial resolution. It is free from ionizing radiation, and it is small, easy, and safe to manipulate. These advantages make PAI a promising method and have great potential for various clinical biomedical imaging applications [188].

Emerging as a novel imaging technique developed over the past 20 years, PAI has garnered significant attention. It has already been subjected to rigorous investigation in diverse clinical applications [189] including domains such as breast imaging [190, 191], dermatologic imaging [192], and musculoskeletal imaging [193].

### Current and future challenges

As shown in the figure 17, based on different fundamental principles of image reconstruction, non-invasive PAI methodologies can be classified into two categories: photoacoustic tomography (PAT) or photoacoustic computer tomography (PACT), and photoacoustic microscopy (PAM). In PAT/PACT, a high-energy laser is used as a light source. The light illumination is diffused to the tissue. The generated acoustic waves arise from the thermally induced expansion of the tissue, subsequently being captured by surface-based detectors for image

reconstruction. In PACT, the spatial resolution typically ranges between 100  $\mu\text{m}$  and 1 mm depending on imaging depth. Integrated with other techniques, such as multi-angle illumination technique, the penetration depth was further improved to approximately 10 cm [194].

On the contrary, PAM is a direct image formation method through focused scanning. It has two forms: acoustic-resolution PAM (AR-PAM) which uses ultrasound focusing, while optical-resolution PAM (OR-PAM) which employs light focusing, both of which targets at improving spatial resolution in images. Different from PACT, it can achieve higher spatial resolution at shallow depths. PAM achieves a penetration depth of approximately 1–2 mm, showcasing spatial resolutions below the 10  $\mu\text{m}$  threshold. While these non-invasive methods yield high resolution and offer a lot of advantages, their imaging depth is limited to several centimeters [195, 196] due to the light attenuation. Therefore, their clinical applications are limited. To overcome this issue, the concept of minimally invasive PAI (miPAI) has emerged, resulting in the development of various miPAI systems in the past decade. Different from the non-invasive methods, miPAI system incorporated an optical fiber within the instrument, enabling direct delivery of the excitation light to internal body tissues. This innovative approach extends PAI to encompass a broader spectrum of applications [197].

PAI has many exciting achievements in biomedical imaging, yet several challenges persist. The utilization of a pulse laser source, though effective, does impose constraints on imaging speed due to inherent limitations in laser rates. Furthermore, the pursuit of higher image resolution and quality warrants further investigations. Although miPAI presents as a promising solution to address the depth limitation of PAI, its clinical applications remain a challenge. Besides the technical challenges, the commercialization of the PAI system is still in the early stage.

### Advances in science and technology to meet challenges

With the development of AI and the tremendous growth of its applications in different fields, the utilization of DL algorithms for imaging reconstruction in the realm of PAI field has attracted a lot of attention. The convergence of novel AI algorithms with PAI holds the potential to propel image quality enhancement, signifying a pivotal trajectory for forthcoming advancements in the PAI domain. The advancement of techniques constitutes a pivotal realm of investigation as well. The enhancement of light sources such as the improvement of pulsed lasers and exploration of alternative laser types can improve the imaging speed. Progress in photoacoustic transducers and detectors, including the utilization of all-optic systems such as Fabry–Perot fiber optic sensors, will be another potential area [198, 199] to improve spatial resolution. Moreover, another crucial field for the future improvement of PAI lies in the exploration of suitable contrast agents. The increase in types of contrast agents has the potential to significantly enhance imaging depth, resolution, and quality.

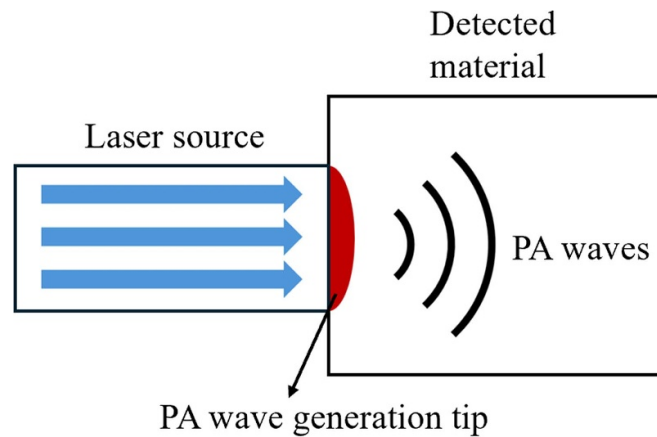


Figure 16. Schematic of photoacoustic principle.

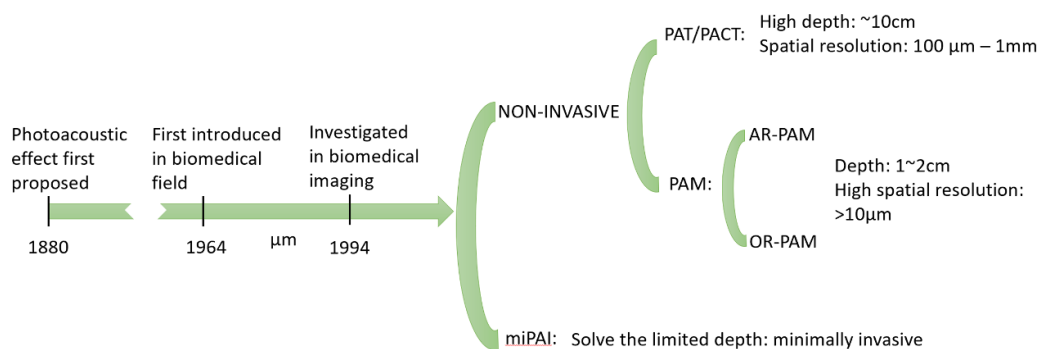


Figure 17. Timeline of the development and the classification of PAI methods.

In addition, the combination of PAI with established imaging methods such as ultrasound imaging and CT is another critical trend and a future direction. This synergistic approach holds the potential to accelerate the integration of PAI into clinical applications, thereby contributing significantly to the ongoing enhancement of the biomedical imaging domain.

**Concluding remarks**

PAI emerged as a novel and promising imaging technique in the biomedical field and has undergone massive growth

in the past two decades. Various methods based on PAI were developed such as PAT/PACT, OR-PAM, AR-PAM, and miPAT. A lot of exciting clinical practices and improvements were investigated as well. It can be expected that the PAI will have a wide application in the biomedical imaging field in the future. To face the challenge, the combination of PAI and established biomedical imaging methods, the integration of DL algorithm for technique improvement including excitation light source, transducer, and detector, as well as the development of contract agent, will collectively stand as transformative steps that are poised to propel PAI into a new chapter of exploration and application.

## 11. Holography

Jianqing Huang<sup>1,2</sup>, Weiwei Cai<sup>1</sup> and Yingchun Wu<sup>3</sup>

<sup>1</sup>Key Laboratory of Education Ministry for Power Machinery and Engineering, School of Mechanical Engineering, Shanghai Jiao Tong University, People's Republic of China

<sup>2</sup>Department of Electrical and Electronic Engineering, the University of Hong Kong, People's Republic of China

<sup>3</sup>State Key Laboratory of Clean Energy Utilization, Zhejiang University, Hangzhou 310027, People's Republic of China

E-mail: huang-j-q@sjtu.edu.cn, cweiwei@sjtu.edu.cn and wuyingchun@zju.edu.cn

### Status

Dennis Gabor invented and named holography in 1947 [200], for which he received the Nobel Prize in Physics in 1971. Further developed by Leith, Denisyuk, and many other researchers around the world, holography becomes an important and versatile imaging technique that is extensively applied in various fields of optical engineering [201]. As illustrated in figure 18, holography is a two-step process, in which the first step records the interference pattern as the hologram, and the second step reconstructs the wavefront from the hologram. Both amplitude and phase distribution of the propagating wavefront can be obtained simultaneously, which is the unique feature of holography in contrast to other conventional imaging techniques. Furthermore, the reconstruction process enables us to change the focus and perspective of the targeted three-dimensional (3D) scene. Consequently, holography is considered as the most promising technique to realize true 3D imaging and display [202].

Digital holography (DH), which records the hologram using digital cameras and numerically reproduce the wavefront, is the fastest growing holographic technique due to the rapid improvements in digital technology and computational power [203]. As a well-established technique, DH has a wide range of practical applications such as 3D sensing, data storage, surface topography, and phase imaging. For example, not only the 3D shape but also the inner structure of transparent and translucent samples can be quantitatively analyzed using digital holographic microscopy [204]. Nowadays, holographic instruments for various purposes are commercially available.

The core of DH is the calculation of the wavefront using diffraction theory, followed by several procedures to improve the image quality or accomplish specific measurement tasks, such as aberration correction, speckle reduction, resolution enhancement, focus prediction, and phase unwrapping. All of these calculations can be performed by physics-based approaches or data-driven methods. The former usually employs explicit analytical formulations of physics models, which enables robust outputs for any valid single-shot measurement. While the data-driven methods can establish implicit relationships between input and output pairs without any prior knowledge of the imaging model. In particular,

the emergence of DL in recent years has substantial influence on the field of DH, showing superior computational efficiency, improved measurement accuracy, and higher image quality [205]. Nevertheless, the data-driven methods applied in DH are still in exploration stage and cannot completely take the place of mature physics-based approaches. To meet the growing demands in the performance of holographic measurements, it is encouraged to put continuous efforts into both types of holographic image processing algorithms.

### Current and future challenges

Despite the successful application of holography in laboratory and industrial practice, there are still several challenges that hinder the further development of holography. The first challenge is to improve the spatial resolution of holographic imaging in both lateral and axial directions. With the finite NA and spatial bandwidth product (SBP) of the imaging system, the spatial resolution is mainly limited by several factors, including wavelength and coherence of the light source, diffraction, image sensor area, and pixel size. Aiming to record the fine holographic fringes, the pixel size of image sensor is usually the primary limitation. Furthermore, owing to the depth-of-focus problem [206], the measurement accuracy and uncertainty of holography in axial direction is significantly inferior to that in lateral direction. Thus, researchers have spent lots of efforts in developing autofocusing algorithms for improved in-focus depth determination.

The second challenge is to enhance the robustness of holography in practical applications with harsh environment. As a versatile imaging technique, DH has been demonstrated in the *in-situ* characterization of complex multiphase flows [207], such as combusting dense particle clouds, fuel sprays, burning aluminized propellants, and shockwaves. However, the measurement accuracy and image quality are inevitably influenced by the harsh environment which usually features high dynamic ranges in temperature, pressure, species, or particle density. For example, refractive index variation in reactive flows caused by the change of media properties, will distort the recorded hologram and consequently deteriorate the reconstructed wavefront [208]. Therefore, it is highly desired to develop new optical configurations, calibration methods, and post-processing algorithms to understand and prevent the impact of harsh environments.

Previous works have demonstrated the great potential that real-time holographic imaging can be realized by using a trained data-driven model [209]. But there are still several important issues that need to be addressed when solving holographic imaging tasks using data-driven methods. Those include (1) a large number of data pairs is usually required for the supervised training of data-driven models; (2) the lack of application-specific holographic datasets hinders the validation of newly designed models; (3) the generalization performance of data-driven methods is limited when performing holographic imaging among various application scenarios; (4) the interpretability of these implicit models is poor, which means



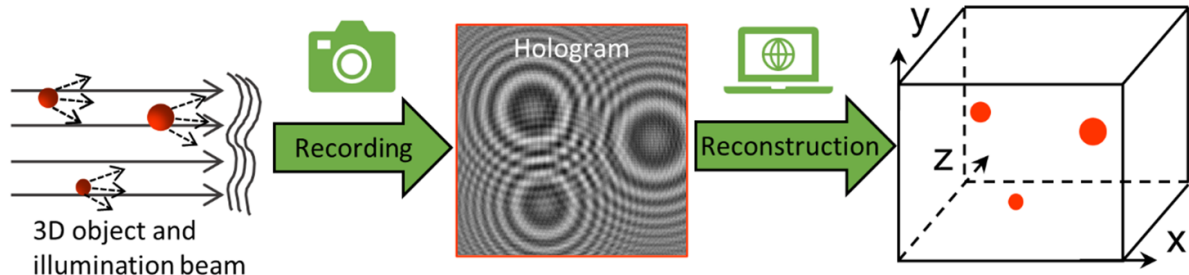


**Figure 18.** Schematic of holography including the recording and reconstruction processes.

the model's architecture is designed empirically and sometimes results in widely erratic outputs.

### Advances in science and technology to meet challenges

From the perspective of system theory, it is an intelligent strategy to optimize the whole light path of the holographic imaging system, including modulation of the light source, transmission of the wavefront, acquisition of interference pattern, and finally reconstruction of the wavefront. Advances in new light sources, optical elements and configurations, image sensors, and processing algorithms are the key enablers to address the challenges and promote holography to new applications.

For example, embedding higher dimensional information in holography using a synthetic aperture can enhance the spatial resolution [210]. Structured illumination, scanning holograms in time series, multiple wavelengths, and polarization encoding are the representative strategies which have been successfully demonstrated in holographic imaging. The corresponding processing algorithms are also developed for decoding the multi-dimensional information in the unusual holograms.

Hybrid holographic imaging system is another remarkable advance, in which a conventional in-line or off-axis holography configuration is combined with other optical techniques, such as optical frequency comb [211], tomography [212], optical metasurface [213], Raman/Mie scattering [214], and imaging pyrometry [215]. It can offer amazing potential in improving image quality and measurement accuracy, and broadening detection capability since more properties of the target object can be measured simultaneously. Nevertheless, such complex imaging systems are not mature in practical applications. A higher level of reliability and flexibility is always required to meet various harsh testing environments.

Finally, several attempts have been made to break the bottlenecks of data-driven methods applied in holography. To reduce the cost of preparing datasets and training data-driven models, specific training strategies have been proposed, such

as semi-supervised learning, unsupervised learning, transfer learning, and even untrained NNs [216]. It has been demonstrated that a comparable result can be output even with limited data pairs. Furthermore, since the principle of holography can be well-described in physics, it is a generally accepted strategy to embed physics knowledge into data-driven models for an improved generalization [217]. It is possible to realize fast and interpretable holographic calculations by creating a physics-informed and data-driven model.

### Concluding remarks

Holography is a powerful imaging technique with the unique advantages in 3D and phase imaging. It is highly desirable to enhance the spatial resolution and robustness of holographic imaging systems, especially in a practical environment with extreme conditions. Advances in hardware and algorithms play an equally important role in the development of holography. Different from traditional simple configurations for holographic imaging, embedding more information of the light source in the hologram recording process enables us to bypass the SBP limitation so that a higher spatial resolution under the same field of view can be achieved. Moreover, integrating holography with other optical techniques makes it possible to broaden the system's detection capability. Data-driven methods can dramatically reduce the computational complexity of hologram calculations, along with the improvement in reconstruction quality. However, it usually suffers from the lack of generalization and interpretability, which hinders the reliable applications in practice. Incorporating physics-based approaches with data-driven models is a promising strategy to overcome the obstacle. It is believed that, in the not-too-distant future, real-time and robust holographic imaging can be extensively applied in industrial practice.

### Acknowledgements

This work was funded by the Hong Kong Scholars Program (XJ2022032) and National Natural Science Foundation of China (52061135108, 51976122).

## 12. Multiphase flow process imaging

Marco J da Silva<sup>1</sup> and Chao Tan<sup>2</sup>

<sup>1</sup>Institute of Measurement Technology, Johannes Kepler University Linz, Austria

<sup>2</sup>School of Electrical and Information Engineering, Tianjin University, People's Republic of China

E-mail: marco.dasilva@jku.at and tanchao@tju.edu.cn

### Status

Multiphase flow denotes the stream of two or more physically distinct and immiscible substances and it is important in a broad range of engineering disciplines and in many other scientific fields such as biology, chemistry and physics. Industrial processes involving multiphase flows are present across many applications, as diverse as steam generation, chemical processing plants, oil and gas production and transport or metallurgical processes. As a consequence, a considerable number of multiphase flow process imaging techniques have been developed and used in the past. Classical imaging techniques such as optical visualization [218] as well as particle imaging velocimetry [219] have been applied in research of multiphase flows for many years. Ultrasound imaging (sonography or ultrasonic Doppler) has found some applications in industry but predominantly in academia too [220]. However, the most prominent imaging technique for multiphase flow is tomographic imaging. Tomography is a powerful imaging technique which has been widely used first in medical diagnostics and later in non-destructive evaluation and dimensional metrology. Tomography to visualize industrial processes has been introduced in the 1980s and the term process tomography was coined [221]. Since then, different imaging modalities have been developed and tested. Examples are electrical [222, 223], magnetic [224], ultrasound [225], microwave [226] and radiation-based [227, 228] process tomography. Other than in medicine, process tomography is required at high scanning speed. Frame rates of thousand images per second and more enable the monitoring of transient and complex flows in industrial plants or equipment. The general principle of CT for multiphase flow process consists of measuring a physical quantity through the pipe or vessel that can be related to the fluid property (e.g. electrical impedance, attenuation coefficient). A number of integral, independent measurements are taken from sensors (or electrodes) placed on the periphery of the test object at different angular positions either by rotation of arrangements or electronic switching. After measurements have been completed, the local properties of the flow can be calculated by means of a so-called reconstruction algorithm. In addition to classical reconstruction methods, AI can be applied to improve system performance [229]. Figure 19 schematically illustrates this process. Variations of the classical scheme are also accepted as tomographic imaging. For instance, in the field of multiphase flow research, an intrusive imaging technique known as wire-mesh sensor has been successfully

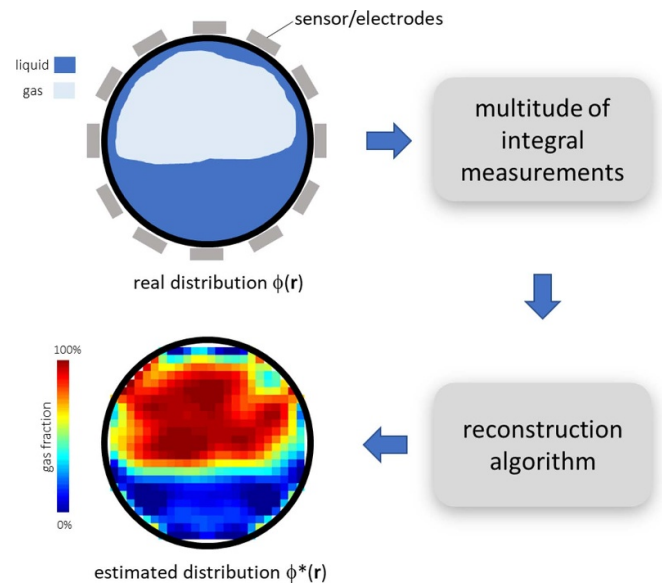


**Figure 19.** Schematic representation of the general approach for tomographic multiphase flow process imaging. The object real distribution is defined as  $\Phi(\mathbf{r})$  where  $\mathbf{r}$  denotes a spatial vector. From the multitude of integral measurements, an image of the estimated distribution  $\Phi^*(r)$  is obtained, which is the best estimate of the real distribution.

applied in the past [230, 231]. Imaging based on nuclear MR is also reported [232]. None of the mentioned technologies can claim the fulfillment of stringent requirements of spatial and temporal resolution as well as of sensor robustness for industrial applications.

### Current and future challenges

The current challenges for multiphase flow process imaging can be divided into two main domains: (1) academic/research and (2) industrial applications.

In the first domain, multiphase flow process imaging provides detailed experimental flow data on which theories can be developed (and then accepted or rejected), as well as for validation of so-called computational fluid dynamics codes, which have been fostered in recent years by the progressively increasing computer power. Also, the new trends in AI have supported the development of more powerful computational codes. Obviously, only sufficiently validated codes can be admitted as reliable [233]. For this aim, small and medium scale multiphase flow experiments with accurate flow imaging is required. Also therefore, multiphase flow process imaging faced more and more challenges regarding spatial and temporal resolution in recent years. Several physical parameters are required in such applications, for instance phase fraction distributions, temperature fields, pressure fields, velocity fields, and concentration fields.

In a second domain, multiphase flow process imaging may be applied for advanced automation and control of several industrial processes [169]. Many industrial applications are

very energy consuming while multiphase flows play a crucial role in process efficiency and safety. Increasing the efficiency of industrial processes is not only an economic issue, it also concerns reduction of carbon dioxide emissions and consequently to climate protection actions. In today's industrial plants, the usual process sensors only provide local measurements (typically temperature, pressure, flow rate and/or level). In most industrial systems, however, such local measurements are not representative of the entire process. Hence, advanced automation and control of such industrial processes can only be achieved by better knowledge of spatially and temporally resolved parameters. Multiphase flow process imaging is therefore urgently needed here being able to generate and process multidimensional data in order to obtain the required additional spatial/temporal information from processes. Additional challenges arrive from the conditions of flow confinement, such as opaque metallic walls, or complex test section geometries. Such constraints may limit the use of some measuring principles. Moreover, the robustness of sensors is an important issue for some industrial applications where harsh environmental conditions occur, i.e. high pressure, high temperature and/or the presence of aggressive media. Further work is still required to ensure that these imaging technologies are actually providing information that can be easily adapted and used in process controlling, which requires a holistic look at these sensing methods and data analysis.

In both domains there is still a clear need for quantitative evaluation of flow parameters and their uncertainty assessment. While the academic/research community is looking for detailed information about the flow in the form of 2D/3D visualization of parameters, the main interest in industrial applications is the safety and efficiency of the processes involved, which requires the transformation and interpretation of flow images into process parameters. Uncertainty evaluation is therefore highly application dependent.

### Advances in science and technology to meet challenges

Since multiphase flow always involve combinations of different fluids, such as gas–water, gas–oil, wet–gas, oil–water, sand–water flows, their flow status changes dramatically with temperature, pressure, diameter, orientation, etc, and the fluids property such as density and salinity would also change with operating condition, there is no universal imaging modality that could deal with a wide range of operating conditions and fluids. Besides, when it comes to mixing more than two fluids, for instance oil–gas–water three-phase flow, single-modality imaging would lose sensitivity to one of the fluids and fails to separate all the three fluids information, where more than one imaging modality is required to fuse different sensitivity to deliver comprehensive information of multiphase flow. Some attempts in this development have been reported in past [230, 234, 235], but there is plenty of room for the combination of several dimensions. Furthermore, for now,

most of process imaging systems are for laboratory research purpose, systems that focus on specific applications and meet industrial installation and data transfer standards are sought. Hence, one challenge of industrial process imaging is that it is more of a customized technology than standardized instruments. For different plants and applications, process imaging tools need re-design and optimization to meet different sensing requirements. Additionally, the industry requires robust and easy installation sensors, therefore, a kind of easy-to-install sensors that are easily adapt to high-temperature and pressure vessels, and multidimensional imaging technology is desired in future development. The term 'dimension' does not only stand for the classic *spatial dimension*, but also for the various modalities: electrical, optical, acoustic, nucleonic—*modality dimension*, for the excitation energy mode(s)—*spectral dimension* as well as the temporal resolution required for production processes—*temporal dimension*. In the short term, multimodality via (software-based) data fusion will continue to be developed, while in the long term, new hardware solutions combining several dimensions shall find their way into industrial applications, for example: high-speed spectroscopic impedance imaging and multimodality optical/acoustic/ET.

For process industries, process control still relies on easy parameters, which have not taken advantages of new observations of the process status to improve control strategies. The process is, however, too complex to be represented by just temperature and pressure, such as in petroleum and chemical engineering. The distinct advantages of multiphase flow process imaging (in special process tomography) provide sufficient process information, such as phase fraction, velocity and flow patterns, to facilitate developing new control strategies to further refine the process. There have been a number of research outcomes focusing on the extraction of key parameters of multiphase flow with process imaging tools, which can be of great help to process control [236] in the short term. However, the control realm is still not aware of such a new observer that can provide direct observations on the target process parameters and status, which would be an emerging area for the process control industry that certainly needs multidisciplinary approach from a control and instrumentation perspective in the long term.

### Concluding remarks

At present, modern industry is marching towards digitalization and intelligence, such as digital twin, which requires abundant information regarding the flow behaviors to diagnose or prognose about the process status and development. This is a newly developing application area of process imaging that is calling for more contributions in sensing methods and data analysis from both the academic and industrial endeavors. Hence, improvement in hardware allied to data fusion of multidimensional (time, energy, mode and space) imaging technology together with AI shall place multiphase flow process imaging into the next level.

### 13. Particle image velocimetry (PIV)

Sayantana Bhattacharya<sup>1</sup> and Pavlos Vlachos<sup>2</sup>

<sup>1</sup> Department of Mechanical Engineering, University of Maryland, Baltimore County, MD 21250, United States of America

<sup>2</sup> School of Mechanical Engineering, Purdue University, West Lafayette, IN 47907, United States of America

E-mail: sbhattac@umbc.edu and pvlachos@purdue.edu

#### Status

PIV is a prevalent technique in the field of non-invasive flow measurement. It measures the instantaneous velocity field by cross-correlating the recorded images of tracer particles in flow. Over decades of evolution in methodology and associated hardware, PIV has established itself in widespread applications. Error analysis and optimization have made PIV viable for planar (two dimensional two component (2D2C) and two dimensional, 3 component (2D3C stereo)), multi-camera volumetric (3D3C), and even single-camera volumetric velocity field measurements. However, the interplay of various independent design parameters and the complexity of the measurement chain still requires an expert user to acquire a reliable velocity field. Uncertainty quantification (UQ) in such measurements [237] is critical for assessing the reliability of measurements, acquiring tolerance on derived quantities that directly affect design decisions, and validating numerical simulations or comparing multi-modal measurements.

During the last decade, a significant effort focused on uncertainty in planar PIV measurements. Indirect UQ methods calibrated the sensitivity of the cross-correlation (CC) plane SNR metrics [238–240] and primary error sources to measurement uncertainty. A more direct approach used statistical analysis of particle image mismatch or ‘disparity’ statistics [241]. A pixel-wise image intensity covariance propagation through correlation peak 3-point fitting also yielded reliable displacement uncertainty estimates [242]. A parallel approach computed the second-order moment [243] of the PDF of error distribution directly extracted from the CC-plane. Comparative analysis [244, 245] (figure 20(a)) for experimental jets and wakes has shown better response and prediction for direct UQ methods. The sensitivity of the direct UQ methods to image SNR perturbations is used to formulate a meta-uncertainty model [246] for improved uncertainty prediction in planar PIV, as shown in figure 20(b).

Subsequent studies have focused on uncertainty propagation in displacement-derived quantities [247], e.g. vorticity, turbulent kinetic energy, Reynolds stress, etc. Velocity uncertainty values have improved pressure field estimation using a generalized least squares method [248]. UQ in background oriented schlieren (BOS) density estimates also incorporate PIV displacement uncertainties [249]. In micro-scale PIV, the existing UQ methods can successfully predict uncertainty in ensemble correlation measurement [250]. For

stereo PIV measurement, an uncertainty model quantifying calibration uncertainty and its contribution to overall 2D3C field uncertainty (figure 20(c)) is established [251]. Though uncertainty propagation through volumetric self-calibration and 2D CC based UQ methods exist [252], a comprehensive framework for 3D PIV UQ is yet to be established.

A prominent growth in PIV uncertainty methodology, its impact on flow measurement reliability and velocity field denoising [253, 254] (figures 21(c) and (d)), and lack of bias and random uncertainty models for complex measurement processes begets the need for further development. In particular, challenges remain for UQ in multi-camera and single-camera volumetric measurements, specific flow applications (high-speed, near wall, optical distortion), processing settings automation (covariance due to grid-overlap, numerical uncertainty due to discretization), dense field estimation (CNN, PINN’s) and data assimilation (using ML algorithms).

#### Current and future challenges

Existing PIV uncertainty estimation methods use an *a-posteriori* image or correlation plane information to predict the error bound on the velocity field. Although these methods reasonably predict the aleatoric uncertainty, the epistemic uncertainty in the different components of the measurement model has not been established. A detailed UQ for each element of the imaging model and processing parameters is critical to better assess the bias uncertainty in the presence of optical distortion, velocity fluctuations, near wall measurement, peak-locking, high dynamic range, particle acceleration, varying window size, grid overlap, and vector field validation. Recent efforts to quantify PIV systematic uncertainty has relied on the calibration of UQ method sensitivity to error sources, e.g. the ‘uncertainty surface’ method [255]. Alternatively, statistical analysis of repeated experiments has reported bias uncertainty on mean velocity for varying experimental factors (e.g. interframe time, aperture, light sheet thickness, etc) in a boundary-layer flow, as shown in figures 21(a) and (b) [256]. Uncertainty in time-averaged fields due to peak locking error was estimated using a multi-interframe time acquisition with least squares regression [257]. However, these approaches are neither exhaustive nor generalized for all types of flows, enabling the need for a direct automated bias uncertainty framework.

Volumetric PIV uses a tomographic reconstruction to estimate the 3D field from 2D projections. Camera calibration, view overlap, viewing angles, varying magnification, depth of field, volume aspect ratio, particle concentration, etc play a significant role in the dispersion of 3D3C measurements. The sensitivity of those parameters is specific to the reconstruction method. The complexity of the measurement chain makes bias and random uncertainty estimation non-trivial. Limited optical access has driven the methodology from multi-camera 3D PIV (multiplicative algebraic reconstruction technique, defocusing PIV, synthetic aperture PIV, coaxial volumetric velocimetry) to single-camera 3D3C measurements (holographic and plenoptic PIV). Recent advancements have focused on

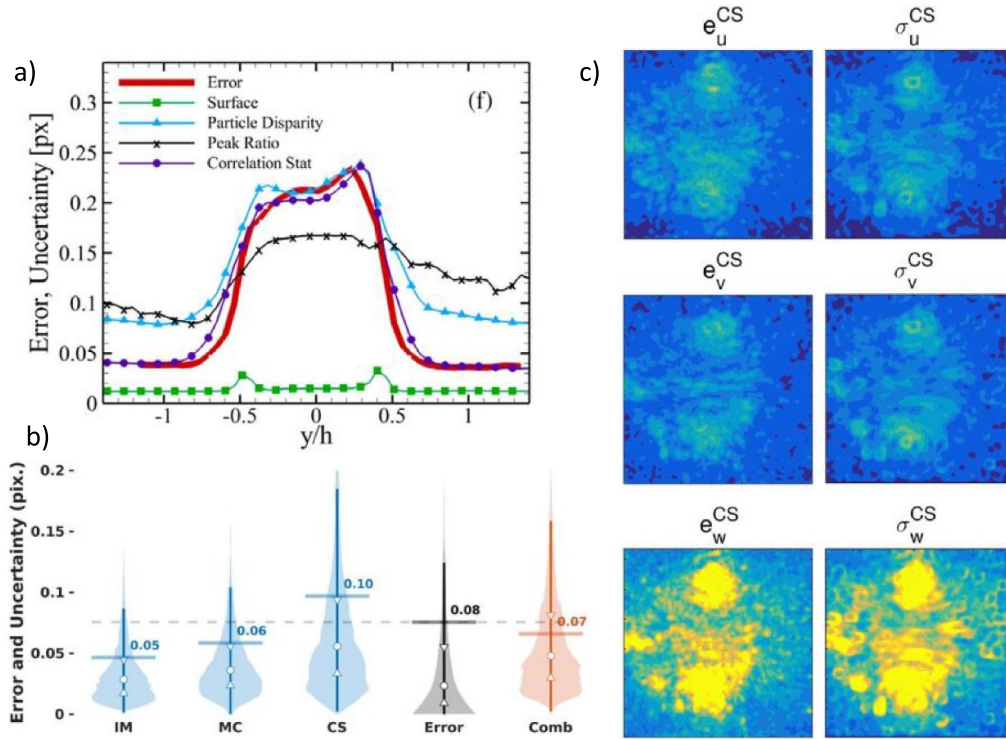


**Figure 20.** (a) Shows comparison of direct and indirect uncertainty methods for benchmark PIV experiments. Reproduced from [244]. © IOP Publishing Ltd. All rights reserved. (b) Further improvement using meta-uncertainty model compared to existing direct methods (IM, MC, CS). Reproduced from [246]. © IOP Publishing Ltd. All rights reserved. (c) Stereo PIV measurement RMS error and RMS uncertainty spatial distributions for 4th PIV challenge case E data. Reproduced from [251]. © IOP Publishing Ltd. All rights reserved.

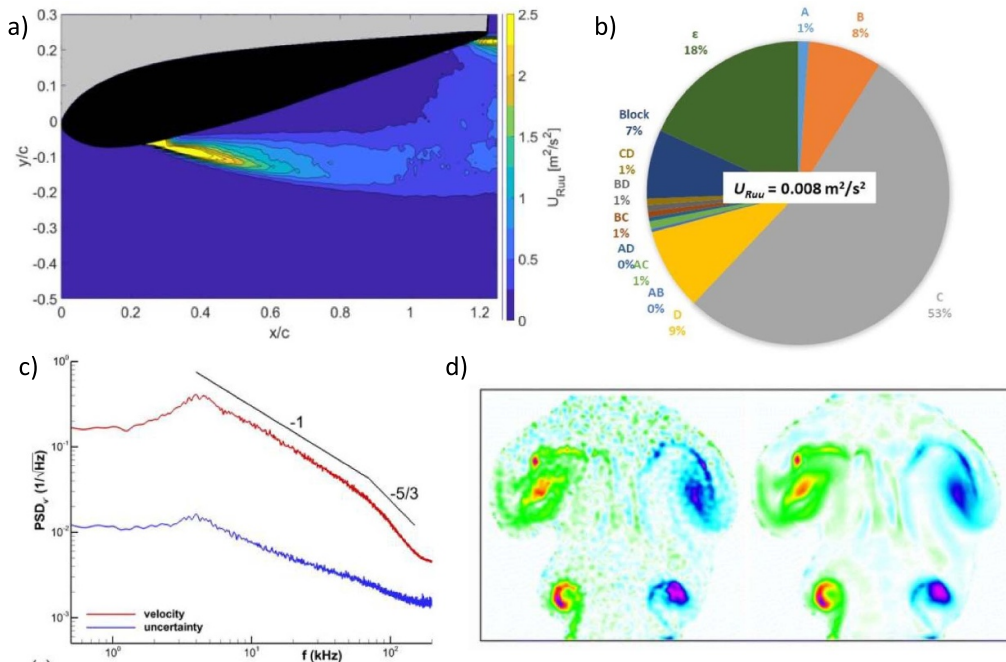


**Figure 21.** (a) Estimated total uncertainty using DOE ANOVA methodology and (b) contribution of systematic uncertainty due to different error sources in potential flow region. Reproduced from [256]. CC BY 4.0. (c) Uncertainty and velocity power spectral density and its correlation in low and middle frequency range for high-speed flow. Reproduced with permission from [254]. (d) Original and filtered vorticity field after uncertainty based denoising for a vortex ring. Reproduced with permission from [253].

x-ray PIV for interior flow measurements. With increased applications, impetus in development, and non-linear combinations and contributions from several experimental parameters, UQ in 3D PIV is critical and an existing challenge in the field.

In flows with refractive index gradients (supersonic flows, density stratified flows), simultaneous estimation of density field variation, and flow velocity poses a significant challenge due to the coupling of measurement errors. Simultaneous PIV-BOS type experiments have been recently performed. However, a systematic analysis of uncertainty propagation is lacking in such applications. In micro-flow applications, confocal imaging with a controlled depth of field using raster scanning of pixels introduce a bias error in measurement. However, uncertainty in microscale measurements and dependence on different confocal system transfer functions is yet to be determined.

### Advances in science and technology to meet challenges

Technological advancements in high energy fast repetition rate lasers and high-resolution, high-speed cameras have standardized time-resolved (TR) regular or multi-pulse PIV measurements, pushing the sampling rate even to the megahertz range. Associated improvements in dynamic velocity range (DVR) and better spatial-temporal resolution can reduce the Cramér-Rao lower bound of the physical variable measurements [258, 259]. Consistent developments in UQ algorithms are required to compare and assess the performance of comparable PIV systems. Especially, error bounds in instantaneous PIV fields with pyramid correlation, multi-pulse systems, and KHz range TRPIV systems should be compared to optimize PIV system requirements for high DVR experiments.

Modern-day computational resources, GPU's and accessible ML algorithms have paved the way for NN based PIV measurements. Data-driven measurements with supervised learning (CNN) can estimate pixel-wise dense displacement fields based on an optical flow network model. However, the predictions are limited by the training dataset. UQ and flow and imaging parameters sensitivity in data-driven PIV fields need further exploration. A recent approach

explored Bayesian formulation for volumetric reconstruction with stochastic gradient descent. Extending the framework to develop a forward model for image intensity distribution and optical system distortion and incorporating a plenoptic [260] or holographic PIV mapping function model can directly benefit the 3D flow field uncertainty estimation. Data assimilation also plays a key role in noise reduction and dense field reconstructions using physics-informed networks (PINN) or multiple measurement modes. Quantification of instantaneous PIV field uncertainty is critical for assessing the reliability of such combined data analysis.

UQ has been applied to denoise data and reduces spatial errors in the post-processing step. Temporal denoising on high-frequency TRPIV data has shown a strong correlation between velocity and uncertainty spectrum for low to midrange frequencies. However, current algorithms are limited in predicting uncertainty bounds for high-frequency fluctuations in PIV measurements. An increasing demand for automated running PIV systems for product design and quality control is observed as PIV technology transitions to industrial applications. Hence, a breakthrough in new algorithms and pathways for PIV UQ will immensely benefit the state-of-the-art in obtaining reliable PIV measurements.

### Concluding remarks

We discussed up-to-date UQ methods and addressed some critical challenges for UQ development in modern PIV techniques. Rapid growth in PIV applications and methodology will require continued growth in modeling uncertainty for instantaneous PIV fields. Upcoming research should focus on volumetric PIV uncertainty estimation for tomographic PIV as well as newer single or multi-camera techniques. Modeling uncertainty in individual components of PIV imaging and processing is critical to quantify systematic uncertainty effectively and, in turn, the overall uncertainty in the measurements. The sensitivity of UQ methods needs exhaustive testing for complex and challenging applications across a broader range of lengths and time scales. Overall, the development of real-time automated end-to-end measurements for PIV systems should significantly benefit from UQ development efforts in this decade.

## 14. Microscopic particle image velocimetry ( $\mu$ PIV)

Christian Cierpka<sup>1</sup> and Massimiliano Rossi<sup>2</sup>

<sup>1</sup>Institute of Thermodynamics and Fluid Mechanics, Technische Universität Ilmenau, Helmholtzring 1, 98693 Ilmenau, Germany

<sup>2</sup>Department of Industrial Engineering, Alma Mater Studiorum Università di Bologna, Via Fontanelle 40, 47121 Forlì, Italy

E-mail: christian.cierpka@tu-ilmenau.de  
and massimiliano.rossi13@unibo.it

### Status

Microfluidic devices, i.e. fluidic systems with typical channel dimensions in the sub-millimetric range, have several advantages in comparison to macroscopic systems. Especially in fields such as process engineering, micro reaction technology, biomedical research, and pharmaceutical applications, the reduction in size allows for a precise handling of small fluid volumes, particles and biological samples. Downscaling is beneficial if expensive chemicals are used, for the investigation and manipulation of individual biological specimens, for automated drug-response screening, or for lowering the amount of energy needed for the production of specific particles/chemicals, to name a few. Due to the different scaling of forces it is also possible to exploit several unconventional physical mechanisms for particle manipulation or flow generation. In this respect, acoustic, electric, magnetic, or even temperature or light fields have been used. Although the flow is typically laminar and the geometries are small, numerical simulations are cumbersome. Often the boundary conditions (e.g. electric potentials, surface chemistry, surface physics, etc) are unknown due to the complex geometries and the uncertainties given by the specific fabrication techniques (lithography, etching, deposition, 3D printing, etc). Therefore, reliable high spatially resolved measurements of the velocity field (and other scalar fields) are necessary. Due to the small dimensions, probes would alter the flow to a large extent and optical methods have to be applied.

$\mu$ PIV was proposed in the late 1990s as an adaptation of the conventional planar PIV to microscopic setups, and it quickly became the standard velocimetry method in this field [261]. The typical  $\mu$ PIV setup has remained basically unchanged since its first application [262, 263] and is shown in figure 22. Small fluorescent tracer particles that should ideally follow the flow are added to the fluid. These particles are illuminated in a volume by a laser light source or an LED and the longer wavelength emitted light is reflected towards the camera whereas the direct reflections are filtered. Two images are recorded one after another and the average particle image displacement inside interrogation windows is estimated using CC as in conventional PIV (comp. section on PIV).

The emergence of global threats such as pandemics and pollution, has given a new impulse to the improvement and development of microfluidic technologies, especially with

respect to biological and biochemical analytical devices. Consequently, improvements in the resolution, accuracy, and capabilities of velocimetry methods for microfluidics will be crucial to support the future technological developments.

### Current and future challenges

Several challenges are inherent in the  $\mu$ PIV technique. Since the seeding concentration is typically low in microfluidics to not alter the fluid properties, the interrogations windows need often to be large with respect to gradients in the flow. In the out-of-plane direction, additional averaging occurs due to the volume illumination and the three-dimensionality of the flow. Particles outside the focal plane still contribute to the CC function which results in a depth wise average, quantified in terms of depth of correlation (DOC, figure 22, right). The DOC is typically in the order of tens of micrometers which may reach a considerable part of the channel dimensions [264]. Although correlation averaging [264] and some advanced algorithms can be used to mitigate these effects [265], these challenges (volume illumination, three-dimensional flow, limited optical access) cannot be avoided in microfluidic imaging techniques, and will inevitably affect  $\mu$ PIV measurements.

At the beginning of 2010s, several research groups start to use slightly modified  $\mu$ PIV setups for 3D Lagrangian particle tracking, essentially exploiting the defocusing principle with different approaches [266]. These methods, here generally referred to as defocusing particle tracking (DPT), have great potential for the full characterization of microfluidic phenomena. DPT methods do not suffer from averaging problems and use the defocus information for 3D particle tracking [266, 267]. For an ideal optical setup, the defocus function is symmetric around the focal plane. In real experiments, optical aberrations or an additional cylindrical lens can provide a non-symmetric (thus unambiguous) defocus function in dependence of the depth coordinate. If a model for the defocus is known, this can be directly used to relate e.g. the size or shape of a particle image to depth. This approach works well for well-defined optical systems, high signal to noise ratios and non-overlapping particle images from point sources with uncertainties in the depth direction of the order of 1%–2% of measurement depth [266, 267, 268]. To avoid image overlap the seeding concentration has to be low, which lowers the resolution. A proper measure for the seeding concentration in the case of large particle images is the source density  $N_s$ , a nondimensional parameter which is the ratio between the sum of the particle image areas and the full image area [269]. Low source densities are especially problematic for non-stationary flows, where time averaging cannot be used to increase the spatial resolution. Another recent approach used a pattern recognition based on the correlation with templates obtained from experimental images [270]. Especially in cases with high seeding concentration, this approach is capable of determining the position of overlapping particle images to a certain extent, corresponding to a source density  $N_s \sim 0.2/0.3$  [3, 270]. However, it still requires a monomodal particle distribution.

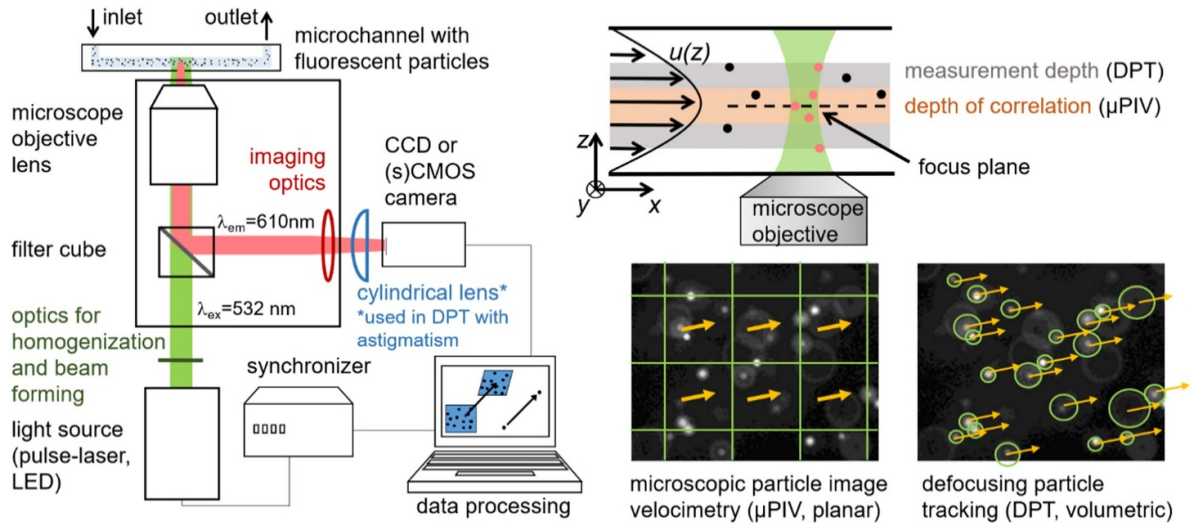


**Figure 22.** Schematic of a typical  $\mu$ PIV setup using fluorescent particles to avoid reflections from the channel walls. In  $\mu$ PIV analysis the images are processed using cross-correlation providing a planar two-components (2D2C) measurement of the flow, averaged across a certain depth of correlation. The same setup (with small modifications, e.g. with a cylindrical lens), can be used for defocusing particle tracking (DPT), obtaining a volumetric three-component (3D3C) measurement of the flow across a measurement depth determined by the imaging system and particle size. Reproduced from [266]. CC BY 4.0.

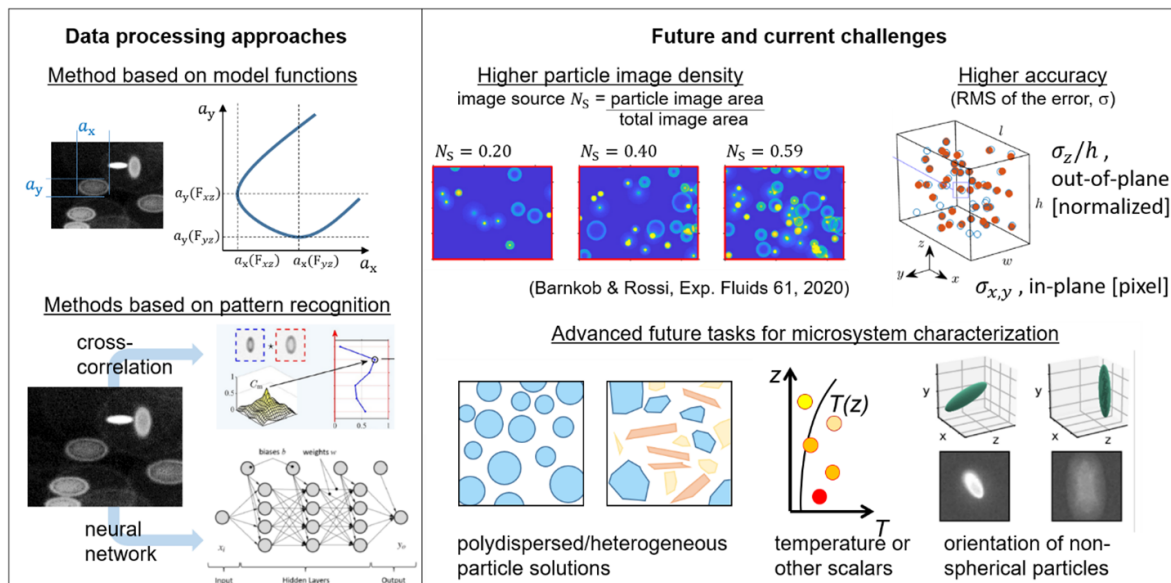


**Figure 23.** Current and future challenges in DPT methods for microfluidics. Development of new algorithms based on ML and neural networks. Improvement of resolution (seeding density) and accuracy. Measurement of monodispersed/heterogeneous particle distribution. Measurement of additional quantities (e.g. temperature, orientation of non-spherical particles). Reproduced from [270], with permission from Springer Nature.

### Advances in science and technology to meet challenges

The DPT approaches with a large future potential are the ones based on ML and in particular NNs, which are however still at an early stage of development, see figure 23, left. ML as a part of AI has gained lot of attention for many different applications in fluid dynamics during recent years, and is currently the most promising candidate to meet the above-mentioned challenges [271]. The basic idea is that a network learns the

behavior of a complex system on the basis of training data without any knowledge of the underlying mechanisms. A use case for ML tools are all the different approaches of defocus  $\mu$ PTV. The first approaches showed a similar performance as for the classical methods and used predefined cropped images [272]. In a recent study, different network architectures were combined to perform the task of particle image detection, depth regression and classification for a multimodal size distribution of particles [273, 274]. The big advantage of such networks is that they show a similar performance in terms of



uncertainty like the classical approach and also work well with overlapping particle images, without the need for monomodal size distribution.

The development of new algorithms based on NNs will allow to process images with a large source density and better accuracy, even with noisy data. These networks can be adopted to also measure scalars or additional quantities (e.g. temperature, pH, concentration, particle type, particle size, particle orientation, etc., see figure 23, right) [271, 275]. If optimized they are also fast enough for a feedback control for example the active sorting of particles or biological specimens. In addition, the networks can be pretrained and adopted easily to different experimental conditions by non-expert users so that they will find a bigger application in medical and biological research as well as in fluid mechanics and engineering.

However, the development of methods based on ML and NN must be supported at the same time by an adequate effort from the DPT community in the preparation and sharing of benchmark datasets with training/validation/test images, as done for instance from the DL and computer vision community with the ImageNet project [276]. This is necessary not only for the development and assessment of the methods, but also to make these methods effectively applicable on real applications.

## Concluding remarks

The future development of velocimetry methods for microfluidics goes in the direction of particle tracking methods based on defocusing, with algorithms relying on ML and NNs. These methods are based on conventional  $\mu$ PIV setups, but have the potential to achieve unprecedented performance in terms of resolution, accuracy, robustness and speed.

Together with the development of new algorithms, it is crucial to establish a systematic and widely-accepted benchmark for evaluation and comparison of the different methods. This aspect has generally been overlooked by the DPT community, and most research groups propose their own method on their own dataset, making impossible to give a fair comparison and to effectively quantify the advancement of the processing techniques. An example of standardized dataset based on synthetic images [269] was recently proposed by the authors [3]. We encourage the community to make use of this dataset and to prepare and share new datasets with different type of images, experimental conditions, and so on. The transition to methods relying on ML will necessarily require a large amount of reference dataset to train and validate the NNs [272] and to make these techniques applicable in real experiments.

## Acknowledgements

CC acknowledges financial support under the German research foundation (DFG) Grant Number 522226046 and 537846345 and the Carl Zeiss Foundation under Grant 'DeepTurb'. MR acknowledges the financial support by the VILLUM foundation, Grant No. 00036098.

## Data availability statement

No new data were created or analyzed in this study.

## ORCID iDs

Jung-Ryul Lee  <https://orcid.org/0000-0003-0742-4722>  
 Hongki Yoo  <https://orcid.org/0000-0001-9819-3135>  
 Chia Chen Ciang  <https://orcid.org/0000-0003-0384-7648>  
 Young-Jin Kim  <https://orcid.org/0000-0002-4271-5771>  
 Daehee Kim  <https://orcid.org/0000-0001-6648-5379>  
 Teow Wee Teo  <https://orcid.org/0000-0003-1897-7488>  
 Zeinab Mahdavi pour  <https://orcid.org/0000-0002-8136-4548>  
 Mohd Zaid Abdullah  <https://orcid.org/0000-0002-5747-9812>  
 Andrew Yacoot  <https://orcid.org/0000-0001-6740-821X>  
 Kyung Chun Kim  <https://orcid.org/0000-0002-7943-9774>  
 Jiamin Ye  <https://orcid.org/0000-0001-5061-6135>  
 Xiao Liang  <https://orcid.org/0000-0001-9127-7096>  
 Jianqing Huang  <https://orcid.org/0000-0002-3480-8513>  
 Weiwei Cai  <https://orcid.org/0000-0003-2333-7282>  
 Marco J da Silva  <https://orcid.org/0000-0003-1955-8293>  
 Chao Tan  <https://orcid.org/0000-0001-5146-4807>  
 Pavlos Vlachos  <https://orcid.org/0000-0002-8040-9257>  
 Christian Cierpka  <https://orcid.org/0000-0002-8464-5513>  
 Massimiliano Rossi  <https://orcid.org/0000-0002-6579-7132>

## References

- [1] Ma S, Yang S and Xing D 2010 Photoacoustic imaging velocimetry for flow-field measurement *Opt. Express* **18** 9991–10000
- [2] Zhao S, Miao Y, Chai R, Zhao J, Bai Y, Wei Z and Ren S 2022 High-precision electrical impedance tomography for electrical conductivity of metallic materials *Adv. Mater. Sci. Eng.* **2022** e3611691
- [3] Barnkob R, Cierpka C, Chen M, Sachs S, Mäder P and Rossi M 2021 Defocus particle tracking: a comparison of methods based on model functions, cross-correlation, and neural networks *Meas. Sci. Technol.* **32** 094011
- [4] Barredo Arrieta A *et al* 2020 Explainable artificial intelligence (XAI): concepts, taxonomies, opportunities and challenges toward responsible AI *Inf. Fusion* **58** 82–115
- [5] Royo S and Ballesta-garcia M 2019 An overview of LIDAR imaging systems for autonomous vehicles *Appl. Sci.* **9** 4093
- [6] Rapp J, Tachella J, Altmann Y, McLaughlin S and Goyal V K 2020 Advances in single-photon Lidar for autonomous vehicles: working principles, challenges, and recent advances *IEEE Signal Process. Mag.* **37** 62–71
- [7] Wang L, Zhang Y and Wang J 2017 Map-based localization method for autonomous vehicles using 3D-LIDAR *IFAC-PapersOnLine* **50** 276–81
- [8] Vodisch N, Unal O, L. K, van Gool L and Dai D 2022 End-to-end optimization of LiDAR beam configuration for 3D object detection and localization *IEEE Robot. Autom. Lett.* **7** 2242–9

- [9] Weiss U and Biber P 2011 Plant detection and mapping for agricultural robots using a 3D LIDAR sensor *Robot. Auton. Syst.* **59** 265–73
- [10] Wang S, Jiang L, Meng J, Xie Y and Ding H 2021 Training for smart manufacturing using a mobile robot-based production line *Front. Mech. Eng.* **16** 249–70
- [11] Zheng L, Fu Z and Xiaoping H 2021 Low-cost retina-like robotic lidar based on incommensurable scanning *IEEE/ASME Trans. Mechatronics* **27** 58–68
- [12] Zhi Y, Li S, Tom D and Nicola B 2019 Multi-sensor online transfer learning for 3D LiDAR-based human detection with a mobile robot *2018 IEEE/RSJ International Conference on Intelligent Robots and Systems (IEEE)* (<https://doi.org/10.1109/IROS.2018.8593899>)
- [13] Kai-Tai S, Chien-Wei C, Li-Ren K, Yu-Xuan S and Ching-Hao M 2020 Autonomous docking in a human-robot collaborative environment of automated guided vehicles *2020 International Automatic Control Conference (IEEE)* (<https://doi.org/10.1109/CACS50047.2020.9289713>)
- [14] Di S, Guang-Mao T and Jiaqi L 2021 Real-time localization measure and perception detection using multi-sensor fusion for automated guided vehicles *2021 40th Chinese Control Conf. (IEEE)* (<https://doi.org/10.23919/CCC52363.2021.9550235>)
- [15] Seigo I, Shigeyoshi H, Mitsuhiro O, Hiroyuki M and Masaru O 2018 Small imaging depth LIDAR and DCNN-based localization for automated guided vehicle *Sensors* **18** 177
- [16] Anusuya Datta Did you know which are the sources for free LiDAR data? (available at: [www.geospatialworld.net/blogs/did-you-know-the-sources-for-free-lidar-data/](http://www.geospatialworld.net/blogs/did-you-know-the-sources-for-free-lidar-data/))
- [17] Robert J Willett Industry 4.0 and Machine Vision- Industry 4.0 (available at: [www.cognex.com/what-is/industry-4-0-machine-vision](http://www.cognex.com/what-is/industry-4-0-machine-vision))
- [18] John S Burgess 1961 The future of radar *IRE Trans. Mil. Electron.* **2** 32–38
- [19] Lee J, Kim Y-J, Lee K, Lee S and Kim S-W 2010 Time-of-flight measurement with femtosecond light pulses *Nat. Photon.* **4** 716–20
- [20] Lamb R A 2010 A technology review of time-of-flight photon counting for advanced remote sensing *Proc. SPIE* **7681** 768107
- [21] Prochazka I 2005 Semiconducting single photon detectors: the state of the art *Phys. Status Solidi c* **2** 1524–32
- [22] Giorgetta F R, Baumann E, Knabe K, Coddington I and Newbury N R 2012 High-resolution ranging of a diffuse target at sub-millisecond intervals with a calibrated FMCW lidar *CLEO 2012 (IEEE)* pp 1–2
- [23] Fumin Z, Lingping Y and Xinghua Q 2020 Simultaneous measurements of velocity and distance via a dual-path FMCW lidar system *Opt. Commun.* **474** 126066
- [24] Godbaz J P, Dorrington A A and Cree M J 2013 Understanding and ameliorating mixed pixels and multipath interference in AMCW lidar *TOF Range-Imaging-Cameras* pp 91–116 (Springer)
- [25] Dingkan W, Lenworth T, Sanjeev K, Yingtao D and Huikai X 2020 A low-voltage, low-current, digital-driven MEMS mirror for low-power LiDAR *IEEE Sens. Lett.* **4** 5000604
- [26] Poulton C V, Russo P, Timurdogan E, Whitson M, Byrd M J, Hosseini E, Moss B, Su Z, Vermeulen D and Watts M R 2018 High-performance integrated optical phased arrays for chip-scale beam steering and LiDAR *CLEO 2018 (OSA)* ([https://doi.org/10.1364/CLEO\\_AT.2018.ATu3R.2](https://doi.org/10.1364/CLEO_AT.2018.ATu3R.2))
- [27] Joule J P 1847 XVII. On the effects of magnetism upon the dimensions of iron and steel bars *London, Edinburgh Dublin Phil. Mag. J. Sci.* **30** 76–87
- [28] Chia C C, Lee S Y, Harmin M Y, Choi Y and Lee J-R 2023 Guided ultrasonic waves propagation imaging: a review *Meas. Sci. Technol.* **34** 052001
- [29] Ahmed H, Mohsin A, Hong S-C, Lee J-R and Ihn J-B 2021 Robotic laser sensing and laser mirror excitation for pulse-echo scanning inspection of fixed composite structures with non-planar geometries *Measurement* **176** 109109
- [30] Bae D-Y and Lee J-R 2015 Development of single channelled serial-connected piezoelectric sensor array and damage visualization based on multi-source wave propagation imaging *J. Intell. Mater. Syst. Struct.* **27** 1861–70
- [31] Flynn E B and Jarmer G S 2013 High-speed, non-contact, baseline-free imaging of hidden defects using scanning laser measurements of steady-state ultrasonic vibration *Proc. IWSHM 2013 (September 2013)* (Destech Publications) pp 1186–93
- [32] Xue H, Yang Y and Zhang B 2022 Topological acoustics *Nat. Rev. Mater.* **7** 974–90
- [33] Schaeffer M, Trainiti G and Ruzzene M 2017 Optical measurement of in-plane waves in mechanical metamaterials through digital image correlation *Sci. Rep.* **7** 42437
- [34] Legrand F, Gérardin B, Bruno F, Laurent J, Lemoult F, Prada C and Aubry A 2021 Cloaking, trapping and superlensing of lamb waves with negative refraction *Sci. Rep.* **11** 23901
- [35] Li L, Jiao J, Gao X, Jia Z, Wu B and He C 2022 A review on nondestructive testing of bonding interface using nonlinear ultrasonic technique *Chin. Sci. Bull.* **67** 621–9
- [36] Yan G, Raetz S, Chigarev N, Blondeau J, Gusev V E and Tournat V 2020 Cumulative fatigue damage in thin aluminum films evaluated non-destructively with lasers via zero-group-velocity Lamb modes *NDT&E Int.* **116** 102323
- [37] Jeon J Y, Kim D, Park G, Flynn E, Kang T and Han S 2020 2D-wavelet wavenumber filtering for structural damage detection using full steady-state wavefield laser scanning *NDT&E Int.* **116** 102343
- [38] Shin A, Park J, Lee H, Choi Y and Lee J-R 2022 Corrosion visualization under organic coating using laser ultrasonic propagation imaging *Smart Struct. Syst.* **29** 301–9
- [39] Abetew A D, Truong T C, Hong S C, Lee J R and Ihn J B 2020 Parametric optimization of pulse-echo laser ultrasonic system for inspection of thick polymer matrix composites *Struct. Health Monit.* **19** 443–53
- [40] Chen J, Fei C, Lin D, Gao P, Zhang J, Quan Y, Chen D, Li D and Yang Y 2022 A review of ultra high frequency ultrasonic transducers *Front. Mater.* **8** 733358
- [41] Saito O, Sen E, Okabe Y, Higuchi N, Ishizuki H and Taira T 2020 Laser wavelengths suitable for generating ultrasonic waves in resin-coated carbon fiber composites *J. Nondestruct. Eval. Diagn. Progn. Eng. Syst.* **3** 031103
- [42] Wang W and Yang Y 2022 Generation of selective single-mode guided waves by d36 type piezoelectric wafer *Appl. Phys. Lett.* **120** 214101
- [43] Miao H and Li F 2021 Shear horizontal wave transducers for structural health monitoring and nondestructive testing: a review *Ultrasonics* **114** 106355
- [44] Shahrim M A A, Chia C C, Ramli H R, Harmin M Y and Lee J-R 2023 Adaptive mode filter for lamb wavefield in the wavenumber-time domain based on wavenumber response function *Aerospace* **10** 4
- [45] Yun H, Rayhana R, Pant S, Genest M and Liu Z 2021 Nonlinear ultrasonic testing and data analytics for damage characterization: a review *Measurement* **186** 110155

- [46] Qi B-L, Wang C-H, Guo D-B and Zhang B 2021 A scanning distortion correction method based on X—Y galvanometer Lidar system *Chin. Phys. B* **30** 044206
- [47] Li Y, Dieuusaert E and Baets R 2022 Miniaturization of laser Doppler vibrometers—a review *Sensors* **22** 4735
- [48] Kilpatrick J M and Markov V B 2010 Full-field laser vibrometer for instantaneous vibration measurement and non-destructive inspection *Key Eng. Mater.* **437** 407–11
- [49] Chang H-Y and Yuan F-G 2020 Visualization of hidden damage from scattered wavefield reconstructed using an integrated high-speed camera system *Struct. Health Monit.* **20** 1475921720940805
- [50] Doan N V, Goo N S, Ko Y, Seo S and Chung M 2022 Design and analysis of micro-vibration isolation system for digital image correlation system-based structural health monitoring *Int. J. Aeronaut. Space Sci.* **23** 711–22
- [51] Chiou Y C and Liu J Z 2011 Recent crack detection of multi-crystalline silicon solar wafer using machine vision techniques *Sens. Rev.* **31** 154–65
- [52] Bidiville A, Wasmer K, Michler J, Nasch P M, Van der Meer M and Ballif C 2010 Mechanisms of wafer sawing and impact on wafer properties *Prog. Photovolt. Res. Appl.* **18** 563–72
- [53] Li Z, Ge P, Bi W, Li C, Wang C and Meng J 2021 Influence of silicon anisotropy on surface shape deviation of wafer by diamond wire saw *Mater. Sci. Semicond. Process.* **133** 105981
- [54] Teo T W, Mahdavi-pour Z and Abdullah M Z 2019 Design of an imaging system for characterizing micro-cracks in crystalline silicon solar cells using light transfection *IEEE J. Photovolt.* **9** 1097–104
- [55] Zimmermann C G 2019 Photoluminescence-based detection of mechanical defects in multijunction solar cells *J. Appl. Phys.* **126** 044503
- [56] Tang W, Yang Q, Hu X and Yan W 2022 Convolution neural network based polycrystalline silicon photovoltaic cell linear defect diagnosis using electroluminescence images *Expert Syst. Appl.* **202** 117087
- [57] Fu Y, Ma X and Zhou H 2021 Automatic detection of multi-crossing crack defects in multi-crystalline solar cells based on machine vision *Mach. Vis. Appl.* **32** 1–14
- [58] Sio H C, Xiong Z, Trupke T and Macdonald D 2012 Imaging crystal orientations in multicrystalline silicon wafers via photoluminescence *Appl. Phys. Lett.* **101** 082102
- [59] Teo T W, Mahdavi-pour Z and Abdullah M Z 2020 Recent advancements in micro-crack inspection of crystalline silicon wafers and solar cells *Meas. Sci. Technol.* **31** 081001
- [60] Zhang X, Hao Y, Shangguan H, Zhang P and Wang A 2020 Detection of surface defects on solar cells by fusing multichannel convolution neural networks *Infrared Phys. Technol.* **108** 103334
- [61] Feldman D, Dummit K, Zuboy J, Heeter J, Xu K and Margolis R 2022 *Spring 2022 Solar Industry Update* (National Renewable Energy Lab) NREL/PR-7A40-82854
- [62] Zafirovska I, Juhl M K, Weber J W, Wong J and Trupke T 2017 Detection of finger interruptions in silicon solar cells using line scan photoluminescence imaging *IEEE J. Photovolt.* **7** 1496–502
- [63] Rahman M R U and Chen H 2020 Defects inspection in polycrystalline solar cells electroluminescence images using deep learning *IEEE Access* **8** 40547–58
- [64] Wang J, Bi L, Sun P, Jiao X, Ma X, Lei X and Luo Y 2022 Deep-learning-based automatic detection of photovoltaic cell defects in electroluminescence images *Sensors* **23** 297–318
- [65] Binomairah A, Abdullah A, Khoo B E, Mahdavi-pour Z, Teo T W, Noor N S M and Abdullah M Z 2022 Detection of microcracks and dark spots in monocrystalline PERC cells using photoluminescence imaging and YOLO-based CNN with spatial pyramid pooling *EJV Photovolt.* **13** 27
- [66] Omisore O M, Han S, Xiong J, Li H, Li Z and Wang L 2020 A review on flexible robotic systems for minimally invasive surgery *IEEE Trans. Syst. Man. Cybern.*
- [67] Pamudurthy V, Lodhia N and Konda V J 2020 Advances in endoscopy for colorectal polyp detection and classification *Baylor University Medical Center Proc.* (Taylor & Francis) pp 28–35
- [68] Ciuti G *et al* 2020 Frontiers of robotic colonoscopy: a comprehensive review of robotic colonoscopes and technologies *J. Clin. Med.* **9** 1648
- [69] Kaur M, Lane P M and Menon C 2021 Scanning and actuation techniques for cantilever-based fiber optic endoscopic scanners—a review *Sensors* **21** 251
- [70] Vasilakakis M, Koulaouzidis A, Marlicz W and Iakovidis D 2020 The future of capsule endoscopy in clinical practice: from diagnostic to therapeutic experimental prototype capsules *Gastroenterol. Rev./Przegląd Gastroenterologiczny* **15** 179–93
- [71] Zidane I F, Khattab Y, Rezeki S and El-Habrouk M 2022 Robotics in laparoscopic surgery—a review *Robotica* **41** 1–48
- [72] Shaukat A and Levin T R 2022 Current and future colorectal cancer screening strategies *Nat. Rev. Gastroenterol. Hepatol.* **19** 1–11
- [73] Iakovidis D K *et al* 2021 Roadmap on signal processing for next generation measurement systems *Meas. Sci. Technol.* **33** 012002
- [74] Khan T, Andrews E G, Gardner P A, Mallela A N, Head J R, Maroon J C, Zenonos G A, Babichenko D and Biehl J T 2022 AR in the OR: exploring use of augmented reality to support endoscopic surgery *ACM Int. Conf. on Interactive Media Experiences* pp 267–70
- [75] Chen W, Yan G, He S, Ke Q, Wang Z, Liu H and Jiang P 2013 Wireless powered capsule endoscopy for colon diagnosis and treatment *Physiol. Meas.* **34** 1545
- [76] Pittiglio G, Lloyd P, da Veiga T, Onaizah O, Pompili C, Chandler J H and Valdastrì P 2022 Patient-specific magnetic catheters for atraumatic autonomous endoscopy *Soft Robot.* **9** 1120–33
- [77] Anwar S, Khan S and Barnes N 2020 A deep journey into super-resolution: a survey *ACM Comput. Surv.* **53** 1–34
- [78] Zhang X, Otoo E-M, Fan Y, Tao C, Wang T and Rhode K 2022 Autostereoscopic 3D augmented reality navigation for laparoscopic surgery: a preliminary assessment *IEEE Trans. Biomed. Eng.* **70** 1413–21
- [79] Koulaouzidis A *et al* 2017 KID Project: an internet-based digital video atlas of capsule endoscopy for research purposes *Endosc. Int. Open* **5** E477–83
- [80] Borgli H *et al* 2020 HyperKvasir, a comprehensive multi-class image and video dataset for gastrointestinal endoscopy *Sci. Data* **7** 1–14
- [81] Rodrigues M, Mayo M and Patros P 2022 Surgical tool datasets for machine learning research: a survey *Int. J. Comput. Vis.* **130** 2222–48
- [82] Angelov P P, Soares E A, Jiang R, Arnold N I and Atkinson P M 2021 Explainable artificial intelligence: an analytical review *Wiley Interdiscip. Rev.* **11** e1424
- [83] Gao W, Xu Z, Han X and Pan C 2022 Recent advances in curved image sensor arrays for bioinspired vision system *Nano Today* **42** 101366
- [84] Hsiao J-H, Chang J-Y and Cheng C-M 2019 Soft medical robotics: clinical and biomedical applications, challenges, and future directions *Adv. Robot.* **33** 1099–111
- [85] Edelmann J, Petruska A J and Nelson B J 2017 Magnetic control of continuum devices *Int. J. Robot. Res.* **36** 68–85

- [86] Kalozoumis P G, Marino M, Carniel E L and Iakovidis D K 2022 Towards the development of a digital twin for endoscopic medical device testing *Digital Twins for Digital Transformation: Innovation in Industry* (Springer) pp 113–45
- [87] Vasilakakis M, Sovatzidi G and Iakovidis D K 2021 Explainable classification of weakly annotated wireless capsule endoscopy images based on a fuzzy bag-of-colour features model and brain storm optimization *Int. Conf. on Medical Image Computing and Computer-Assisted Intervention* (Springer) pp 488–98
- [88] Kaur Dhoot M, Fan I-S and Skaf Z 2020 Review of robotic systems for aircraft inspection *9th Int. Conf. on Through-life Engineering Service (TES)* (<https://doi.org/10.2139/ssrn.3718054>)
- [89] Gupta M, Khan M A, Butola R and Singari R M 2022 Advances in applications of non-destructive testing (NDT): a review *Adv. Mater. Process. Technol.* **8** 2286–307
- [90] Wei D, Hu S, Zhou Y, Ren X, Huo X, Yin J and Wu Z 2023 A magnetically actuated miniature robotic fish with the flexible tail fin *IEEE Robot. Autom. Lett.* **8** 6099–106
- [91] Sheppard C J R 2003 *Scanning Confocal Microscopy* (Marcel Dekker)
- [92] Yoo H, Lee S, Kang D, Kim T, Gweon D, Lee S and Kim K 2006 Confocal scanning microscopy: a high-resolution nondestructive surface profiler *Int. J. Precis. Eng. Manuf.* **7** 3–7
- [93] Hamilton D K and Wilson T 1982 Three-dimensional surface measurement using the confocal scanning microscope *Appl. Phys. B* **27** 211–3
- [94] Fabich M 2009 Advancing confocal laser scanning microscopy: the advantage of optical metrology *Opt. Photon.* **2** 40–44
- [95] Jordan H J, Wegner M and Tiziani H 1998 Highly accurate non-contact characterization of engineering surfaces using confocal microscopy *Meas. Sci. Technol.* **9** 1142–51
- [96] Conroy M and Armstrong J 2005 A comparison of surface metrology techniques *7th Int. Symp. on Measurement Technology and Intelligent Instruments* vol 13 pp 458–65
- [97] Sheppard C J R and Cogswell C J 1990 3-Dimensional image-formation in confocal microscopy *J. Microsc.* **159** 179–94
- [98] Lyda W, Gronle M, Fleischle D, Mauch F and Osten W 2012 Advantages of chromatic-confocal spectral interferometry in comparison to chromatic confocal microscopy *Meas. Sci. Technol.* **23** 054009
- [99] Kim C S and Yoo H 2021 Three-dimensional confocal reflectance microscopy for surface metrology *Meas. Sci. Technol.* **32** 102002
- [100] Sahl S J, Hell S W and Jakobs S 2017 Fluorescence nanoscopy in cell biology *Nat. Rev. Mol. Cell Biol.* **18** 685–701
- [101] Tanaami T, Otsuki S, Tomosada N, Kosugi Y, Shimizu M and Ishida H 2002 High-speed 1-frame/ms scanning confocal microscope with a microlens and Nipkow disks *Appl. Opt.* **41** 4704–8
- [102] Patel Y G, Rajadhyaksha M and DiMarzio C A 2011 Optimization of pupil design for point-scanning and line-scanning confocal microscopy *Biomed. Opt. Express* **2** 2231–42
- [103] Berge B and Peseux J 2000 Variable focal lens controlled by an external voltage: an application of electrowetting *Eur. Phys. J. E* **3** 159–63
- [104] Ruprecht A K, Wiesendanger T F and Tiziani H J 2004 Chromatic confocal microscopy with a finite pinhole size *Opt. Lett.* **29** 2130–2
- [105] Chun B S, Kim K and Gweon D 2009 Three-dimensional surface profile measurement using a beam scanning chromatic confocal microscope *Rev. Sci. Instrum.* **80** 073706
- [106] Kim T, Kim S H, Do D, Yoo H and Gweon D 2013 Chromatic confocal microscopy with a novel wavelength detection method using transmittance *Opt. Express* **21** 6286–94
- [107] Sun Y B, Zhao W Q, Qiu L R, Li R J and Wang Y 2019 Axial high-resolution differential confocal microscopy *Meas. Sci. Technol.* **30** 125402
- [108] Lee D R, Kim Y D, Gweon D G and Yoo H 2014 High speed 3D surface profile without axial scanning: dual-detection confocal reflectance microscopy *Meas. Sci. Technol.* **25** 125403
- [109] Yang C, Shi K B, Zhou M D, Zheng S Y, Yin S Z and Liu Z W 2012 Z-microscopy for parallel axial imaging with micro mirror array *Appl. Phys. Lett.* **101** 231111
- [110] Badon A, Bensussen S, Gritton H J, Awal M R, Gabel C V, Han X and Mertz J 2019 Video-rate large-scale imaging with multi-Z confocal microscopy *Optica* **6** 389–95
- [111] Wertheim D and Gillmore G 2014 Application of confocal microscopy for surface and volume imaging of solid state nuclear track detectors *J. Microsc.* **254** 42–46
- [112] Nanoscope Systems, Inc. 2023 (available at: [www.nanoscope.co.kr/](http://www.nanoscope.co.kr/))
- [113] Binnig G, Quate C F and Gerber C 1986 Atomic force microscope *Phys. Rev. Lett.* **56** 930–3
- [114] Yacoot A and Koenders L 2008 Aspects of scanning force microscope cantilevers and tips and their effects on dimensional measurement *J. Phys. D: Appl. Phys.* **41** 103001
- [115] Zhang L, Sakai T, Sakuma N, Ono T, Nakayama K, Sakuma N, Ono T and Nakayama K 1999 Nanostructural conductivity and surface-potential study of low-field-emission carbon films with conductive scanning probe microscopy *Appl. Phys. Lett.* **75** 3527–9
- [116] Hurley D C 2009 *Applied Scanning Probe Methods* ed B Bhushan and H Fuchs *et al* (Springer) pp 97–138
- [117] Melitz W, Shen J, Kummel A C and Lee S 2011 Kelvin probe force microscopy and its application *Surf. Sci. Rep.* **66** 1–27
- [118] Hartmann U 1988 Magnetic force microscopy: some remarks from the micromagnetic point of view *J. Appl. Phys.* **64** 1561–4
- [119] Betzig E, Trautmann J K, Harris T D, Weiner J S and Kostelak R L 1991 Breaking the diffraction barrier: optical microscopy on a nanometric scale *Science* **251** 1468–70
- [120] Reddick R C, Warmack R J and Ferrell T L 1991 New form of scanning optical microscopy *Phys. Rev. B* **39** 767–70
- [121] Uruma T, Satoh N, Yamamoto H and Iwata F 2020 Development of scanning capacitance force microscopy using the dissipative force modulation method *Meas. Sci. Technol.* **31** 035904
- [122] Xu J B, Lauger K, Dransfeld K and Wilson I H 1994 Thermal sensors for investigation of heat transfer in scanning probe microscopy *Rev. Sci. Instrum.* **65** 2262–6
- [123] Park H, Jung J, Min D K, Kim S, Hong S and Shin H 2004 Scanning resistive probe microscopy: imaging ferroelectric domains *Appl. Phys. Lett.* **84** 1734–6
- [124] Yacoot A and Koenders L 2011 Recent developments in dimensional nanometrology using AFMs *Meas. Sci. Technol.* **22** 122001
- [125] Yacoot A *et al* 2020 How accurate is your atomic force microscope? A comparison of dimensional measurements made using different AFMs *Microsc. Anal.* **34** S4–S9
- [126] Ando T 2012 High-speed atomic force microscopy coming of age *Nanotechnology* **23** 062001
- [127] Payton O D, Picco L and Scott T B 2016 High-speed atomic force microscopy for materials science *Int. Mater. Rev.* **61** 473–94

- [128] Ando T *et al* 2018 The 2018 correlative microscopy techniques roadmap *J. Phys. D: Appl. Phys.* **51** 4433001
- [129] Eaton P and West P 2010 *Atomic Force Microscopy* (ISBN-13: 9780199570454) (Oxford Scholarship online)
- [130] Villarubia J 2004 *Tip Characterization for Dimensional Metrology*, in *Applied Scanning Probe Methods I* ed B Bushan, H Fuchs and S Hosaka (Springer) pp 147–68
- [131] Hussain D and Ahmad K Song J and Xie H 2016 Advances in the atomic force microscopy for critical dimension metrology *Meas. Sci. Technol.* **28** 012001
- [132] Klapetek P, Yacoot A, Grolich P, Valtr M and Nečas D 2017 GwyScan: a library to support non-equidistant scanning probe microscope measurements *Meas. Sci. Technol.* **28** 034015
- [133] Nečas D and Klapetek P 2012 Gwyddion: an open-source software for SPM data analysis *Cent. Eur. J. Phys.* **10** 181–8
- [134] Sun X, Heaps E, Yacoot A, Yang Q, Grolich P and Klapetek P 2021 Three-dimensional drift correction of scan data from atomic force microscopy using Lissajous scanning paths *Meas. Sci. Technol.* **32** 115010
- [135] Alunda B O, Otieno L O, Park S J, Choi S G, Kim J H and Lee Y J 2020 Development of a photo-thermal scan head for high-speed atomic force microscope *Meas. Sci. Technol.* **31** 047003
- [136] Penedo M, Yurtsever A, Miyazawa K, Furusho H, Ishii K-A and Fukuma T 2020 Photothermal excitation efficiency enhancement of cantilevers by electron beam deposition of amorphous carbon thin films *Sci. Rep.* **10** 17436
- [137] Holz M, Reuter C, Ahmad A, Reum A, Hofmann M, Ivanov T and Rangelow I W 2019 Correlative microscopy and nanofabrication with AFM integrated with SEM *Microsc. Today* **27** 24–30
- [138] Zawierta M, Jeffery R D, Putrino G, Dilusha Silva K K M B, Keating A, Martyniuk M and Faraone L 2019 Atomic force microscopy with integrated on-chip interferometric readout *Ultramicroscopy* **205** 75–83
- [139] Fan P, Gao J, Mao H, Geng Y, Yan Y, Wang Y, Goel S and Luo X 2022 Scanning probe lithography: state-of-the-art and future perspectives *Micromachines* **13** 228
- [140] Marciniak L, Kniec K, Elżbieciak-Piecka K, Trejgis K, Stefanska J and Dramićanin M 2022 Luminescence thermometry with transition metal ions. A review *Coord. Chem. Rev.* **469** 214671
- [141] Paul N 1937 Device for indicating the temperature distribution of hot bodies *Google Patents*
- [142] Abram C, Pougin M and Beyrau F 2016 Temperature field measurements in liquids using ZnO thermographic phosphor tracer particles *Exp. Fluids* **57** 115
- [143] Cai T, Park Y, Mohammadshahi S and Kim K C 2021 Rise time-based phosphor thermometry using  $\text{Mg}_4\text{FGeO}_6:\text{Mn}^{4+}$  *Meas. Sci. Technol.* **32** 015201
- [144] Zhang Y, Wang X, Li Y, Li Y and Yao X 2018 Excellent up-conversion temperature sensing sensitivity and broad temperature range of Er-doped strontium tungstate multiphase phosphors *Opt. Mater. Express* **8** 12–23
- [145] Allison S, Beshears D, Cates M, Scudiere M, Shaw D and Ellis A 2020 Luminescence of YAG: Dy and YAG: Dy, Er crystals to 1700 °C *Meas. Sci. Technol.* **31** 044001
- [146] Dramićanin M D 2016 Sensing temperature via downshifting emissions of lanthanide-doped metal oxides and salts. A review *Methods Appl. Fluorescence* **4** 042001
- [147] Feist J, Heyes A and Nicholls J 2001 Phosphor thermometry in an electron beam physical vapour deposition produced thermal barrier coating doped with dysprosium *Proc. Inst. Mech. Eng. G* **215** 333–41
- [148] Abram C, Fond B and Beyrau F 2018 Temperature measurement techniques for gas and liquid flows using thermographic phosphor tracer particles *Prog. Energy Combust. Sci.* **64** 93–156
- [149] Ayers Z, Fisher J, Brown A, Son S F and Meyer T R 2019 kHz-rate temperature imaging using time-domain thermographic phosphorescence *AIAA Scitech 2019 Forum*
- [150] Ojo A O, Escofet-Martin D, Abram C, Fond B and Peterson B 2022 Precise surface temperature measurements at kHz-rates using phosphor thermometry to study flame-wall interactions in narrow passages *Combust. Flame* **240** 111984
- [151] Cai T, Peng D, Liu Y Z, Zhao X F and Kim K C 2017 A novel lifetime-based phosphor thermography using three-gate scheme and a low frame-rate camera *Exp. Therm Fluid Sci.* **80** 53–60
- [152] Cai T, Han J, Kim M and Kim K C 2021 Two-dimensional lifetime-based kHz surface temperature measurement technique using phosphor thermometry *Appl. Phys. Lett.* **119** 244101
- [153] Zentgraf F, Stephan M, Berrocal E, Albert B, Böhm B and Dreizler A 2017 Application of structured illumination to gas phase thermometry using thermographic phosphor particles: a study for averaged imaging *Exp. Fluids* **58** 82
- [154] Marciniak L, Piotrowski W, Szalkowski M, Kinzhybalov V, Drozd M, Dramićanin M and Bednarkiewicz A 2022 Highly sensitive luminescence nanothermometry and thermal imaging facilitated by phase transition *Chem. Eng. J.* **427** 131941
- [155] Xuan G, Fan L, Beyrau F and Fond B 2023 High spatial resolution fluid thermometry in boundary layers by macroscopic imaging of individual phosphor tracer particles *Exp. Therm Fluid Sci.* **148** 110977
- [156] Someya S 2021 Particle-based temperature measurement coupled with velocity measurement *Meas. Sci. Technol.* **32** 042001
- [157] Massing J, Kaden D, Kähler C J and Cierpka C 2016 Luminescent two-color tracer particles for simultaneous velocity and temperature measurements in microfluidics *Meas. Sci. Technol.* **27** 115301
- [158] Anderson B R, Livers S, Gunawidjaja R and Eilers H 2019 Fiber-based optical thermocouples for fast temperature sensing in extreme environments *Opt. Eng.* **58** 097105
- [159] Song M, Wang L, Wang J and Du P 2022 Constructing double perovskite  $\text{Eu}^{3+}/\text{Mn}^{4+}$ -codoped  $\text{La}_2\text{Mg}_{1.33}\text{Ta}_{0.67}\text{O}_6$  phosphors for high sensitive dual-mode optical thermometers *J. Lumin.* **252** 119347
- [160] Piotrowski W M, Trejgis K, Dramićanin M and Marciniak L 2021 Strong sensitivity enhancement in lifetime-based luminescence thermometry by co-doping of  $\text{SrTiO}_3$ :  $\text{Mn}^{4+}$  nanocrystals with trivalent lanthanide ions *J. Mater. Chem. C* **9** 10309–16
- [161] Fonger W H and Struck C W 1978 Unified model of energy transfer for arbitrary Franck-Condon offset and temperature *J. Lumin.* **17** 241–61
- [162] Feuk H, Nilsson S and Richter M 2022 Laser excitation effects in lifetime-based high-speed phosphor thermometry *J. Lumin.* **250** 119106
- [163] Cai T, Chen B, Han J, Kim M, Yeom E and Kim K C 2022 Effect of excitation duration on phosphorescence decay and analysis of its mechanisms *J. Lumin.* **252** 119423
- [164] Yang L, Peng D, Shan X, Guo F, Liu Y, Zhao X and Xiao P 2018 “Oxygen quenching” in Eu-based thermographic phosphors: mechanism and potential application in oxygen/pressure sensing *Sens. Actuators B* **254** 578–87
- [165] Stelter M, Martins F J, Beyrau F and Fond B 2021 Three-dimensional temperature and velocity measurements in fluids using thermographic phosphor tracer particles *14th Int. Symp. on Particle Image Velocimetry* vol 1

- [166] Cai T, Mohammadshahi S, Lee T and Kim K C 2021 Simultaneous measurement of two-dimensional temperature and strain fields based on thermographic phosphor and digital image correlation *Meas. Sci. Technol.* **32** 095204
- [167] Cai T, Jung J, Li D, Kim M, Jeon C-H and Kim K C 2022 Simultaneous sensing of oxygen concentration and temperature utilizing rise and decay of the phosphorescence of  $Y_2O_3: Eu^{3+}$  in high-temperature environments *Sens. Actuators B* **370** 132394
- [168] Wei K, Qiu C and Primrose K 2016 Super-sensing technology: industrial applications and future challenges of electrical tomography *Phil. Trans. R. Soc. A* **374** 20150328
- [169] Hampel U *et al* 2022 A review on fast tomographic imaging techniques and their potential application in industrial process control *Sensors* **22** 2309
- [170] Wang H and Yang W 2020 Application of electrical capacitance tomography in circulating fluidised beds—a review *Appl. Therm. Eng.* **176** 115311
- [171] Bera T K 2018 Applications of electrical impedance tomography (EIT): a short review *IOP Conf. Ser.: Mater. Sci. Eng.* **331** 012004
- [172] Wang Q, Jia X and Wang M 2019 Fuzzy logic based multi-dimensional image fusion for gas–oil–water flows with dual-modality electrical tomography *IEEE Trans. Instrum. Meas.* **69** 1948–61
- [173] Hjertaker B T, Maad R and Johansen G A 2011 Dual-mode capacitance and gamma-ray tomography using the landweber reconstruction algorithm *Meas. Sci. Technol.* **22** 104002
- [174] Pusppanathan J, Abdul Rahim R, Phang F A, Mohamad E J, Nor Ayob N M, Fazalul Rahiman M H and Kok Seong C 2017 Single-plane dual-modality tomography for multiphase flow imaging by integrating electrical capacitance and ultrasonic sensors *IEEE Sens. J.* **17** 6368–77
- [175] Razzak S A, Barghi S and Zhu J X 2007 Electrical resistance tomography for flow characterization of a gas–liquid–solid three-phase circulating fluidized bed *Chem. Eng. Sci.* **62** 7253–63
- [176] Maimaitijiang Y, Roula M A, Watson S, Patz R, Williams R J and Griffiths H 2008 Parallelization methods for implementation of a magnetic induction tomography forward model in symmetric multiprocessor systems *Parallel Comput.* **34** 497–507
- [177] Ma L, Banasiak R and Soleimani M 2016 Magnetic induction tomography with high performance GPU implementation *Prog. Electromagn. Res. B* **65** 49–63
- [178] Jeon J, Park C S, Lee S, Chae H Y, Kim J J and Son H 2022 Magnetic induction tomography using multi-channel phase-domain transceiver for structural health monitoring *IEEE Trans. Instrum. Meas.* **71** 1–9
- [179] Park C S, Jeon J, Oh B, Chae H Y, Park K, Son H and Kim J J 2018 A portable phase-domain magnetic induction tomography transceiver with phase-band auto-tracking and frequency-sweep capabilities *Sensors* **18** 3816
- [180] Xiao Z, Tan C and Dong F 2019 3-d hemorrhage imaging by cambered magnetic induction tomography *IEEE Trans. Instrum. Meas.* **68** 2460–8
- [181] Zeeshan Z, Zuccarelli C E, Acero D O, Marashdeh Q M and Teixeira F L 2018 Enhancing resolution of electrical capacitive sensors for multiphase flows by fine-stepped electronic scanning of synthetic electrodes *IEEE Trans. Instrum. Meas.* **68** 462–73
- [182] Li K, Chandrasekera T C, Li Y and Holland D J 2018 A non-linear reweighted total variation image reconstruction algorithm for electrical capacitance tomography *IEEE Sens. J.* **18** 5049–57
- [183] Andryani N A C, Sudiana D and Gunawan D 2018 Compressive sensing approach with double layer soft threshold for ECVT static imaging *Proc. 2018 5th International Conf. on Information Technology, Computer, and Electrical Engineering (ICITACEE)* pp 379–84
- [184] Bell A G 1881 On the production and reproduction of sound by light *Proc. Am. Assoc. Adv. Sci.* **29** 115–36
- [185] Amar L 1964 Detection d'omes elastiques (ultrasonores) sur l'os occipital, induites par impulsions laser dans l'oeil d'un lapin *CR Acad. Sc. Paris* **259** 3653–5
- [186] Oraevsky A A *et al* 1994 Laser-based optoacoustic imaging in biological tissues *Proc. SPIE* **2134** 122–8
- [187] Manohar S and Razansky D 2016 Photoacoustics: a historical review *Adv. Opt. Photonics* **8** 586–617
- [188] Das D *et al* 2021 Another decade of photoacoustic imaging *Phys. Med. Biol.* **66** 05TR01
- [189] Attia A B E, Balasundaram G, Moothanchery M, Dinish U S, Bi R, Ntziachristos V and Olivo M 2019 A review of clinical photoacoustic imaging: current and future trends *Photoacoustics* **16** 100144
- [190] Oraevsky A A *et al* 2001 Laser optoacoustic imaging of breast cancer in vivo *Proc. SPIE* **4256** 6–15
- [191] Heijblom M, Piras D, Brinkhuis M, van Hespden J C G, van den Engh F M, van der Schaaf M, Klaase J M, van Leeuwen T G, Steenbergen W and Manohar S 2015 Photoacoustic image patterns of breast carcinoma and comparisons with magnetic resonance imaging and vascular stained histopathology *Sci. Rep.* **5** 1–16
- [192] Moran M S *et al* 2014 Society of surgical oncology–American society for radiation oncology consensus guideline on margins for breast-conserving surgery with whole-breast irradiation in stages I and II invasive breast cancer *Int. J. Radiat. Oncol. Biol. Phys.* **88** 553–64
- [193] Janggun J, Tian C, Xu G, Sarazin J, Schioppa E, Gandikota G and Wang X 2018 Photoacoustic tomography for human musculoskeletal imaging and inflammatory arthritis detection *Photoacoustics* **12** 82–89
- [194] Li M, Vu T, Sankin G, Winship B, Boydston K, Terry R, Zhong P and Yao J 2020 Internal-illumination photoacoustic tomography enhanced by a graded-scattering fiber diffuser *IEEE Trans. Med. Imaging* **40** 346–56
- [195] Lin L, Hu P, Shi J, Appleton C M, Maslov K, Li L, Zhang R and Wang L V 2018 Single-breath-hold photoacoustic computed tomography of the breast *Nat. Commun.* **9** 1–9
- [196] Chitgupi U *et al* 2019 Surfactant-stripped micelles for NIR-II photoacoustic imaging through 12 cm of breast tissue and whole human breasts *Adv. Mater.* **31** 1902279
- [197] Zhao T, Desjardins A E, Ourselin S, Vercauteren T and Xia W 2019 Minimally invasive photoacoustic imaging: current status and future perspectives *Photoacoustics* **16** 100146
- [198] Zhou J *et al* 2020 All-optical fiber ultrasound imaging system based on the photoacoustic principle *Proc. SPIE* **11319** 237–42
- [199] Zhang E Z and Beard P C 2011 A miniature all-optical photoacoustic imaging probe *Proc. SPIE* **7899** 291–6
- [200] Gabor D 1948 A new microscopic principle *Nature* **161** 777–8
- [201] Schnars U, Falldorf C, Watson J and Jüptner W 2015 Digital holography *Digital Holography and Wavefront Sensing* (Springer) pp 39–68
- [202] Blanche P-A 2021 Holography, and the future of 3D display *Light Adv. Manuf.* **2** 446–59

- [203] Trolinger J D and Mansoor M M 2022 History and metrology applications of a game-changing technology: digital holography *J. Opt. Soc. Am. A* **39** A29–43
- [204] Wu Y and Ozcan A 2018 Lensless digital holographic microscopy and its applications in biomedicine and environmental monitoring *Methods* **136** 4–16
- [205] Zeng T, Zhu Y and Lam E Y 2021 Deep learning for digital holography: a review *Opt. Express* **29** 40572–93
- [206] Katz J and Sheng J 2010 Applications of holography in fluid mechanics and particle dynamics *Annu. Rev. Fluid Mech.* **42** 531–55
- [207] Huang J, Cai W, Wu Y and Wu X 2022 Recent advances and applications of digital holography in multiphase reactive/nonreactive flows: a review *Meas. Sci. Technol.* **33** 022001
- [208] Mazumdar Y C, Smyser M E, Heyborne J D, Slipchenko M N and Guildenbecher D R 2020 Megahertz-rate shock-wave distortion cancellation via phase conjugate digital in-line holography *Nat. Commun.* **11** 1129
- [209] Situ G 2022 Deep holography *Light Adv. Manuf.* **3** 278–300
- [210] Gao P and Yuan C 2022 Resolution enhancement of digital holographic microscopy via synthetic aperture: a review *Light Adv. Manuf.* **3** 105
- [211] Vicentini E, Wang Z, Van Gasse K, Hänsch T W and Picqué N 2021 Dual-comb hyperspectral digital holography *Nat. Photon.* **15** 890–4
- [212] Balasubramani V, Kus A, Tu H Y, Cheng C J, Baczewska M, Krauze W and Kujawinska M 2021 Holographic tomography: techniques and biomedical applications [Invited] *Appl. Opt.* **60** B65–80
- [213] Huang L, Zhang S and Zentgraf T 2018 Metasurface holography: from fundamentals to applications *Nanophotonics* **7** 1169–90
- [214] Liebel M, Pazos-Perez N, van Hulst N F and Alvarez-Puebla R A 2020 Surface-enhanced Raman scattering holography *Nat. Nanotechnol.* **15** 1005–11
- [215] Chen Y, Guildenbecher D R, Hoffmeister K N G, Cooper M A, Stauffacher H L, Oliver M S and Washburn E B 2017 Study of aluminum particle combustion in solid propellant plumes using digital in-line holography and imaging pyrometry *Combust. Flame* **182** 225–37
- [216] Wang F, Bian Y, Wang H, Lyu M, Pedrini G, Osten W, Barbastathis G and Situ G 2020 Phase imaging with an untrained neural network *Light Sci. Appl.* **9** 77
- [217] Chen H, Huang L, Liu T and Ozcan A 2022 Fourier imager network (FIN): a deep neural network for hologram reconstruction with superior external generalization *Light Sci. Appl.* **11** 254
- [218] Do Amaral C E F, Alves R F, da Silva M J, Arruda L V R, Dorini L, Morales R E M and Pipa D R 2013 Image processing techniques for high-speed videometry in horizontal two-phase slug flows *Flow Meas. Instrum.* **33** 257–64
- [219] Li Y, Blois G, Kazemifar F and Christensen K T 2021 A particle-based image segmentation method for phase separation and interface detection in PIV images of immiscible multiphase flow *Meas. Sci. Technol.* **32** 095208
- [220] Tan C, Murai Y, Liu W, Tasaka Y, Dong F and Takeda Y 2021 Ultrasonic Doppler technique for application to multiphase flows: a review *Int. J. Multiphase Flow* **144** 103811
- [221] 2022 *Industrial Tomography* (Elsevier) (<https://doi.org/10.1016/c2019-0-05207-7>)
- [222] Rashed S, Faraj Y, Wang M and Wilkinson S 2022 Electrical resistance tomography-based multi-modality sensor and drift flux model for measurement of oil–gas–water flow *Meas. Sci. Technol.* **33** 094006
- [223] Rasel R K, Chowdhury S M, Marashdeh Q M and Teixeira F L 2022 Review of selected advances in electrical capacitance volume tomography for multiphase flow monitoring *Energies* **15** 5285
- [224] Vauhkonen M, Hänninen A, Jauhainen J and Lehtikangas O 2019 Multimodal imaging of multiphase flows with electromagnetic flow tomography and electrical tomography *Meas. Sci. Technol.* **30** 094001
- [225] Liu H, Tan C, Liu W and Dong F 2022 Tomographic pulse wave ultrasonic Doppler method for cross-sectional velocity distribution imaging of dispersed oil-water two-phase flow *Exp. Fluids* **63** 73
- [226] Lin Y, Yang W, Wu Z and Wang H 2020 Monitoring of high-moisture content particle drying in a fluidized bed by microwave and capacitance tomographic sensors *Drying Technol.* **40** 1153–67
- [227] Neumann M, Bieberle M, Wagner M, Bieberle A and Hampel U 2019 Improved axial plane distance and velocity determination for ultrafast electron beam x-ray computed tomography *Meas. Sci. Technol.* **30** 084001
- [228] Ziauddin M *et al* 2022 Comparing wire-mesh sensor with neutron radiography for measurement of liquid fraction in foam *J. Phys.: Condens. Matter* **51** 015101
- [229] Wang G, Zhang Y, Ye X and Mou X 2019 *Machine Learning for Tomographic Imaging* (IOP Publishing) (<https://doi.org/10.1088/978-0-7503-2216-4>)
- [230] Dos Santos E N, Vendruscolo T P, Morales R E M, Schleicher E, Hampel U and Da Silva M J 2015 Dual-modality wire-mesh sensor for the visualization of three-phase flows *Meas. Sci. Technol.* **26** 105302
- [231] de Assis Dias F, Wiedemann P, Schleicher E, da Silva M J and Hampel U 2022 Improvement of wire-mesh sensor accuracy via adapted circuit design and integrated energy loss measurement *Meas. Sci. Technol.* **33** 084002
- [232] Bruscheckski M, John K, Wüstenhagen C, Rehm M, Hadžić H, Pohl P and Grundmann S 2021 Commissioning of an MRI test facility for CFD-grade flow experiments in replicas of nuclear fuel assemblies and other reactor components *Nucl. Eng. Des.* **375** 111080
- [233] Prasser H-M 2008 Novel experimental measuring techniques required to provide data for CFD validation *Nucl. Eng. Des.* **238** 744–70
- [234] Koulountzios P, Rymarczyk T and Soleimani M 2021 A triple-modality ultrasound computed tomography based on full-waveform data for industrial processes *IEEE Sens. J.* **21** 20896–909
- [235] Liu H, Dong F and Tan C 2021 Multifrequency ultrasonic tomography for oil–gas–water three-phase distribution imaging using transmissive attenuation spectrum *IEEE Trans. Instrum. Meas.* **70** 1–11
- [236] Hlava J and Abouelazayem S 2022 Control systems with tomographic sensors—a review *Sensors* **22** 2847
- [237] Sciacchitano A 2019 Uncertainty quantification in particle image velocimetry *Meas. Sci. Technol.* **30** 092001
- [238] Charonko J J and Vlachos P P 2013 Estimation of uncertainty bounds for individual particle image velocimetry measurements from cross-correlation peak ratio *Meas. Sci. Technol.* **24** 065301
- [239] Xue Z, Charonko J J and Vlachos P P 2014 Particle image velocimetry correlation signal-to-noise ratio metrics and measurement uncertainty quantification *Meas. Sci. Technol.* **25** 115301
- [240] Xue Z, Charonko J J and Vlachos P P 2015 Particle image pattern mutual information and uncertainty estimation for particle image velocimetry *Meas. Sci. Technol.* **26** 74001
- [241] Sciacchitano A, Wieneke B and Scarano F 2013 PIV uncertainty quantification by image matching *Meas. Sci. Technol.* **24** 045302

- [242] Wieneke B 2015 PIV uncertainty quantification from correlation statistics *Meas. Sci. Technol.* **26** 074002
- [243] Bhattacharya S, Charonko J J and Vlachos P P 2018 Particle image velocimetry (PIV) uncertainty quantification using moment of correlation (MC) plane *Meas. Sci. Technol.* **29** 115301
- [244] Sciacchitano A, Neal D R, Smith B L, Warner S O, Vlachos P P, Wieneke B and Scarano F 2015 Collaborative framework for PIV uncertainty quantification: comparative assessment of methods *Meas. Sci. Technol.* **26** 074004
- [245] Boomsma A, Bhattacharya S, Troolin D, Pothos S and Vlachos P 2016 A comparative experimental evaluation of uncertainty estimation methods for two-component PIV *Meas. Sci. Technol.* **27** 94006
- [246] Rajendran L K, Bhattacharya S, Bane S P M and Vlachos P P 2021 Meta-uncertainty for particle image velocimetry *Meas. Sci. Technol.* **32** 104002
- [247] Sciacchitano A and Wieneke B 2016 PIV uncertainty propagation *Meas. Sci. Technol.* **27** 084006
- [248] Zhang J, Bhattacharya S and Vlachos P P 2020 Using uncertainty to improve pressure field reconstruction from PIV/PTV flow measurements *Exp. Fluids* **61** 131
- [249] Rajendran L, Zhang J, Bane S and Vlachos P 2020 Uncertainty-based weighted least squares density integration for background-oriented schlieren *Exp. Fluids* **61** 1–12
- [250] Ahmadzadegan A, Bhattacharya S, Ardekani A M and Vlachos P P 2022 Uncertainty estimation for ensemble particle image velocimetry *Meas. Sci. Technol.* **33** 085302
- [251] Bhattacharya S, Charonko J J and Vlachos P P 2017 Stereo-particle image velocimetry uncertainty quantification *Meas. Sci. Technol.* **28** 15301
- [252] Bhattacharya S and Vlachos P P 2020 Volumetric particle tracking velocimetry (PTV) uncertainty quantification *Exp. Fluids* **61** 1–18
- [253] Wieneke B 2017 PIV anisotropic denoising using uncertainty quantification *Exp. Fluids* **58** 94
- [254] Beresh S J 2018 Denoising 400-kHz ‘postage-stamp PIV’ using uncertainty quantification 2018 AIAA Aerospace Sciences Meeting (27 December 2022) (<https://doi.org/10.2514/6.2018-2034>)
- [255] Timmins B H, Wilson B W, Smith B L and Vlachos P P 2012 A method for automatic estimation of instantaneous local uncertainty in particle image velocimetry measurements *Exp. Fluids* **53** 1133–47
- [256] Adatrao S, van der Velden S, van der Meulen M J, Bordes M C and Sciacchitano A 2022 Design of experiments: a statistical tool for PIV uncertainty quantification *Meas. Sci. Technol.* **34** 015201
- [257] Adatrao S, Bertone M and Sciacchitano A 2021 Multi- $\Delta t$  approach for peak-locking error correction and uncertainty quantification in PIV *Meas. Sci. Technol.* **32** 054003
- [258] Rajendran L K, Bane S P M and Vlachos P P 2020 Uncertainty amplification due to density/refractive index gradients in background-oriented schlieren experiments *Exp. Fluids* **61** 139
- [259] Westerweel J 2000 Theoretical analysis of the measurement precision in particle image velocimetry *Exp. Fluids* **29** S003–12
- [260] Hall E M, Guildenbecher D R and Thurow B S 2017 Uncertainty characterization of particle location from refocused plenoptic images *Opt. Express* **25** 21801
- [261] Lindken R, Rossi M, Große S and Westerweel J 2009 Micro-particle image velocimetry (microPIV): recent developments, applications, and guidelines *Lab Chip* **9** 2551–67
- [262] Santiago J G, Wereley S T, Meinhart C D, Beebe D J and Adrian R J 1999 A particle image velocimetry system for microfluidics *Exp. Fluids* **25** 316–9
- [263] Meinhart C D, Wereley S T and Santiago J G 2000 A PIV algorithm for estimating time-averaged velocity fields *J. Fluids Eng.* **122** 285–9
- [264] Rossi M, Segura R, Cierpka C and Kähler C J 2012 On the effect of particle image intensity and image preprocessing on depth of correlation in micro-PIV *Exp. Fluids* **52** 1063–75
- [265] Kähler C J, Astarita T, Vlachos P P, Sakakibara J, Hain R, Discetti S, La Foy R and Cierpka C 2016 Main results of the fourth international PIV challenge *Exp. Fluids* **57** 1–17
- [266] Cierpka C and Kähler C J 2012 Particle imaging techniques for volumetric three-component (3D3C) velocity measurements in microfluidics *J. Vis.* **15** 1–31
- [267] Cierpka C, Rossi M, Segura R, Mastrangelo F and Kähler C J 2012 A comparative analysis of the uncertainty of astigmatism- $\mu$ PTV, stereo- $\mu$ PIV, and  $\mu$ PIV *Exp. Fluids* **52** 605–15
- [268] Franchini S, Charogiannis A, Markides C N, Blunt M J and Krevor S 2019 Calibration of astigmatic particle tracking velocimetry based on generalized Gaussian feature extraction *Adv. Water Resour.* **124** 1–8
- [269] Rossi M 2019 Synthetic image generator for defocusing and astigmatic PIV/PTV *Meas. Sci. Technol.* **31** 017003
- [270] Barnkob R and Rossi M 2020 General defocusing particle tracking: fundamentals and uncertainty assessment *Exp. Fluids* **61** 1–14
- [271] Discetti S and Lui Y 2022 Machine learning for flow field measurements: a perspective *Meas. Sci. Technol.* **34** 021001
- [272] König J, Chen M, Rösing W, Boho D, Mäder P and Cierpka C 2020 On the use of a cascaded convolutional neural network for three-dimensional flow measurements using astigmatic PTV *Meas. Sci. Technol.* **31** 074015 open access
- [273] Sachs S, Ratz M, Mäder P, König J and Cierpka C 2023 Particle detection and size recognition based on defocused particle images: a comparison of a deterministic algorithm and a deep neural network *Experiments in Fluids* **64** 21
- [274] Ratz M, Sachs S, König J and Cierpka C 2023 A deep neural network architecture for reliable 3D position and size determination of Lagrangian particle tracking using a single camera *Meas. Sci. Technol.* **34** 105203
- [275] Deng Z, König J and Cierpka C 2022 Astigmatism particle tracking velocimetry and lifetime imaging using LED and low-speed cameras *Meas. Sci. Technol.* **33** 115301
- [276] Russakovsky O *et al* 2015 ImageNet large scale visual recognition challenge *Int. J. Comput. Vis.* **115** 211–52